Application of Optimal Control Theory to Launch Vehicles

FINAL TECHNICAL REPORT

July 1968

GPO PRICE $ _____

CSFTI PRICE(S) $ _____

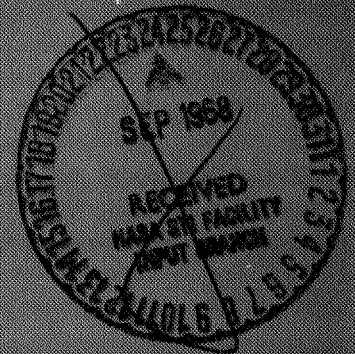Hard copy (HC) __ .

Microfiche (MF) __ .

ff 653 July 65

HONEYWELL SYSTEMS & RESEARCH DIVISION

APPLICATION OF OPTIMAL CONTROL THEORY

TO LAUNCH VEHICLES

FINAL TECHNICAL REPORT

Prepared for

National Aeronautics and Space Administration
George C. Marshall Space Flight Center
Huntsville, Alabama

Contract NAS 8-21063

Prepared by: C. A. Harvey   Approved by:

V. S. Levadi
Aerospace Sciences
Research Manager

Reviewed by:

G. B. Skelton
Flight Mechanics
Research Section Chief

HONEYWELL INC.

Systems and Research Division
Research Department
St. Paul, Minnesota 55113

ACKNOWLEDGMENT

FOREWORD

This document is the final technical summary of an investigation of application of optimal control theory to the design of control systems for launch vehicles performed for the National Aeronautics and Space Administration, George C. Marshall Space Flight Center under Contract NAS 8-21063.

Mr. J. R. Redus of the Astrodynamics and Guidance Theory Division of the Aero-Astrodynamics Laboratory was the technical monitor. The study was carried out by the Systems and Research Division of Honeywell Inc. Dr. Grant B. Skelton was initially the principal investogator and later served as the technical supervisor for the program. Dr. C. A. Harvey succeeded Dr. Skelton as principal investigator. Mr. M. D. Ward did all of the digital computer programming, and Mr. C. R. Stone provided consulting assistance for the load distribution model.

ABSTRACT

This report is a technical summary of an investigation of the application of optimal control theory to the design of launch vehicle control systems. The goal of this study was the development of a practical design technology based on optimization theory for launch vehicle attitude control systems.

In a previous study Honeywell developed a stochastic constrained-response theory and demonstrated its applicability to the control of a rigid launch vehicle. This optimization theory was applied in the present study to a vehicle model which included three flexure modes and three fuel-slosh modes as well as the rigid dynamics.

The development of a practical design technology requires the development of a method for simplifying the optimal controller produced by the optimization theory. For a practical controller this simplification technique must yield a controller which uses a practical sensor complement. Thus, a method for choosing a set of feedback sensors and sensor locations for the simplified controller must be developed concurrently with the simplification technique. The attempts to develop such techniques are described following descriptions of the mathematical model employed in the study and the formulation of the optimization problem.

Formal methods for solving the controller simplification and sensor choice problems failed to give satisfactory results. This led to a series of experiments performed to determine the significance of certain feedbacks of the optimal controller.

The experimentation is described followed by a description of a simplified controller designed on the basis of results from the series of experiments.

Quantitative results obtained during the course of the investigation are presented, followed by general conclusions and recommendations for further study.

The appendices contain a discussion of the distributed aerodynamic loading included in the model for this study, a display of matrix coefficients appearing in the model equations of motion, a derivation of the optimum fixed-form controller, and a display of gains for controllers derived from the optimization theory.

CONTENTS

CONTENTS (Continued)

LIST OF ILLUSTRATIONS

LIST OF TABLES

NOMENCLATURE

D	Axial aerodynamic drag of vehicle

I_{yy} — Pitch moment of inertia of vehicle about center of gravity (cg)

M — Total mass of vehicle $= \int M(x)\,dx$

M_{s_j} — Sloshing mass of fuel in j^{th} tank

M_i — Generalized mass of ith flexure mode

$M_\alpha'(x_o)$ — Structural bending moment at x_o due to angle of attack

$M_{\dot{\phi}}'(x_o)$ — Structural bending moment at x_o due to pitch rate

N — Aerodynamic side force due to a unit angle-of-attack $= \int \frac{d\widetilde{t}}{d\alpha}\,dx$

N_{η_1} — Aerodynamic side force due to a unit i^{th} flexure mode displacement $= \int \frac{d\widetilde{t}}{d\alpha} Y_i'(x)\,dx$

$N_{\dot{\eta}_i}$ — Aerodynamic side force due to a unit i^{th} flexure mode rate $= \int \frac{d\widetilde{t}}{d\alpha} Y_i(x)\,dx$

$N_{\eta_{ii}}$ — Aerodynamic coupling of ith flexure mode due to a unit i^{th} flexure mode displacement $= \int \frac{d\widetilde{t}}{d\alpha} Y_i(x) Y_i'(x)\,dx$

$N_{\dot{\eta}_{ii}}$ — Aerodynamic coupling of ith flexure mode due to a unit i^{th} flexure mode rate $= \int \frac{d\widetilde{t}}{d\alpha} [Y_i(x)]^2\,dx$

R' Thrust of gimbaled engines $= \dfrac{4}{5} T$

T Total thrust of engines

$T_{\dot{\varphi}}$ Aerodynamic pitching moment due to a unit pitch rate

$$= \int \frac{d\tilde{t}}{d\alpha}(x-x_{cg})^2 dx$$

T_{η_i} Aerodynamic pitching moment due to a unit i^{th} flexure mode

displacement $= \int \frac{d\tilde{t}}{d\alpha} Y_i{}'(x)\,(x-x_{cg})dx$

$T_{\dot{\eta}_i}$ Aerodynamic pitching moment due to a unit i^{th} flexure mode

rate $= \int \frac{d\tilde{t}}{d\alpha} Y_i(x)\,(x-x_{cg})dx$

V Nominal flight path velocity of vehicle

$Y_i(x)$ Normalized modal deflection of ith flexure mode

$Y_i{}'(x)$ Normalized modal slope of ith flexure mode

c_1 Coefficient in wind filter $= 10^{-2}\sqrt{1.9 + 1.47(0.91)\cdot 10^{-8}}$

c_2 Coefficient in wind filter

$$= 10^{-2}\sqrt{[1.9 - 1.47(0.91)\cdot 10^{-8}]}\; c_5 - 1.9\cdot 10^{-4}\, c_1$$

c_3 Coefficient in wind filter $= 1$

c_4 Coefficient in wind filter $= 1.9\cdot 10^{-4}$

c_5 Coefficient in wind filter $= [(0.95)^2 + (0.735)^2]\cdot 10^{-8}$

$h(t)$ Altitude of vehicle

ℓ_{cp} Aerodynamic moment arm $= x_{cp} - x_{cg}$

$v_w(x, t)$	Wind component orthogonal to missile
$\bar{v}_w(x, t)$	Mean value of $v_w(x, t)$
x	Distance along vehicle measured from tail
x_β	Control engines gimbal location
x_{cg}	Location of vehicle center of gravity
x_{cp}	Location of aerodynamic center of pressure
x_{s_j}	Location of jth fuel-sloshing center of mass
z	Lateral displacement normal to nominal flight path
z_{s_j}	Displacement of jth sloshing mass normal to vehicle centerline
β	Gimbal angle
β_c	Commanded gimbal angle
ζ_i	Equivalent viscous damping factor of ith flexure mode
ζ_{s_j}	Equivalent viscous damping factor of jth fuel-sloshing mode
η_i	Generalized deflection of ith flexure mode
σ_{v_w}	Standard deviation of $v_w(t)$
φ	Angular pitch displacement
ω_i	Natural frequency of ith flexure mode
ω_{s_j}	Natural frequency of jth fuel-sloshing mode

SECTION I
INTRODUCTION AND SUMMARY

The goal of this study was the development of a practical design technology based on optimization theory for the launch vehicle attitude control problem. In a previous study, under contract NAS 8-20155, Honeywell developed a stochastic constrained-response theory and demonstrated its applicability to the control of a rigid booster. These results are reported in reference 1. The present study is an extension of the earlier work in two respects. The vehicle model for the present study includes three flexure modes and three fuel-slosh modes as well as the rigid dynamics. The second extension is in the realm of simplification of the optimal controller produced by the above stochastic theory and, concurrently, the choice of feedback sensors and sensor locations.

The booster control problem consists of designing a gimbal controller that compensates for undesired wind-induced bending, rotations, and translations. The goal of the design is to produce a controller which maintains bending moments within structural strength limits throughout the flight and provides satisfactory errors in terminal drift, drift rate, and angle of attack.

In reference 1 the incident winds and corresponding responses were described as random processes, and an event of mission failure was defined. The event of mission failure is that one or more responses fall outside pre-selected limits at burnout or during the flight. The optimization problem is the minimization of an upper bound of the likelihood of occurrence of the event of mission failure. This problem was formulated in a manner that permitted its solution by means of known optimization theories. The solution yields a linear, finite-time controller with time-varying gains.

The Saturn V/Voyager with a 45-foot shroud length was taken as the study vehicle for the present study. This model was chosen because a Load Relief Study for this vehicle was performed by the Aerospace Division of Honeywell

under contract NAS 8-21171, and their reduced vehicle data, presented in reference 2, became available during the contract period.

The response constraints assumed for this study are:

- Magnitude of terminal drift = $|z(160)| < 30,000$ meters

- Magnitude of terminal drift rate = $|\dot{z}(160)| < 70$ meters/second

- Magnitude of terminal angle of attack = $|\alpha(160)| < 0.05934$ radian

- Magnitude of gimbal angle = $|\beta(t)| < 0.0873$ radian

- Magnitude of IB1 = $|IB1(t)| < 9 \cdot 10^6$ Newton meters

- Magnitude of IB2 = $|IB2(t)| < 1.7 \cdot 10^6$ Newton meters

- Magnitude of IB3 = $|IB3(t)| < 5 \cdot 10^5$ Newton meters

where IB1 is the bending moment at the fuselage station 1541 inches forward of the gimbal station, IB2 is the bending moment at the fuselage station 2747 inches forward of the gimbal station, and IB3 is the bending moment at the fuselage station 3256 inches forward of the gimbal station. The constant values used for the bending moment limits in this study are lower bounds for the actual time-varying maximum allowable bending moments.

The optimization is most easily applied to the case in which it is assumed that every desired vehicle and wind measurement can be made (i.e., the complete state can be measured). Optimization for this case yields the best possible controller in terms of performance, but the controller is idealized and impractical. The performance of this controller indicates the significant responses to be controlled and significant feedback responses. These results provide guides for simplification of the controller.

Optimization with complete measurement capability was accomplished in eleven iterations using the concept of quadratic equivalence described in reference 1. The resulting controller, denoted as controller A, and its

2

performance were used to define analytical measures of quality for comparing candidate sensor complements. When evaluated, the measures of quality developed were found to be unsatisfactory in that they yielded little insight and poor results. Controller simplification analysis based on investigations to determine degradation in performance caused by deleting the feedback of certain states from controller A was then begun. In analyzing the results of these investigations, it was found that the coefficient of attitude rate in the bending moment expression was in error; this caused the attitude rate contributions to the bending moment response covariances to be unrealistically large. The error was that division of the attitude rate coefficient by the negative of the nominal flight-path velocity had not been performed in the data preparation. This caused the bending moments computed to be overly sensitive to attitude rate. The error did not affect the vehicle state-transition equations.

When the error was discovered, there were two possible approaches to obtain meaningful results for the corrected model. One approach was to evaluate the performance of controller A, repeating all of the simplification results for the corrected model. The second approach was to proceed with optimization with complete measurement for the corrected model to obtain a new optimal controller, and then to perform simplification analyses for this new optimal controller. The second approach required a much larger expenditure of money than did the first approach, since the computations involved in the first approach could utilize most of the computational results previously obtained for the incorrect model (since the state covariances were not affected by the error). Fortunately, controller A proved to be a good controller for the corrected model. It was decided to repeat the simplifications of the first approach and to then proceed with the second approach as far as time and money permitted.

For the corrected model the upper bound of the probability that mission failure would occur with controller A with complete measurement was $8 \cdot 10^{-4}$ with no mean wind input and $8.2 \cdot 10^{-4}$ with the mean wind input and an adjusted deterministic input. The only response which significantly

contributed to this likelihood was IB3 during the time interval of high dynamic pressure.

The simplification analyses indicated that controller A was very sensitive to the high-frequency third flexure mode, wind, and load-distribution states. Deleting the fuel-slosh, fuel-slosh rate, drift, and second flexure mode feedbacks from controller A caused only slight degradation in performance. These results led to the design of a simplified controller involving a fifth-order state estimator, and feedbacks of five accelerometer signals and the first and second integrals of these signals. This controller exhibited reasonably good performance, yielding a value of 0.017 for the upper bound of the probability of mission failure with a mean wind input of zero.

Following the second approach, the optimization with complete measurement was performed for the corrected model with the same optimization criterion as used for determining controller A. One subsequent iteration of the optimization criterion provided a controller, denoted as controller B, which exhibited much improved performance. The nature of this controller differed significantly from that of controller A. The upper bound of the probability that mission failure would occur for controller B with complete measurement was 10^{-6} with no mean wind input and $1.7 \cdot 10^{-6}$ with the mean wind input. The only response which significantly contributed to this likelihood was the gimbal deflection near the terminal time. In comparison, the upper bound on the likelihood of IB3 exceeding its limits during the interval of high dynamic pressure was $2 \cdot 10^{-18}$. Subsequent iterations could undoubtedly have reduced the likelihood of the gimbal angle exceeding its limit near the terminal time, but expenditure limitations prevented further iterations. However, there is a clear difference in the control characteristics of controller B and controller A.

In addition to the differences in the significant responses contributing to the probability of occurrence of mission failure, these controllers exhibited the following differences in standard deviations of states at maximum dynamic pressure. The standard deviation of attitude error was 0.05 radian for controller B and 0.007 radian for controller A, indicating that controller A is a

4

tighter attitude controller. The standard deviation of the first fuel-slosh mode displacement was 11 centimeters for controller B and 4 centimeters for controller A, indicating that controller B permits somewhat more fuel sloshing than does controller A.

The limited simplification analyses performed with controller B showed that deleting the fuel-slosh and drift feedbacks caused extreme degradation of the controller. The performance with these feedbacks deleted was unsatisfactory after 75 seconds, and the probability of occurrence of mission failure was essentially one (certainty). Thus it appears that the remarkable load-relief capability of controller B is achieved by significant utilization of the fuel-slosh feedbacks. Hence, measurement or estimation of the motion of the fuel could produce greater load-relief capability.

The mathematical model, problem formulation, controller simplification analyses, and quantitative results are described in Sections II, III, IV and V. Conclusions and recommendations are presented in Section VI.

Differential equations describing the missile dynamics, the wind filter, and the distribution of aerodynamic loads are presented in Section II. Difference equations used to approximate the differential equations are also given there.

Section III is a brief summary of the formulation of the load-relief problem as a stochastic minimization problem and the equivalent quadratic method used in its solution. Complete derivations of this material are presented in reference 1.

The approaches to sensor choice and controller simplification are described in Section IV. The quantitative results generated during the study are summarized in Section V.

SECTION II
MATHEMATICAL MODEL

The differential equations used to describe the missile dynamics, the wind random process, and the distribution of the wind loads are presented. The difference equations approximation to the differential equations are also given.

Missile Dynamics

The Saturn V booster with a Voyager payload was used as a study vehicle. The payload configuration consisted of a cylindrical section 45 feet long. The model included rigid-body dynamics, three flexure modes, three fuel-slosh modes and a first-order actuator. Engine-inertia effects were ignored.

Vehicle perturbation equations, a summary of data supplied by MSFC, and reduced data computed by Honeywell's Aerospace Division are presented in reference 2. The particular set of response perturbation equations used in this study were:

Drift:
$$M\ddot{z} = (T-D)\varphi + R'\beta + \int \frac{d\tilde{t}}{d\alpha} \alpha \, dx + (T-D) \sum_{i=1}^{3} Y_i'(x_\beta)\eta_i$$
$$- \sum_{j=1}^{3} M_{s_j} \ddot{z}_{s_j} + \sum_{i=1}^{3} \int \frac{d\tilde{t}}{d\alpha} \left(Y_i'(x)\,\eta_i - Y_i(x)\frac{\dot{\eta}_i}{V} \right) dx \qquad (2.1)$$

Pitch:
$$I_{yy}\ddot{\varphi} = -R'(x_{cg}-x_\beta)\beta + \int \frac{d\tilde{t}}{d\alpha}(x-x_{cg})\alpha \, dx - T \sum_{i=1}^{3} [(x_{cg}-x_\beta)\, Y_i'(x_\beta)$$
$$+ Y_i(x_\beta)]\eta_i + \sum_{j=1}^{3} M_{s_j} \left[\left(\frac{T-D}{M}\right) z_{s_j} + (x_{cg}-x_{s_j})\,\ddot{z}_{s_j} \right]$$
$$+ \sum_{i=1}^{3} \int \frac{d\tilde{t}}{d\alpha}(x-x_{cg}) \left[Y_i'(x)\eta_i - Y_i(x)\frac{\dot{\eta}_i}{V} \right]dx \qquad (2.2)$$

i^{th} Flexure Mode:

$$M_i(\ddot{\eta}_i + 2\zeta_i \omega_i \dot{\eta}_i + \omega_i^2 \eta_i) = R'Y_i(x_\beta)\beta + \int \frac{d\tilde{t}}{d\alpha} Y_i(x)\alpha \, dx$$

$$+ \sum_{j=1}^{3} M_{s_j} \left[\left(\frac{T-D}{M} \right) Y_i'(x_{s_j}) z_{s_j} - Y_i(x_{s_j}) \ddot{z}_{s_j} \right]$$

$$+ \int \frac{d\tilde{t}}{d\alpha} Y_i(x) \left[Y_i'(x)\eta_i - Y_i(x) \frac{\dot{\eta}_i}{V} \right] dx \qquad (2.3)$$

j^{th} Fuel-Slosh Mode:

$$\ddot{z}_{s_j} + 2\zeta_{s_j} \omega_{s_j} \dot{z}_{s_j} + \omega_{s_j}^2 z_{s_j} = \left(\frac{T-D}{M} \right) \left[\varphi + \sum_{i=1}^{3} Y_i'(x_{s_j})\eta_i \right]$$

$$- \ddot{z} + (x_{cg} - x_{s_j})\ddot{\varphi} - \sum_{i=1}^{3} Y_i(x_{s_j})\ddot{\eta}_i \qquad (2.4)$$

Actuator: $\quad \dot{\beta} + 11.9\beta = 11.9\beta_c \qquad (2.5)$

where $\frac{d\tilde{t}}{d\alpha}$ denotes the side force on the vehicle per unit length per unit angle of attack

$$\alpha(x, t) = \varphi(t) + \frac{v_\omega(x, t) - \dot{z}(t) - [x - x_{cg}(t)]\dot{\varphi}(t)}{V(t)} \qquad (2.6)$$

which denotes the angle of attack at a station x. The other notation employed is defined under <u>Nomenclature</u>.

The structural bending moment at station x_o was assumed to be given by

$$I_b(x_o) = M_\beta'\beta + \sum_{i=1}^{3} M'_{\ddot{\eta}_i} \ddot{\eta}_i + \int \frac{d\tilde{t}}{d\alpha} [(x - x_{cg})\gamma_1 + \gamma_2 + (x_o - x) \chi(x_o - x)]\alpha \, dx$$

$$(2.7)$$

where

$$M_\beta' = R'[x_o - x_\beta + \gamma_2 - \gamma_1(x_{cg} - x_\beta)]$$

$$M_{\ddot{\eta}_i}' = \int_o^x (x - x_o) \, M(x) \, Y_i(x) \, dx$$

$$\gamma_1(x_o, t) = \frac{I_T + M_T(x_T - x_{cg})(x_T - x_o)}{I_{yy}}$$

$$\gamma_2(x_o, t) = \frac{M_T(x_T - x_o)}{M}$$

$$\chi(x_o - x) = \begin{cases} 1 \text{ if } 0 \leq x \leq x_o \\ 0 \text{ if } x > x_o \end{cases}$$

M_T = mass of section of vehicle from 0 to x_o

x_T = center of gravity of section of vehicle from 0 to x_o

I_T = pitch moment of inertia of vehicle section from 0 to x_o about x_T

$M(x)$ = mass density of vehicle

All integrals without indicated limits represent integrals over the length of the vehicle.

Using equation (2.6) to eliminate α from equations (2.1) - (2.4) and (2.7) yielded

$$\ddot{z} = \frac{(T - D + N)}{M} \varphi - \frac{N\dot{z}}{MV} + \frac{R'}{M} \beta - \frac{N\ell_{cp}}{MV} \dot{\varphi} - \sum_{j=1}^{3} \frac{M_{s_j}}{M} \ddot{z}_{s_j}$$

$$+ \frac{1}{M} \sum_{i=1}^{3} [(T - D) Y_i'(x_\beta) + N_{\eta_i}] \eta_i - \sum_{i=1}^{3} \frac{N_{\dot{\eta}_i}}{MV} \dot{\eta}_i + \frac{1}{M} \int \frac{d\widetilde{t}}{d\alpha} \frac{v_\omega}{V} dx \qquad (2.8)$$

$$\ddot{\varphi} = \frac{N\ell_{cp}}{I_{yy}} \varphi - \frac{N\ell_{cp}}{I_{yy}V} \dot{z} - \frac{R'}{I_{yy}} (x_{cg}-x_\beta)\beta - \frac{T_{\dot{\varphi}}}{I_{yy}V} \dot{\varphi}$$

$$+ \frac{1}{I_{yy}} \sum_{j=1}^{3} M_{s_j} \left[(x_{cg}-x_{s_j})\ddot{z}_{s_j} + \left(\frac{T-D}{M}\right) z_{s_j} \right]$$

$$+ \frac{1}{I_{yy}} \sum_{i=1}^{3} [T_{\eta_i} - T(x_{cg}-x_\beta) Y_i'(x_\beta) - TY_i(x_\beta)] \eta_i$$

$$- \sum_{i=1}^{3} \frac{T_{\dot{\eta}_i}}{I_{yy}V} \dot{\eta}_i + \frac{1}{I_{yy}} \int \frac{d\tilde{t}}{d\alpha} (x-x_{cg}) \frac{v_\omega}{V} dx \qquad (2.9)$$

$$(\ddot{\eta}_i + 2\varsigma_i \omega_i \dot{\eta}_i + \omega_i^2 \eta_i) = \frac{N_{\eta_i}}{M_i V} \varphi - \frac{N_{\dot{\eta}_i}}{M_i V} \dot{z} + \frac{R'}{M_i} Y_i(x_\beta)\beta - \frac{T_{\dot{\eta}_i}}{M_i V} \dot{\varphi}$$

$$- \frac{1}{M_i} \sum_{j=1}^{3} M_{s_j} \left[Y_i(x_{s_j})\ddot{z}_{s_j} - \frac{T-D}{M_i} Y_i'(x_{s_j})z_{s_j} \right]$$

$$+ \frac{1}{M_i} \left[N_{\eta_{ii}} \eta_i - \frac{N_{\dot{\eta}_{ii}}}{V} \eta_i \right] + \frac{1}{M_i} \int \frac{d\tilde{t}}{d\alpha} Y_i(x) \frac{v_\omega}{V} dx$$

$$(2.10)$$

$$I_b(x_o) = M_\alpha'\varphi - \frac{M_\alpha'}{V} \dot{z} + M_\beta'\beta - \frac{M_{\dot{\varphi}}'}{V} \dot{\varphi} + \sum_{i=1}^{3} M_{\ddot{\eta}_i}' \ddot{\eta}_i$$

$$+ \int \frac{d\tilde{t}}{d\alpha} [(x-x_{cg}) \gamma_1 + \gamma_2 + (x_o-x) \chi(x_o-x)] \frac{v_\omega}{V} dx \qquad (2.11)$$

where all newly introduced coefficients are defined in the Nomenclature. The integrals remaining in these equations will be discussed further under wind loads.

Wind Model

The wind model used in this study was essentially the same as the wind model described in reference 1. The only changes incorporated in this study were changes in the mean wind and wind standard deviations.

The wind filter equations employed were taken from reference 1; they are

$$v_w = \bar{v}_w + \sigma_{v_w} w \tag{2.12}$$

$$\begin{bmatrix} \dot{w} \\ \dot{x} \end{bmatrix} = \begin{bmatrix} 0 & \dot{h}c_3 \\ -\dot{h}c_5 & -\dot{h}c_4 \end{bmatrix} \begin{bmatrix} w \\ x \end{bmatrix} + \begin{bmatrix} c_1 \sqrt{\dot{h}} \\ c_2 \sqrt{\dot{h}} \end{bmatrix} \eta \tag{2.13}$$

where $\dot{h}$ is the vertical component of vehicle velocity and η is a unity white noise input.

In the study reported in reference 1, the mean wind and wind standard deviations were smoothed to have zero values at burnout. In this study $\bar{v}_w$ was smoothed to be zero for $t \geq 130$ seconds and σ_{v_w} was assumed constant for $t \geq 125$ seconds.

Wind Loads

As discussed in reference 1, an anomaly arises in the expression for the time-derivative of the bending moment if the integral in equation (2.11) is approximated by assuming that v_w is constant over the length of the vehicle and the above wind model is used. For, then, $I_b(x_0)$ contains a term $\frac{M_\alpha'}{V} v_w$, and hence $\frac{d}{dt} I_b(x_0)$ will contain a term $\frac{M_\alpha'}{V} \dot{v}_w$ where $\dot{v}_w = \dot{\bar{v}}_w + \dot{\sigma}_{v_w} w + \sigma_{v_w}$ $(\dot{h}c_3 x + c_1 \sqrt{\dot{h}} \eta)$. Thus the wind shear, $\dot{v}_w$, and the bending moment ratio contain white noise, and their standard deviations are infinite.

10

Removal of the white noise contribution from the wind shear would require construction of a different wind filter. Wind shear data for such a construction was not adequate. The white noise contribution to the bending moment rate can be removed by replacing the constant wind approximation with a distributed wind load approximation. Such an approximation was described in reference 1. Essentially the same approximation was used in this study. That is, integrals of the form

$$\int \frac{v_\omega(x, t)}{V(t)} \frac{d\tilde{t}(x, t)}{d\alpha} f(x, t) \, dx$$

were approximated by an expression of the form

$$a(t) \, x_1(t) + b(t) \, x_2(t)$$

where $a(t)$ and $b(t)$ were relatively slowly-varying time functions, and $x_1(t)$ and $x_2(t)$ satisfied

$$\dot{x}_1 = -\frac{V}{X_1} x_1 + \frac{v_\omega(t)}{X_1} \qquad (2.14)$$

$$\dot{x}_2 = \frac{-4V}{X_2} x_2 - \frac{6V}{X_2} x_3 - \frac{5}{X_2} v_\omega(t) \qquad (2.15)$$

$$\dot{x}_3 = \frac{V}{X_2} x_2 + \frac{v_\omega(t)}{X_2} \qquad (2.16)$$

The input $v_\omega(t)$ in (2.14) - (2.16) denotes the wind at the nose of the vehicle. The values of X_1 and X_2 were chosen to be 160/9 and 200/3 respectively. These values are 2/3 of the values used in the previous study, since the vehicle of that study was approximately one and one-half times as long as the Saturn V/Voyager.

The integrals in equations (2.8), (2.9), (2.10) and (2.11) for the three bending moment stations considered were approximated as

$$\int \frac{d\tilde{t}}{d\alpha} \frac{v_\omega}{V} \, dx = a_1 x_1 + a_2 x_2 \tag{2.17}$$

$$\int \frac{d\tilde{t}}{d\alpha} (x-x_{cg}) \frac{v_\omega}{V} \, dx = a_3 x_1 + a_4 x_2 \tag{2.18}$$

$$\int \frac{d\tilde{t}}{d\alpha} Y_i(x) \frac{v_\omega}{V} \, dx = a_{3+2i} x_1 + a_{4+2i} x_2 \tag{2.19}$$

$$\int \frac{d\tilde{t}}{d\alpha} [(x-x_{cg}) \gamma_1 + \gamma_2 + (x_j-x) \chi(x_j-x)] \frac{v_\omega}{V} \, dx = a_{9+2j} x_1 + a_{10+2j} x_2 \tag{2.20}$$

The derivation of the values of the $a_i(t)$ used is given in Appendix A.

State Equations (Continuous)

The quadratic theory used in this study requires that vehicle and wind filter equations be expressed as first-order vector differential equations of the form

$$\dot{x}(t) = F(t)x(t) + G_1(t)u(t) + G_2(t)\eta(t) + G_3(t) \overline{v}_\omega(t) \tag{2.21}$$

and responses to be controlled be expressed as

$$r(t) = H(t)x(t) + D_1(t)u(t) + D_2(t) \overline{v}_\omega(t) \tag{2.22}$$

To obtain the state and response equations in this form, let x be the vector $[\dot{\varphi}, \dot{z}, \dot{\eta}_1, \dot{\eta}_2, \dot{\eta}_3, \dot{z}_{s_1}, \dot{z}_{s_2}, \dot{z}_{s_3}, \varphi, z, \eta_1, \eta_2, \eta_3, z_{s_1}, z_{s_2}, z_{s_3}, \beta, \omega, x, x_1, x_2, x_3]^T$, let $u = \beta_c$, and let $r = [\beta, \dot{\beta}, IB1, \dot{IB1}, IB2, \dot{IB2}, IB3, \dot{IB3},$

12

α, $\dot{\varphi}$, $\dot{z}$, φ, $z]^T$, where IB1 = I_b (1541 in.), IB2 = I_b (2747 in.) and IB3 = I_b (3256 in.). With this notation equations (2.4) - (2.6) and (2.8) - (2.20) may be combined to yield

$$A\dot{x} = Bx + Cu + D\eta + E\overline{v}_\omega \qquad (2.23)$$

$$\widetilde{r} = H_1 x + H_2 \dot{x} + \widetilde{C}u + \widetilde{E}\overline{v}_\omega \qquad (2.24)$$

where $\widetilde{r} = [\beta, \dot{\beta}, \text{IB1}, \text{IB2}, \text{IB3}, \alpha, \dot{\varphi}, \dot{z}, \varphi, z]^T$. The coefficient matrices are displayed in Appendix B. By defining $F = A^{-1}B$, $G_1 = A^{-1}C$, $G_2 = A^{-1}E$, the state equations may be expressed in the form (2.21). It is shown in Appendix B that $H_2 A^{-1}C = H_2 A^{-1}E = 0$ so that $\widetilde{r} = (H_1 + H_2 A^{-1}B)x + \widetilde{C}u + \widetilde{E}\overline{v}_\omega$. Letting $\widetilde{H}_1 = H_1 + H_2 A^{-1}B$ and defining a matrix J such that $J\widetilde{r} = [\text{IB1}, \text{IB2}, \text{IB3}]^T$, the bending moment rates are given by

$$\frac{d}{dt}(J\widetilde{r}) = J[\dot{\widetilde{H}}_1 x + \widetilde{H}_1 A^{-1}(Bx + Cu + D\eta + E\overline{v}_\omega)]$$

It is also shown in Appendix B that $J\widetilde{H}_1 A^{-1}D = 0$, so that the response equations have the desired form of (2.22) with H(t), D_1(t) and D_2(t) appropriately defined.

The matrix manipulations required to obtain the literal elements of the coefficient matrices in (2.21) and (2.22) were too complicated to be performed. The manipulations were therefore performed with the numerical data. The numerical computatios were carried out for each multiple of 5 seconds on the interval from zero to 160 seconds. The computations associated with the state equations and a portion of the response vector, $\widetilde{r}$, were straightforward. The coefficients in the bending moment rate expressions involved the time derivative of $J\widetilde{H}_1$. These were computed using the average of first divided differences for adjacent 5-second intervals.

The end result was a set of state equations and response equations of the form (2.21) and (2.22) with the time-varying coefficients defined numerically at 5-second intervals.

State Equations (Discrete)

Difference approximations. -- For computational purposes the differential equations (2.21) were approximated by difference equations. The difference equations were derived with two constraints in mind. Both of the constraints were based on the desire to achieve reasonable computation time for the optimization program and at the same time maintain a sufficiently accurate approximation of the differential equations.

The simplest difference approximation to equation (2.21) is

$$\frac{x[(k+1)\Delta t]}{\Delta t} = \left[\frac{I}{\Delta t} + F(k\Delta t)\right] x(k\Delta t) + G_1(k\Delta t)u(k\Delta t) + G_2(k\Delta t)\eta(k\Delta t)$$

$$+ G_3(k\Delta t) \bar{v}_\omega (k\Delta t) \tag{2.25}$$

This approximation would be sufficiently accurate if Δt was chosen sufficiently small. But the computation time is inversely proportional to Δt; to reduce computation time it is desirable to choose Δt to be as large as possible. For a given value of Δt a more accurate approximation to equation (2.21) is given by the sample-data form

$$x[(k+1)\Delta t] = e^{\Delta t F(k\Delta t)} \left\{ x(k\Delta t) + F^{-1}(k\Delta t) \left[I - e^{-\Delta t F(k\Delta t)}\right] \left[G_1(k\Delta t)u(k\Delta t)\right.\right.$$

$$\left.\left. + G_2(k\Delta t)\eta(k\Delta t) + G_3(k\Delta t) \bar{v}_\omega (k\Delta t)\right]\right\} \tag{2.26}$$

This form is approximate in that the various coefficients are not constant over the Δt intervals, and the control $u(t)$ is continuous and not piecewise constant. The major disadvantage of equation (2.26) is that almost all of the elements of

14

the coefficient matrices are nonzero, whereas in equation (2.25) the majority of the elements of the coefficient matrices are zero. Computation time increases at least linearly with the number of nonzero elements. A compromise was made between these approximations by incorporating sample-data approximations for the high-frequency dynamics and the simple difference form for the low-frequency dynamics of the system.

Preliminary considerations indicated that a value of $\Delta t = 0.02$ second would yield reasonable computation time and provide sufficient accuracy. Initially, the simple difference approximation for the first sixteen scalar equations and the sample-data approximation for the last six scalar equations were implemented. Recall that the seventeenth state is gimbal deflection, the eighteenth and nineteenth are the wind states and the final three are states associated with load distribution. The accuracy of this initial set of difference equations was found not to be adequate, so sample-data approximations for the flexure modes were incorporated. This gave a satisfactory approximation for the computation of an optimal controller.

The time-varying coefficients were obtained by linear interpolation between the 5-second data points.

The gimbal actuator. -- It was shown in reference 1 that the results of optimization are not dependent on the particular first-order dynamics assumed for the actuator in the continuous case. If the simple difference approximation to the actuator equation is used, this result carries over to the discrete case. With $\Delta t = 0.02$, the simple difference approximation to the actuator equation (2.5) was not adequate, so the sample-data approximation was used. In this case the optimization results are dependent on the actuator dynamics, and hence the controller obtained should truly be considered a sampled-data controller.

SECTION III
OPTIMIZATION: MATHEMATICAL FORMULATION

The formulation of the load-relief problem as a stochastic minimization problem and the equivalent quadratic method for its solution presented in reference 1 are briefly summarized in this section.

Formulation

The load-relief problem is essentially one of ensuring that missile response are within prescribed limits. Some of the limits must be met throughout the booster flight, $0 < t < T$ and the others must be met only at burnout, $t = T$. For a given wind input let $r_i(t)$, $i = 1, 2, \ldots, m_1$, be the deviations from the ideal values of the booster responses which are to meet constraints at $t = T$, and let $r_i(t)$, $i = m_1 + 1, \ldots, m_2$, be the deviations from the ideal values of the responses which are to meet constraints on $0 < t < T$. Let γ_i, $i = 1, 2, \ldots, m_1$, be positive constants and let $\gamma_i(t)$, $i = m_1 + 1, \ldots, m_2$, be positive functions defined on $0 < t < T$ such that γ_i represents the prescribed limit for r_i. Let a_i denote the event

$$|r_i(T)| < \gamma_i \tag{3.1}$$

and $\overline{a}_i$ denote the event

$$|r_i(T)| \geq \gamma_i \tag{3.2}$$

for $i = 1, 2, \ldots, m_1$. Let $b_i(j)$, $i = m_1 + 1, \ldots, m_2$, denote the event that the condition

$$|r_i(t)| = \gamma_i \text{ and } \frac{d}{dt} [r_i(t)]^2 > 0 \tag{3.3}$$

is met exactly j times in the interval $0 \leq t \leq T$. Then the event of mission success is the event that all of the events a_1, a_2, ..., a_{m_1}, $b_{m_1+1}(0)$, ...,

$b_{m_2}(0)$ occur. The probability of mission success is the joint probability $P[a_1, \ldots, a_{m_1}, b_{m_1+1}(0), \ldots, b_{m_2}(0)]$, and the probability of mission failure which we shall denote by J is

$$J = 1 - P[a_1, \ldots, a_{m_1}, b_{m_1+1}(0), \ldots, b_{m_2}(0)] \qquad (3.4)$$

Minimizing J would be a meaningful basis for control design, but no analytical expression for J is known, even for Gaussian processes.

It is proven in reference 1 that

$$J^* = \sum_{i=1}^{m_2} P(\overline{a}_i) + \sum_{i=m_1+1}^{m_2} E\left\{N_i\right\} \qquad (3.5)$$

is an upper bound for J, (i.e., $J^* \geq J$), where $E\left\{N_i\right\}$ is the expected number of occasions that $r_i(t)$ exceeds its limit in the interval $[0, T]$, i.e.

$$E\left\{N_i\right\} = \sum_{j=0}^{\infty} j \, P[b_i(j)] \qquad (3.6)$$

Analytical expressions for $P(\overline{a}_i)$ and $E\left\{N_i\right\}$ are derived in reference 1 under the assumption that the response $r_i(t)$ are nonstationary Gaussian processes. The functional, J^*, is chosen as the performance index to be minimized and the control $u(t)$ is required to be a linear transformation of measured responses $m(t)$. Thus the optimal control problem is:

Given the system described by equations (2.21) and (2.22), find the linear controller (the linear transformation of measured responses) that minimizes J^*.

The linear transformation of measured responses may be restricted as desired to include only current responses, present and past responses, or only past responses, and by defining the particular measurements available. For all formulations where the present state can be completely measured, the optimal linear transformation can be reduced to

17

$$u = K(t)x(t) \tag{3.7}$$

in which case one can search for $K(t)$ directly.

Method of Solution

The functional $J*$ to be minimized may be written in the form

$$J* = f_1[S(T), R(T)] + \int_0^T f_2[S(t), R(t)] \, dt \tag{3.8}$$

where $S(t)$ is the response covariance matrix defined by

$$S(t) = E\left\{ [r(t) - \bar{r}(t)] [r(t) - \bar{r}(t)]' \right\} \tag{3.9}$$

$R(t)$ is the mean-response product matrix defined by

$$R(t) = \bar{r}(t) [\bar{r}(t)]' \tag{3.10}$$

and $\bar{r}(t)$ is the vector of mean responses defined by

$$\bar{r}(t) = E\left\{ r(t) \right\} \tag{3.11}$$

The prime as a superscript indicates transposition; i.e., x' = the transpose of x.

The method for solving the optimization problem involves iteratively solving optimization problems with performance functionals which are quadratic in $S(t)$ and $R(t)$ of the form

$$J** = TR\left\{ Q(T)S(T) + V(T)R(T) + \int_0^T [Q(t)S(t) + V(t)R(t)]dt \right\} \tag{3.12}$$

18

where TR indicates the trace and Q and V are non-negative definite symmetric matrices. The aim of the iterations is to obtain such Q and V matrices that minimizing J** is equivalent to minimizing J* in the sense that the same linear control minimizes each functional. A necessary condition for this equivalence is that

$$Q(T) = \frac{\partial f_1}{\partial S}, \quad V(T) = \frac{\partial f_1}{\partial R}, \quad Q(t) = \frac{\partial f_2}{\partial S}, \quad V(t) = \frac{\partial f_2}{\partial R} \tag{3.13}$$

where the partial derivatives are evaluated at S_o and R_o, the response covariance and mean-response product matrices produced by the optimal controller for J**.

An iteration procedure to attain the condition (3.13) is:

(a) Choose values for Q and V

(b) Find the minimizing control for J** by application of the quadratic theories

(c) Compute the corresponding R and S matrices

(d) Compute the matrices $\frac{\partial f}{\partial S}$ and $\frac{\partial f}{\partial R}$ and compare with the chosen Q and V matrices

(e) Rechoose Q and V and repeat (b), (c) and (d) until the condition (3.13) is satisfied

This iterative process was not completely automated in that the choice of new Q and V matrices was based on the response behavior previously obtained as well as the error in satisfying condition (3.13).

A major simplification which was found to be satisfactory in the previous study reported in reference 1 was incorporated in this study. This simplification consisted of setting

$$V(t) = Q(t), \quad 0 \leq t \leq T \tag{3.14}$$

Satisfactory mean responses were obtained and no attempt was made to match V to $\partial f / \partial R$.

The Quadratic Problem

The iteration procedure described above involves the solution of a quadratic problem. The solution of this problem as given in Appendix G of reference 1 for the difference equation formulation is presented below.

Suppose the system is given as

$$x(n+1) = A(n)x(n) + B_1 u(n) + B_2 \bar{v}_w(n) + B_3(n)\eta(n)$$

$$r(n) = H_1(n)x(n) + D_1(n)u(n) + D_2(n)\bar{v}_w(n)$$

$$m(n) = H_2(n)x(n) + \xi(n)$$

where m(n) is a vector of sensor outputs, and $\xi(n)$ is a white noise input

$$E\left\{\eta(i)\eta(j)'\right\} = (\Delta t)^{-1} W_1(i)\delta_{ij}$$

$$E\left\{\xi(i)\xi(j)'\right\} = (\Delta t)^{-1} W_2(i)\delta_{ij}$$

$$E\left\{\eta(i)\xi(j)'\right\} = (\Delta t)^{-1} W_3(i)\delta_{ij}$$

$$\delta_{ii} = 1, \quad \delta_{ij} = 0 \text{ if } i \neq j$$

$$E\left\{x(0)\right\} = \bar{x}(0), \quad E\left\{[x(0) - \bar{x}(0)][x(0) - \bar{x}(0)]'\right\} = X(0)$$

and $N = (\Delta t)^{-1} T$ and the common (incomplete) notation suppressing Δt in the arguments is used. The optimization problem is to find the linear transformation of present and past measured responses

$$u(n) = \sum_{i=o}^{n} L(n, i) \, m(i)$$

that minimizes the quadratic functional

$$J** = TR\left\{Q(N)[S(N) + R(N)] + \sum_{n=0}^{N-1} \Delta t \, Q(n)[S(n) + R(n)]\right\}$$

where $R(n) = \bar{r}(n) \, \bar{r}(n)'$, $\bar{r}(n) = E\{r(n)\}$ and $S(n) = E\left\{[r(n) - \bar{r}(n)][r(n) - \bar{r}(n)]'\right\}$.
Assuming that $Q(n)$ is symmetric and non-negative definite for $n = 0, 1, \ldots$,
N, and $[D_1(n)]' Q(n) D_1(n)$ is positive for $n < N$ and $Q(N) D_1(N) = 0$ (all true in
the present problem), the solution is

$$u(n) = K(n)\hat{x}(n) + f(n)$$

where $\hat{x}(n)$ is the conditional estimate of the state

$$\hat{x}(n) = E\left\{x(n)\,|\,m(0), \ldots, m(n), u(0), \ldots, u(n-1), \bar{v}_{\omega}(0), \ldots, \bar{v}_{\omega}(n-1)\right\}$$

and $K(n)$ and $f(n)$ satisfy

$$K(n) = -[B_1'P(n+1)B_1 + \Delta t D_1(n)'Q(n)D_1(n)]^{-1} \lceil B_1'P(n+1)A(n)$$

$$+\Delta t D_1(n)'Q(n)H_1(n)]$$

$$f(n) = -[B_1'P(n+1)B_1 + \Delta t D_1(n)'Q(n)D_1(n)]^{-1} \left\{B_1'[g(n+1)\right.$$

$$\left.+P(n+1)B_2\bar{v}_{\omega}(n)] + \Delta t D_1(n)'Q(n)D_2(n)\bar{v}_{\omega}(n)\right\}$$

$$P(n) = [A(n)+B_1K(n)]'P(n+1)[A(n)+B_1K(n)] + \Delta t[H_1(n)$$

$$+D_1(n)K(n)]'Q(n)\lceil H_1(n)+D_1(n)K(n)]$$

$$g(n) = [A(n)+B_1K(n)]'g(n+1) + P(n+1)[B_1f(n)+B_2\bar{v}_{\omega}(n)]$$

$$+\Delta t[H_1(n)+D_1(n)K(n)]'Q(n)[D_2(n)\bar{v}_{\omega}(n)+D_1(n)f(n)]$$

with $P(N) = H_1(N)'Q(N)H_1(N)$ and $g(N) = H_1(N)'Q(N)D_2(N)\bar{v}_{(1)}(N)$. The solution to the state estimation problem is

$$\hat{x}(n) - \bar{x}(n) = \tilde{x}(n)$$

$$\tilde{x}(n+1) = [A(n) - L(n) H_2(n)]\tilde{x}(n) + L(n)m(n)$$

$$\bar{x}(n+1) = [A(n) + B_1(n)K(n)]\bar{x}(n) + B_2(n)\bar{v}_w(n) + B_1(n)f(n)$$

where $\bar{x}(n)$ is the a priori mean state, $\bar{x}(n) = E\{x(n)\}$, and $L(n)$ satisfies

$$\Delta t L(n) = [A(n)\hat{P}(n)H_2(n)'\Delta t + B_3(n)W_3(n)][H_2(n)\hat{P}(n)H_2(n)'\Delta t + W_2(n)]^{-1}$$

$$\hat{P}(n+1) = A(n)\hat{P}(n)A(n)' + (\Delta t)^{-1}B_3(n)W_1(n)B_3(n)'$$
$$- \Delta t L(n) [H_2(n)\hat{P}(n)H_2(n)'\Delta t + W_2(n)]L(n)'$$

with $\hat{P}(0) = X(0)$. The matrix $\hat{P}(n)$ is the covariance matrix of the estimation error, $x(n) - \hat{x}(n)$. This completes the description of the solution to the minimization problem.*

The state covariance matrix

$$X(n) = E\{[x(n) - \bar{x}(n)] [x(n) - \bar{x}(n)]'\}$$

satisfies the difference equation

$$X(n+1) = [A(n)+B_1K(n)] [X(n) - \hat{P}(n)] [A(n)+B_1K(n)]'$$
$$+ A(n)\hat{P}(n)A(n)' + (\Delta t)^{-1}B_3(n)W_1(n)B_3(n)'$$

---

*As discussed in Section IV, the $L(n)$ and $\hat{P}(n+1)$ equations may be simplified considerably from the form presented here when current values of portions of the state $x(t)$ can be measured perfectly.

The response covariance matrix, $S(n) = E\left\{[r(n) - \bar{r}(n)][r(n) - \bar{r}(n)]'\right\}$, may be obtained as follows:

$$r(n) - \bar{r}(n) = H_1(n)[x(n)-\bar{x}(n)] + D_1(n)K(n)[\hat{x}(n)-\bar{x}(n)]$$

$$= [H_1(n)+D_1(n)K(n)][x(n)-\bar{x}(n)] - D_1(n)K(n)[x(n)-\hat{x}(n)]$$

$$S(n) = [H_1(n)+D_1(n)K(n)]X(n)[H_1(n)+D_1(n)K(n)]'$$

$$+D_1(n)K(n)\hat{P}(n)K'(n)D_1'(n) - [H_1(n)+D_1(n)K(n)] E\left\{[x(n)\right.$$

$$\left. - \bar{x}(n)][x(n)-\hat{x}(n)]'\right\} K'(n)D_1'(n) - D_1(n)K(n) E\left\{[x(n)\right.$$

$$\left. - \hat{x}(n)][x(n)-\bar{x}(n)]'\right\}[H_1(n)+D_1(n)K(n)]'$$

$$= [H_1(n)+D_1(n)K(n)] X(n) [H_1(n)+D_1(n)K(n)]'$$

$$+ D_1(n)K(n)\hat{P}(n)K'(n)D_1'(n) - [H_1(n)+D_1(n)K(n)]\hat{P}(n)K'(n)D_1'(n)$$

$$- D_1(n)K(n)\hat{P}(n) [H_1(n)+D_1(n)K(n)]'$$

$$= [H_1(n)+D_1(n)K(n)][X(n)-\hat{P}(n)][H_1(n)+D_1(n)K(n)]'$$

$$+ H_1(n)\hat{P}(n)H_1'(n)$$

For the special case in which it is assumed that the complete state can be measured exactly, $m(n) = x(n)$ and the above results are simplified since $\hat{x}(n) = x(n)$ and $\hat{P}(n) = 0$.

SECTION IV
SENSOR CHOICE AND CONTROLLER SIMPLIFICATION

Optimization with complete measurement capability provides a very good controller with respect to performance, but complete measurement of the state is generally impractical and often impossible. Thus the optimal control with complete measurement capability is a standard for comparison of controller

performance. It also serves as a starting point for the synthesis of a practical controller and may contain information which can be used to select the best sensor complement for controller performance from a set of possible sensor complements.

The sensor choice and controller simplification problems, the general relationships concerning practicable controllers, the analytical measures of quality of sensor complements developed, the controller simplification analyses performed, and the simplified controller designed in the study are described in this section. The numerical results pertaining to these topics are presented together with the numerical results obtained during optimization in Section V, and the overall conclusions are given in Section VI.

Two analytical measures of quality of sensor complements were developed which were based on the optimal controller with complete measurement capability. These measures of quality did not prove to be satisfactory when applied to the study vehicle with controller A. The major cause of the inadequacy of these measures of quality was attributed to the fact that they fail to properly emphasize the states which are significant feedbacks. Thus, the investigation of controller simplification focused on determining the significant degrees of freedom as a means of identifying the states which would have to be measured and/or estimated. This investigation indicated that for controller A the states associated with the load-distribution and wind filter were significant, but the drift and states associated with fuel sloshing were not significant. Incorporating the wind and load-distribution states in the controller required the synthesis of an estimator. Such an estimator is described at the end of this section.

General Considerations

The fundamental goal of this study was the development of analytical techniques which make practicable the design of controllers for launch vehicles by application of optimal control theory. There were several approaches which

could be taken to reach this goal. The approach chosen for this study was to use optimal control theory to find the optimal linear controller with no constraints on the available feedback signals or simplicity of the controller. If necessary, fictitious sensors were assumed to exist. Then it was intended to develop a technique, which utilized the optimal controller, to find the best sensor complement from a set of such complements in terms of controller capability for linear controllers constrained to feedback only the outputs from the sensor complements and signals obtained from simple filters used in conjunction with the sensor complements. This second stage of the approach was called the sensor choice and controller simplification problem.

The optimal controller, assuming complete measurement capability, may be written as

$$u(x, t) = K^O(t)x + f^O(t) \tag{4.1}$$

where $u(x, t)$ is the input to the actuator, $K^O(t)$ is a gain (row) vector, and $f^O(t)$ is a deterministic input. Given any sensor complement, the sensor outputs can be arranged as a measurement (column) vector, $m(t)$ which may be written as

$$m(x, t) = M(t)x \tag{4.2}$$

where the dimension of $m(t)$ and the values of the elements of the matrix $M(t)$ depend upon the given sensor complement. A controller consisting of a deterministic input plus linear feedback of the measurement vector may be expressed as

$$u(x, t) = K(t)M(t)x + f(t) \tag{4.3}$$

where $K(t)$ is a gain (row) vector, the dimension of $K(t)$ being the same as the dimension of $m(t)$.

If for some sensor complement it is the case that $K^O(t)$ can be written as a linear combination of the rows of $M(t)$, then the controller given by equation (4.3) can be made to be identical to the optimal controller given by equation (4.1) by choosing $f(t) = f^O(t)$ and $K(t)$ properly. Thus, it is appropriate to consider the general properties of a measurement vector or sensor complement in terms of the algebraic properties of the corresponding matrix $M(t)$.

Consider a sensor complement consisting of outputs of linear accelerometers, angular accelerometers, integrals of the angular accelerometer signals, integrals of linear combinations of the linear accelerometer signals and integrals of the angular accelerometer signals, and a measurement of gimbal angle. Two general statements can be made concerning such a sensor complement. The first is that the columns of the associated matrix, $M(t)$, corresponding to the wind state w, the wind-shear state x, and the internal load-distribution state x_3 are zero; that is, these states are not directly measurable. The second is that if the complement includes angular accelerometers located at three distinct stations along the vehicle and linear accelerometers located at two of these stations, then generally, assuming knowledge of the mode shapes and center of gravity, the states associated with rigid-body and flexure degrees of freedom can be independently measured, and inclusion of integrals of other accelerometer outputs is redundant. These results may be obtained as follows:

The output of a lateral accelerometer located at x_A is given by

$$\ddot{r}_A = \ddot{z} + (x_A - x_{cg}) \ddot{\varphi} + \sum_{i=1}^{3} Y_i(x_A) \ddot{\eta}_i - [(T-D)/M][\varphi + \sum_{i=1}^{3} Y_i'(x_A) \eta_i] \quad (4.4)$$

and the output of an angular accelerometer located at x_A is given by

$$\ddot{\varphi}_A = \ddot{\varphi} + \sum_{i=1}^{3} Y_i'(x_A) \ddot{\eta}_i \quad (4.5)$$

From equation (2.23) and the explicit form of the B matrix displayed in Appendix B it can be observed that the states, w, x and x_3, do not enter into

26

the $\ddot{z}$, $\ddot{\varphi}$, and $\ddot{\eta}_i$ equations. Let m_1, m_2, and m_3 denote the integrals of the outputs of angular accelerometers at stations x_{A1}, x_{A2}, and x_{A3} respectively. Let m_{i+5} denote the integral of m_i for $i = 1$, 2, 3. For $i = 4$, 5 let m_i denote the integral of the sum of the output of a lateral accelerometer at station $x_{A(i-2)}$ and $[(T-D)/M]m_{i+3}$. Then

$$
\begin{bmatrix} m_1 \\ m_2 \\ m_3 \\ m_4 \\ m_5 \end{bmatrix} = \begin{bmatrix} 1 & 0 & Y_1'(x_{A1}) & Y_2'(x_{A1}) & Y_3'(x_{A1}) \\ 1 & 0 & Y_1'(x_{A2}) & Y_2'(x_{A2}) & Y_3'(x_{A2}) \\ 1 & 0 & Y_1'(x_{A3}) & Y_2'(x_{A3}) & Y_3'(x_{A3}) \\ x_{A2}-x_{cg} & 1 & Y_1(x_{A2}) & Y_2(x_{A2}) & Y_3(x_{A2}) \\ x_{A3}-x_{cg} & 1 & Y_1(x_{A3}) & Y_2(x_{A3}) & Y_3(x_{A3}) \end{bmatrix} \begin{bmatrix} \dot{\varphi} \\ \dot{z} \\ \dot{\eta}_1 \\ \dot{\eta}_2 \\ \dot{\eta}_3 \end{bmatrix} \qquad (4.6)
$$

The coefficient matrix in equation (4.6) is generally nonsingular, and hence the components $\dot{\varphi}$, $\dot{z}$, $\dot{\eta}_i$, of the state vector may be obtained from the signals m_1, m_2, m_3, m_4, and m_5 assuming knowledge of the mode shape, axial acceleration $= (T-D)/M$, and the center of gravity. For the study vehicle the coefficient matrix in equation (4.6) is nonsingular for $t > 0$ with x_{A1}, x_{A2} and x_{A3} taken to be stations 1541, 2686 and 3240 inches respectively. Knowing the components, $\dot{\varphi}$, $\dot{z}$, $\dot{\eta}_i$ of the state vector, their integrals φ, z, η_i may be obtained. Thus, in this case all states except those associated with fuel sloshing, the wind filter, and the load distribution can be measured directly.

If a lateral accelerometer located at station x_{A1} is added to the above sensor complement it is redundant in that the sum of the integral of this output and $[(T-D)/M]m_6$ is linearly dependent on m_1, m_2, m_3, m_4 and m_5.

This algebraic analysis shows that complete measurement of the state is not possible and hence that there is no hope of matching the controller of equation (4.3) to that of equation (4.1) if the states that cannot be measured significantly contribute to the optimal controller. This suggests that the following approach to the fundamental goal might have been more profitable.

Solve the optimal control problem with the controller constrained to utilize only directly measurable states and estimates of those states which cannot be measured directly. Then, with this controller as a starting point, the sensor choice and controller simplification problems could be treated. There is additional complexity in this approach since solving the associated optimal control problem involves the iterative solution of a two-point boundary value problem within each iteration of weight adjustment to attain quadratic equivalence. However, it is felt that this approach holds promise because the controller upon which the simplification is based would have a behavior more closely related to the controllers utilizing realizable sensor complements.

This difference in behavior between the optimal controller with complete measurement and the optimal controller with partial measurement is believed to be the cause of the inadequacy of the first measure of quality described below.

Analytical Measures of Quality

The first measure of quality is based on an approximation to the optimal controller with a specified set of observation vectors. The approximation consists of replacing the Riccati and state covariance matrices for the fixed-form control problem, described below, by the corresponding matrices for the control problem with complete measurement.

The second measure of quality is based on the following observation. The optimal control input is a deterministic input plus the scalar product of the gain vector times the state vector. A sensor output is the scalar product of an observation vector times the state vector. If the gain vector lies in the subspace spanned by the observation vectors associated with some sensor complement, then the optimal controller may be attained with that sensor complement. Thus a measure of quality may be defined in terms of the accuracy of approximating the optimal gain vector by a linear combination of observation vectors.

<u>The first measure of quality.</u> -- The vehicle equations of motion are assumed to be in the form

$$\dot{x}(t) = F(t)x(t) + G_1(t)u(t) + G_2(t)\eta(t) + G_3(t)\bar{v}_\omega(t) \tag{4.7}$$

$$r(t) = H(t)x(t) + D_1(t)u(t) + D_2(t)\bar{v}_\omega(t) \tag{4.8}$$

$$m(t) = M(t)x(t) \tag{4.9}$$

where x(t) denotes the state vector, r(t) denotes the response vector, u(t) denotes the scalar control input, $\eta(t)$ denotes a scalar Gaussian white noise input, $\bar{v}_\omega(t)$ denotes the scalar mean wind input and m(t) denotes the vector of sensor outputs. In the following discussion the dependence on t will be suppressed, and it will be assumed that $\bar{v}_\omega = 0$.

The control problem can be formulated as the following fixed-form optimization problem. Choose the (row) vector K such that with u = K Mx the functional

$$J(M, K) = TR[Q(T)S(T)] + \int_o^T TR[Q(t)S(t)]dt \tag{4.10}$$

is minimized, where TR(QS) indicates the trace of the matrix QS and S is the response covariance matrix. In this formulation the matrix M denotes the observation matrix. The values of the elements and the rank of M depend on the sensor complement chosen. Complete measurement capability is equivalent to M being nonsingular (the number of measurements m would equal the dimension of x) in which case, without loss of generality, M may be assumed to be the identity. The positive semidefinite matrix, Q, is assumed to be independent of M.

Assuming $D_1'QD_1$ to be nonsingular for $0 \leq t < T$, the solution to the optimization problem is*

---

*This solution is derived in Appendix C.

$$K = -(D_1'QD_1)^{-1} [D_1'QH - G_1'P] XM' (MXM')^{-1} \qquad (4.11)$$

$$-\dot{P} = (F + G_1KM)' P + P(F + G_1KM) + (H + D_1KM)' Q(H + D_1KM) \qquad (4.12)$$

$$\dot{X} = (F + G_1KM)X + X(F + G_1KM)' + G_2NG_2' \qquad (4.13)$$

$$P(T) = H'(T) Q(T) H(T), \; X(0) \text{ given} \qquad (4.14)$$

where X is the state covariance matrix and N is the variance of η.

It may be seen from the above equations that, if M is nonsingular, the solution is independent of X. If the rank of M is less than the dimension of x, however, the solution depends on X and involves a two-point boundary value problem.* Thus the simplest problem to solve is the one in which M is non-singular. Furthermore, defining $J[M, K_o(M)]$ to be

$$J[M, K_o(M)] = \min_K J(M, K) \qquad (4.15)$$

the minimum value of $J[M, K_o(M)]$ is obtained with M nonsingular. Solving the problem with M taken to be the identity provides ideal values of $J[M, K_o(M)]$, K, P, X, and S, which will be denoted by J^o, K^o, P^o, X^o, and S^o.

Let the gain vector, K*, be defined as

$$K* = -(D_1'QD_1)^{-1} [D_1'QG + G_1'P^o]X^oM'(MX^oM')^{-1}$$

$$= K^oX^oM'(MX^oM')^{-1} \qquad (4.16)$$

Then the measure of quality of the sensor complement corresponding to the observation matrix M is defined to be $J(M, K*)$. This measure of quality is an

---

*In the case where the rank of M is less than the dimension of x, the solution may be expressed in the form $u(t, x(t)) = L(t)\hat{x}(t)$ where L(t) is a linear time-varying row vector and $\hat{x}(t)$ is the least-mean-square-error estimate of x(t). This assertion is proved in Appendix C.

approximation to the exact measure of quality of the sensor complement $J[M, K_o(M)]$. It is difficult to estimate the accuracy of the approximation, but clearly the relation $J(M, K*) \geq J[M, K_o(M)] \geq J^o$ holds. Also, if M is nonsingular, then $J(M, K*) = J^o$. It was conjectured that the approximation would be adequate for comparing the quality of different sensor complements. However, as described below and shown in Section V, this did not prove to be the case for the study vehicle.

A very simple example for which analytical solutions may be obtained is presented to demonstrate the nature of the measure of quality defined above.

The state and response vectors are assumed to be two-dimensional, the system is assumed to be autonomous, and the performance functional is assumed to be the integral over the infinite interval of $r'Qr$. Specifically, consider the system represented by:

$$ F = \begin{bmatrix} 0 & 1 \\ 0 & 0 \end{bmatrix} \;,\; G_1 = D_1 = \begin{bmatrix} 0 \\ 1 \end{bmatrix} \;,\; G_2 = \begin{bmatrix} 1 \\ 1 \end{bmatrix} \;, $$

$$ H = \begin{bmatrix} 1 & 0 \\ 1 & 1 \end{bmatrix} \;,\; N = 1,\; Q = \begin{bmatrix} 5.25 & 0 \\ 0 & 1 \end{bmatrix} . $$

$$ J = \int_o^\infty TR[Q(t)S(t)]\, dt = \int_o^\infty TR[Q(H+D_1KM)\, X(t)\, (H+D_1KM)']dt $$

For this example the equations defining the optimal control are

$$ K = -[1 + p_{12},\; 1 + p_{22}]\, XM'(MXM')^{-1} $$

$$ 0 = (F+G_1KM)'\, P + P(F+G_1KM) + (H+D_1KM)'\, Q(H+D_1KM) $$

$$ 0 = (F+G_1KM)X + X(F+G_1KM)' + \begin{bmatrix} 1 & 1 \\ 1 & 1 \end{bmatrix} $$

Taking M to be the identity yields

$$[K_1{}^o, K_2{}^o] = -[1 + p_{12}{}^o, \ 1 + p_{22}{}^o]$$

$$\begin{bmatrix} 0 & 0 \\ 0 & 0 \end{bmatrix} = \begin{bmatrix} 0 & K_1{}^o \\ 1 & K_2{}^o \end{bmatrix} \begin{bmatrix} p_{11}{}^o & p_{12}{}^o \\ p_{12}{}^o & p_{22}{}^o \end{bmatrix} + \begin{bmatrix} p_{11}{}^o & p_{12}{}^o \\ p_{12}{}^o & p_{22}{}^o \end{bmatrix} \begin{bmatrix} 0 & 1 \\ K_1{}^o & K_2{}^o \end{bmatrix}$$

$$+ \begin{bmatrix} 1 & 1+K_1{}^o \\ 0 & 1+K_2{}^o \end{bmatrix} \begin{bmatrix} 5.25 & 0 \\ 0 & 1 \end{bmatrix} \begin{bmatrix} 1 & 0 \\ 1+K_1{}^o & 1+K_2{}^o \end{bmatrix}$$

$$\begin{bmatrix} 0 & 0 \\ 0 & 0 \end{bmatrix} = \begin{bmatrix} 0 & 1 \\ K_1{}^o & K_2{}^o \end{bmatrix} \begin{bmatrix} x_{11}{}^o & x_{12}{}^o \\ x_{12}{}^o & x_{22}{}^o \end{bmatrix} + \begin{bmatrix} x_{11}{}^o & x_{12}{}^o \\ x_{12}{}^o & x_{22}{}^o \end{bmatrix} \begin{bmatrix} 0 & K_1{}^o \\ 1 & K_2{}^o \end{bmatrix} + \begin{bmatrix} 1 & 1 \\ 1 & 1 \end{bmatrix} .$$

The solution to these equations is

$$p_{11}{}^o = 4, \quad p_{12}{}^o = 1.5, \quad p_{22}{}^o = 1, \quad x_{11}{}^o = 1.15, \quad x_{12}{}^o = -0.5, \quad x_{22}{}^o = 0.875$$

$$K_1{}^o = -2.5, \quad K_2{}^o = -2$$

and the corresponding value of J is $J^o = 8$, and the corresponding S is

$$S^o = \begin{bmatrix} 1.15 & -1.225 \\ -1.225 & 1.9625 \end{bmatrix}$$

Now consider the case in which $M = [m_1, \ m_2]$ and K is a scalar. Then the equations defining the optimal control are

$$K = \frac{-[1+p_{12}, \ 1+p_{22}][m_1 x_{11} + m_2 x_{12}, \ m_1 x_{12} + m_2 x_{22}]'}{m_1{}^2 x_{11} + 2 m_1 m_2 x_{12} + m_2{}^2 x_{22}}$$

32

$$\begin{bmatrix} 0 & 0 \\ 0 & 0 \end{bmatrix} = \begin{bmatrix} 0 & m_1K \\ 1 & m_2K \end{bmatrix} \begin{bmatrix} p_{11} & p_{12} \\ p_{12} & p_{22} \end{bmatrix} + \begin{bmatrix} p_{11} & p_{12} \\ p_{12} & p_{22} \end{bmatrix} \begin{bmatrix} 0 & 0 \\ m_1K & m_2K \end{bmatrix}$$

$$+ \begin{bmatrix} 1 & 1+m_1K \\ 0 & 1+m_2K \end{bmatrix} \begin{bmatrix} 5.25 & 0 \\ 0 & 1 \end{bmatrix} \begin{bmatrix} 1 & 0 \\ 1+m_1K & 1+m_2K \end{bmatrix}$$

$$\begin{bmatrix} 0 & 0 \\ 0 & 0 \end{bmatrix} = \begin{bmatrix} 0 & 1 \\ m_1K & m_2K \end{bmatrix} \begin{bmatrix} x_{11} & x_{12} \\ x_{12} & x_{22} \end{bmatrix} + \begin{bmatrix} x_{11} & x_{12} \\ x_{12} & x_{22} \end{bmatrix} \begin{bmatrix} 0 & m_1K \\ 1 & m_2K \end{bmatrix} + \begin{bmatrix} 1 & 1 \\ 1 & 1 \end{bmatrix}$$

The solution to these equations is

$$p_{11} = \frac{-\left[8m_1m_2K + 25(m_1 - m_2^2K) + 4m_1^2K(1+m_1K)\right]}{8m_1m_2K}$$

$$p_{12} = \frac{-\left[8m_1K + 25 + 4m_1^2K^2\right]}{8m_1K}$$

$$p_{22} = \frac{-\left[8m_1m_2K^2 - 25 + 4m_1K(m_2^2K^2 - 1 - m_1K)\right]}{8m_1m_2K^2}$$

$$x_{11} = \frac{-\left[2m_2K - 1 + m_1K - m_2^2K^2\right]}{2m_1m_2K^2}$$

$$x_{12} = -\frac{1}{2}, \quad x_{22} = \frac{m_1K - 1}{2m_2K}$$

with $K_o(M)$ a real root of the equation

$$4m_1(m_1 + m_2)^2K^3 - (21m_1 + 50m_2)K + 50 = 0$$

Thus to obtain the exact solution it is necessary to solve for the real root of the above cubic equation.

The value of K* is readily obtained, in the case being considered, as

$$K^* = [-2.5, -2] \, X^0 \begin{bmatrix} m_1 \\ m_2 \end{bmatrix} \, (m_1^2 x_{11}^0 + 2m_1 m_2 x_{12}^0 + m_2^2 x_{22}^0)^{-1}$$

$$= \frac{-1.875m_1 - 0.5m_2}{1.15m_1^2 - m_1 m_2 + 0.875m_2^2}$$

Then $J(M, K^*)$ may be computed for any (m_1, m_2) by evaluating K^* and the expression

$$J(M, K^*) = \left[\frac{21}{4} + (1 + m_1 K^*)^2 \right] \left(\frac{1 + m_2^2 K^{*2} - 2m_2 K^* - m_1 K^*}{2m_1 m_2 K^{*2}} \right)$$

$$- 1 - m_1 K^* - m_2 K^* - m_1 m_2 K^{*2} + (1 + m_2 K^*)^2 \, \frac{m_1 K^* - 1}{2m_2 K^*}$$

For $m_1 = 5$ and $m_2 = 4$, $K^* = \frac{-11.325}{22.75} = -\frac{1}{2}$ and $J(M, K^*) = 8$. Of course, in this case $m_1 K^*$ and $m_2 K^* = K_2^0$ so that $X = X^0$ and $S = S^0$.

Numerical results were obtained for the following three other cases:

Case I: $m_1 = m_2 = 1$

Case II: $m_1 = 3$, $m_2 = 4$

Case III: $m_1 = 1$, $m_2 = 0.633$.

For this example the observation matrix M is essentially a function of only one parameter, which may be taken to be $\theta = \tan^{-1}(m_2/m_1)$. The optimal θ is $\theta^0 = \tan^{-1}(0.8)$. Case I corresponds to $\theta_I = \tan^{-1}(1)$ and Case III was chosen

34

to correspond to $\theta_{III} = \theta^O - (\theta_I - \theta^O)$. Case II corresponds to $\theta_{II} = \tan^{-1}(4/3) > \theta_I > \theta^O$. The results are as follows:

Case	K*	J(M, K*)	K_{opt}	$J[M, K_O(M)]$
I	-2.32	8.18	-2.40	8.16
II	-0.617	9.07	-0.75	8.74
III	-2.53	8.21	-2.60	8.17

These results indicate that J(M, K*) is a good approximation of $J[M, K_O(M)]$ if the observation vector (m_1, m_2) is near the optimal observation vector (5, 4) in the sense that $|\theta - \theta_O|$ is small. Furthermore, the measure of quality J(M, K*) properly distinguishes the quality of observation for control.

The second measure of quality. -- The feedback gains of the optimal controller with complete measurement are conveniently represented as a time-varying vector $K^O(t)$. If a sensor complement with observation matrix M(t) has the property that there exists a vector, K(t), such that

$$K(t) \, M(t) = K^O(t) \tag{4.17}$$

Then this sensor complement is equivalent in terms of control performance to complete measurement. In general, sensor complements are of such a nature that equation (4.17) cannot be satisfied for any K(t). Thus a mathematically appealing measure of quality of a sensor complement is the minimum error that can be achieved with the given sensor complement in satisfying equation (4.17). Of course there are many ways of defining the error, and one such definition is the weighted least-square-error,

$$E[K(t)] = [K(t)M(t) - K^O(t)] \, W(t) \, [K(t)M(t) - K^O(t)]' \tag{4.18}$$

where W(t) is a non-negative definite symmetric matrix. With this type of error definition it is a simple matter to compute the measure of quality

$$J_{W(t)}[M(t)] = [\hat{K}(t;W, M)M(t) - K^O(t)]W(t)[\hat{K}(t;W, M)M(t) - K^O(t)]' \tag{4.19}$$

where

$$\hat{K}(t;W, M) = K^O(t)W(t)M'(t) [M(t)W(t)M'(t)]^{-1} \qquad (4.20)$$

and it is assumed that W(t) is chosen so that (MWM') is nonsingular. This measure of quality has the attribute of ease of computation. Its major deficiency is that it is an indirect measure of controller performance. Hence this measure of quality can be used only to discern gross differences in sensor complements.

A sensor complement consisting of linear accelerometers, angular accelerometers, and rate gyros located at stations 1541 and 2686 inches, an angular accelerometer, a rate gyro, an attitude gyro and the integral of a linear accelerometer located at station 3240 inches, and the gimbal-angle pickoff was chosen to evaluate the acceptability of the measures of quality defined above. For this sensor complement the first measure of quality and the gains associated with the second measure of quality with W(t) taken to be the identity were computed. The first measure of quality defined a controller $u^* = K^*Mx$ and the second defined a controller $\hat{u} = \hat{K}Mx$. Response covariances for these controllers were computed; the results were catastrophic. The response covariances for u^* were excessive after 10 seconds and those for $\hat{u}$ were excessive after 35 seconds. Magnitudes of the covariances were so large that the values computed were meaningless except that they indicated unsatisfactory control. Numerical errors introduced by matrix inversions and interpolation in the computation of K^*M and $\hat{K}M$ may be a partial cause of the unsatisfactory nature of the controllers. But, the major causes of the unsatisfactory control are believed to be that the first and second integrals of the linear accelerometer signals and the attitude signals at stations 1541 and 2686 were not included in the measurement vector and that the columns of M corresponding to the wind states, ω and x, and the internal load distribution state, x_3 were zero. This conclusion is based on the results of the analyses described below.

36

Controller Simplification Analyses

Since the analytical measures of quality proved to be unsatisfactory, a series of experiments was performed to attempt to identify the states which must be measured or estimated to achieve good performance. In the following description of the series of experiments performed, the cost associated with a particular response is an upper bound for the likelihood that the particular response exceeds its limit, and the total cost is the sum of the costs for all responses included in the performance functional. The corrected model was used in these experiments.

The first experiment was performed to determine the importance of the w, x, and x_3 feedbacks, since these three states cannot be measured. In this experiment the performance of the controller obtained by using the gains of controller A for all states except w, x, and x_3 with the gains for these three states equal to zero was computed. The performance of this controller was not very good during the time of high dynamic pressure in that the IB3 cost was large. Thus, it appears necessary to include these states in the controller, and, since they do not explicitly appear in any sensor output, an estimator for these states is required.

The second experiment was performed to determine the significance of the wind states. The above controller was modified by adding the gain of controller A for x_3. The performance of this controller was worse than that of the controller in the previous experiment. The cost for IB3 in the interval of high dynamic pressure was larger than in the first experiment and there were significant costs for β and $\dot{z}$ at burnout. These results demonstrate a significant degree of coupling of wind and load-distribution states.

These two experiments demonstrate very clearly that the optimal controller for a fixed form of feedback is not, in general, the controller defined by the least-squares approximation to the optimal gains. That is, if the controller is required to be of the form

$$u(t) = K(t)M(t)x(t) \qquad (4.21)$$

where M(t) is fixed, then the controller corresponding to $\hat{K}(t;I, M(t))$ defined by (4.20) is generally not optimal. The controllers in the two experiments can be considered as fixed-form controllers in that every state except ω and x is measured; i.e., M is the matrix obtained by deleting the rows corresponding to ω and x from the identity matrix. Then $\hat{K}(t; I, M)$ yields the controller of the second experiment. The cost associated with this controller was more than twenty times the cost of the controller in the first experiment, which is in turn greater than or equal to the cost of the optimal controller of this fixed form.

Thus, conclusions reached from this series of experiments are given subject to an awareness that the controller obtained by deleting specific feedbacks does not necessarily represent the optimal controller of the fixed form which utilizes the remaining feedbacks.

The third experiment was performed to determine the degradation in performance caused by deleting the fuel-sloshing degrees of freedom from controller A. The contribution of these states to the IB3 response and to an estimate of the control at 75 seconds for the system with controller A was insignificant, so it was expected that the degradation would not be great. The cost at 75 seconds with sloshing deleted from the controller was about one and one-half times the optimal cost. This is not a severe degradation, but there was a serious degradation in performance in the interval between 140 and 145 seconds, well beyond the interval of high dynamic pressure. This poor performance late in the flight is one of the many results of the experiments for which there is no clear explanation. Clues to the cause of this particular phenomenon are the behavior of the optimal gain on the third sloshing mode displacement, which has a slight peak in this interval, and the fact that the third slosh-mode frequency has crossed over the first flexure-mode frequency.

The drift makes no contribution to bending moment and its contribution to the control is small. The purpose of the fourth experiment was to determine the performance of the controller with this state and the fuel-slosh states deleted from controller A. There was no noticeable change in the performance caused by deleting drift.

The contribution of the second flexure-mode displacement to controller A at 75 seconds was small, and although this state did contribute significantly to the IB3 response at 75 seconds, this state and the fuel-sloshing states and drift were deleted from controller A in the fifth experiment. In comparison to the previous experiment, the performance of this controller showed a slight degradation during the interval of high dynamic pressure and nine orders of magnitude improvement in the cost in the interval between 140 and 145 seconds.

The sixth experiment consisted of deleting the third-flexure mode displacement from the controller in addition to the states deleted in the fifth experiment. The purpose was to determine the significance of this highest-frequency mode. In comparison to the previous experiment, the performance of this controller displayed a slight improvement during the interval of high dynamic pressure, but extreme degradation for the interval between 110 and 150 seconds. In this latter interval the costs were greater than one indicating almost certainty for the likelihood of mission failure. The differences in the performance of this controller and the controllers of the two previous experiments in the interval between 115 and 150 seconds are an indication of significant coupling of the high-frequency modes in this interval.

The contribution of the wind-filter state, x, to bending moment was zero and its contribution to controller A at 75 seconds was small. This motivated the seventh experiment which consisted of evaluating the performance obtained with this state deleted from the controller of the fifth experiment. There was no significant difference in the performance between this controller and that of the fifth experiment. This demonstrates that there is no serious degradation in performance caused by deleting this state from the control.

The controller for the eighth experiment was obtained by deleting the internal-load-distribution state, x_3, from the controller of the previous experiment. The contribution of this state to bending moment was zero, but its contribution to controller A at 75 seconds was significant. This controller exhibited very good performance during the interval of high dynamic pressure. In fact, its performance there was better than that of controller A. But, the

performance at burnout was rather poor. This indicates that the feedback of x_3 is quite important; however, the underlying relationship of this feedback to controller performance is not understood.

The ninth experiment was conducted to determine the effect of complete removal of the second flexure degree of freedom in addition to the fuel-slosh degrees of freedom and the drift state. The controller for this experiment was the same as in the fifth experiment except that the second flexure-mode rate feedback was deleted. The performance of this controller was somewhat worse than that of the fifth experiment in the interval of high dynamic pressure, but not enough to represent a serious degradation.

The final experiment consisted of deleting the third flexure-mode rate and displacement feedbacks from the controller of the previous experiment. This experiment was conducted to determine the significance of the third-mode degree of freedom. The performance of this controller was completely unsatisfactory for $t \geq 70$ seconds. This is a further indication of the significant role of the high-frequency dynamics in the performance of the controller.

The conclusions reached on the basis of these experiments are:

- The states ω and x_3 should be estimated.
- Feedback of the fuel-slosh states is not necessary.
- The highest-frequency flexure mode is very significant.

Simplified Controller

The experiments described above indicate the necessity of including measurements or estimates of the wind state, ω, and the load-distribution state, x_3, in the controller. Since these states do not contribute directly to any sensor output, their inclusion in the controller can only be achieved with an estimator. Such an estimator was derived from the following considerations.

The states associated with rigid-body and flexure degrees of freedom can be measured by means of integrals of five accelerometer signals as shown above. The load-distribution states, x_1 and x_2, can be measured by linear combinations of two accelerometer signals and the rigid-body and flexure states, assuming the fuel-slosh states are zero. In fact, the fuel-slosh states do contribute to the measurements of x_1 and x_2, but this contribution appears to be negligible for $40 \le t \le 125$.

Let $m_1, \ldots, m_8$ be defined as in the General Considerations with x_{1A}, x_{2A}, and x_{3A} denoting stations 1541, 2686, and 3240 inches respectively. Let m_9 denote the output of an angular accelerometer at station 3240 inches, and let m_{10} denote the output of a lateral accelerometer at station 2686 inches. From the state equations and equations (4.4) and (4.5), the following equation may be obtained:

$$\begin{bmatrix} m_9 \\ m_{10} \end{bmatrix} = \tilde{H}_2 x \tag{4.25}$$

Let $\tilde{m}_9$ denote m_9 minus the known contributions to m_9 from $\dot{\varphi}$, $\ddot{z}$, $\ddot{\eta}_i$, φ, z, η_i, and β. Similarly define $\tilde{m}_{10}$. Then

$$\begin{bmatrix} \tilde{m}_9 \\ \tilde{m}_{10} \end{bmatrix} = M^* \begin{bmatrix} x_1 \\ x_2 \end{bmatrix} + M^{**} \, [\dot{z}_{s1}, \, \dot{z}_{s2}, \, \dot{z}_{s3}, \, z_{s1}, \, z_{s2}, \, z_{s3}]^T \tag{4.26}$$

with M^* nonsingular except at $t = 0$. The elements of $(M^*)^{-1} M^{**}$ are less than 0.08 for $40 \le t \le 125$. Thus $(M^*)^{-1} (\tilde{m}_9, \, \tilde{m}_{10})^T$ is assumed to be a fairly accurate measurement of $(x_1, x_2)^T$ during this interval.

Assuming noisy measurement of the states, x_1 and x_2, an estimator can be derived for states, x_1, x_2, x_3, ω and x. The estimator is designed on the assumption that M^{**} is zero, but the performance of the controller with the estimator is determined with the actual M^{**}. That is, the estimator is designed on the basis of the equations (assuming for simplicity $\bar{v}_\omega = 0$).

$$
\begin{bmatrix} \dot{\omega} \\ \dot{x} \\ \dot{x}_1 \\ \dot{x}_2 \\ \dot{x}_3 \end{bmatrix} = \hat{B}_{44} \begin{bmatrix} \omega \\ x \\ x_1 \\ x_2 \\ x_3 \end{bmatrix} + \hat{D}_4 \, \eta, \quad \begin{bmatrix} \hat{m}_9 \\ \hat{m}_{10} \end{bmatrix} = M^* \begin{bmatrix} x_1 \\ x_2 \end{bmatrix} + \begin{bmatrix} \xi_1 \\ \xi_2 \end{bmatrix}
\tag{4.27}
$$

where $\hat{B}_{44}$ is obtained by deleting the first row and column from B_{44} of Appendix B and $\hat{D}_4$ is the last 5 rows of D_4 of Appendix B and ξ_1 and ξ_2 are independent white noise inputs. This yields estimator equations

$$
\begin{bmatrix} \dot{\hat{\omega}} \\ \dot{\hat{x}} \\ \dot{\hat{x}}_1 \\ \dot{\hat{x}}_2 \\ \dot{\hat{x}}_3 \end{bmatrix} = [\hat{B}_{44} - LM] \begin{bmatrix} \hat{\omega} \\ \hat{x} \\ \hat{x}_1 \\ \hat{x}_2 \\ \hat{x}_3 \end{bmatrix} + L \begin{bmatrix} \hat{m}_9 \\ \hat{m}_{10} \end{bmatrix}, \quad M = \begin{bmatrix} 0 & 0 & & 0 \\ 0 & 0 & M^* & 0 \end{bmatrix}
\tag{4.28}
$$

where L denotes the estimator gain matrix which is obtained from the difference equations

$$
\Delta t L(n) = [\hat{B}_{44}(n)\hat{P}(n)M(n)'\Delta t + \hat{D}_4(n)W_3(n)][M(n)\hat{P}(n)M(n)'\Delta t + W_2(n)]^{-1}
\tag{4.29}
$$

$$
\hat{P}(n+1) = \hat{B}_{44}(n)\hat{P}(n)\hat{B}_{44}(n)' + (\Delta t)^{-1}\hat{D}_4(n)W_1(n)\hat{D}_4(n)'
$$

$$
- \Delta t L(n)[M(n)\hat{P}(n)M(n)'\Delta t + W_2(n)]L(n)
\tag{4.30}
$$

$\hat{P}(0) = \hat{X}(0)$ where $\hat{X}(0)$ is the lower right-hand 5 x 5 submatrix of X(0), and $W_1 = E[\eta^2]$, $W_2 = E[\xi \xi']$, and $W_3 = E[\xi \eta]$. In place of the above estimate, the estimate obtained with $\hat{m}_9$ and $\hat{m}_{10}$ replaced by $\tilde{m}_9$ and $\tilde{m}_{10}$ is used to obtain an estimate of the Kalman form satisfying

$$
\begin{bmatrix} \dot{y}_1 \\ \dot{y}_2 \\ \dot{y}_3 \\ \dot{y}_4 \\ \dot{y}_5 \end{bmatrix} = [\hat{B}_{44} - LM] \begin{bmatrix} y_1 \\ y_2 \\ y_3 \\ y_4 \\ y_5 \end{bmatrix} + L \begin{bmatrix} \tilde{m}_9 \\ \tilde{m}_{10} \end{bmatrix} \tag{4.31}
$$

with

$$
\begin{bmatrix} \tilde{m}_9 \\ \tilde{m}_{10} \end{bmatrix} = \begin{bmatrix} \hat{m}_9 \\ \hat{m}_{10} \end{bmatrix} + M^{**}[\dot{z}_{s1}, \dot{z}_{s2}, \dot{z}_{s3}, z_{s1}, z_{s2}, z_{s3}]
$$

Redefining the state vector x to consist of 27 components, the first 22 being the original state vector and the last 5 being y_1, y_2, y_3, y_4, and y_5 in that order, the control vector associated with the resulting system is

$$
[K_1, K_2, K_3, K_4, K_5, 0, 0, 0, K_9, K_{10}, K_{11}, K_{12}, K_{13}, 0, 0, 0, K_{17}, 0, 0, 0, 0, 0,
$$

$$
K_{18}, K_{19}, K_{20}, K_{21}, K_{22}]
$$

A controller was designed for the corrected model in the manner just described with $E[\xi \ \xi'] = \frac{1}{10} \begin{bmatrix} 1 & 0 \\ 0 & 1 \end{bmatrix}$ $E[\eta^2]$ and $E[\xi\eta] = \begin{bmatrix} 0 \\ 0 \end{bmatrix}$. The quality of the estimates obtained was very poor. However the controller yielded fairly good performance. The total cost was associated with the IB3 response during the interval of high dynamic pressure. In view of the poor quality of the estimates obtained and the results of the seventh and eighth experiments, it is believed that the performance of this controller could be improved by modifying the gains for the estimates of the states, x and x_3. However, time and money limitations precluded investigating this possibility.

SECTION V
QUANTITATIVE RESULTS

This section presents summaries of the numerical results generated in the optimization with complete measurement and sensor choice and controller simplification calculations. The performance of the controller is described as the sum of response costs. Such a response cost is an upper bound on the likelihood of the response exceeding its limit.

Optimization

The iteration procedure described in Section III was used to design controller A for the incorrect model, assuming complete measurement capability. Eleven iterations were required. The sample time employed was 0.02 second. The terminal constraints were met satisfactorily by the third iteration and the significant response was the IB3 response during the interval of high dynamic pressure. The weight on IB3 was increased by two orders of magnitude in the fourth iteration; this produced a reduction of about 4 percent in the IB3 cost. The weights for the fifth iteration were chosen to be the same as for the fourth iteration with the exception that the weight on $\dot{I}B3$ was increased by a factor of 5. This produced a reduction of about 2 percent in the $\dot{I}B3$ covariance at the expense of more than doubling the IB3 covariance and an increase of two orders of magnitude in the IB3 cost. The next three iterations were consecutive reductions in the weight on $\dot{I}B3$ with the other weights unchanged. Improved performance was obtained at each iteration. The weights on each of the bending-moment-rate responses were reduced in the ninth iteration with an accompanying improvement in performance of less than 10 percent. The tenth iteration consisted of increasing the weight on IB3 at 75 seconds by three orders of magnitude; this produced an improvement in performance of less than 10 percent. The weight on IB3 at 75 seconds was reduced by a factor of two and the peak of the time varying weight on IB3 was narrowed in the eleventh iteration. This produced an improvement in performance of approximately a 15 percent reduction in cost. The cost corresponding to this controller was $1.9 \cdot 10^{-3}$,

and this controller, designated as controller A, was accepted as the "optimal" controller.

Optimization was performed with this last set of weights using a sample time of 0.01 second to determine the effect of sampling. The controllers derived for the two sample times were qualitatively the same. The value of the performance functional obtained with the 0.01 second sampling was approximately one-half the value obtained with the 0.02 second sampling. The major differences in the gains for the two cases were those associated with the highest-frequency fuel-slosh and flexure modes, $K_{\dot{z}_3}$ and $K_{\dot{\eta}_3}$, and the gimbal deflection gain, K_β, during the interval of high-dynamic pressure. These gain changes indicate the significance of the high-frequency dynamics in the control problem.

The above results are summarized in Tables 1, 2, and 3. The quadratic weights are shown in Table 1. Peak values of mean responses and response covariances are given in Tables 2 and 3 respectively. The bending moment equations (2.11) used in the above iterations was in error. The erroneous equation

$$I_b(x_o) = M_\alpha{}'\varphi - \frac{M_\alpha{}'}{V}\dot{z} + M_\beta{}'\beta + M_\varphi{}'\dot{\varphi} + \sum_{i=1}^{3} M_{\ddot{\eta}_i}{}'\ddot{\eta}_i$$

$$+ \int \frac{dt}{d\alpha}\ [(x-x_{cg})\gamma_1 + \gamma_2 + (x_o-x)\ \chi\ (x_o-x)]\ \frac{v_\omega}{V}\ dx$$

was used in place of the correct equation

$$I_b(x_o) = M_\alpha{}'\varphi - \frac{M_\alpha{}'}{V}\dot{z} + M_\beta{}'\beta - \frac{M_\varphi{}'}{V}\dot{\varphi} + \sum_{i=1}^{3} M_{\ddot{\eta}_i}{}'\ddot{\eta}_i$$

$$+ \int \frac{dt}{d\alpha}\ [(x-x_{cg})\gamma_1 + \gamma_2 + (x_o-x)\ \chi\ (x_o-x)]\ \frac{v_\omega}{V}\ dx$$

The erroneous bending moment was overly dependent on pitch rate, and this dependence increased with time because velocity increases with time.

Table 1. Quadratic Weights

Iteration	$Q_\alpha(160)$	$\dot{Q}_z(160)$	$Q_z(160)$	$Q_\beta(t)$	$\dot{Q}_\beta(t)$	Q_{IB1}	$\dot{Q}_{IB1}$	C_1	C_2	C_4	C_5	C_6	C_7	τ	C_3
1	$1.42 \cdot 10^7$	$2.04 \cdot 10^3$	$1.11 \cdot 10^{-2}$	$1.31 \cdot 10^4$	$1.31 \cdot 10^4$	$1.23 \cdot 10^{-10}$	$3.09 \cdot 10^{-11}$	$3.46 \cdot 10^{-9}$	2	0.25	$4.0 \cdot 10^{-8}$	9	0.25	80	400
2	$8.52 \cdot 10^6$	$1.02 \cdot 10^3$	$5.56 \cdot 10^{-3}$	$6.57 \cdot 10^3$	$1.64 \cdot 10^3$	$6.17 \cdot 10^{-11}$	$1.54 \cdot 10^{-11}$	$1.73 \cdot 10^{-9}$	2	0.25	$4.0 \cdot 10^{-8}$	9	0.25	80	100
3	$2.84 \cdot 10^8$	$2.04 \cdot 10^3$	$1.11 \cdot 10^{-2}$	$1.31 \cdot 10^4$	$1.31 \cdot 10^4$	$1.23 \cdot 10^{-10}$	$3.09 \cdot 10^{-11}$	$3.46 \cdot 10^{-9}$	2	0.25	$4.0 \cdot 10^{-7}$	9	0.25	75	100
4	$2.84 \cdot 10^9$	$2.04 \cdot 10^3$	$1.11 \cdot 10^{-2}$	$7.88 \cdot 10^5$	$7.88 \cdot 10^5$	$1.23 \cdot 10^{-10}$	$3.09 \cdot 10^{-11}$	$3.46 \cdot 10^{-9}$	2	0.25	$4.0 \cdot 10^{-7}$	99	0.25	75	100
5	$2.84 \cdot 10^9$	$2.04 \cdot 10^3$	$1.11 \cdot 10^{-2}$	$7.88 \cdot 10^5$	$7.88 \cdot 10^5$	$1.23 \cdot 10^{-10}$	$3.09 \cdot 10^{-11}$	$3.46 \cdot 10^{-9}$	2	0.25	$4.0 \cdot 10^{-7}$	99	5	75	100
6	$2.84 \cdot 10^9$	$2.04 \cdot 10^3$	$1.11 \cdot 10^{-2}$	$7.88 \cdot 10^5$	$7.88 \cdot 10^5$	$1.23 \cdot 10^{-10}$	$3.09 \cdot 10^{-11}$	$3.46 \cdot 10^{-9}$	2	0.25	$4.0 \cdot 10^{-7}$	99	0.125	75	100
7	$2.84 \cdot 10^9$	$2.04 \cdot 10^3$	$1.11 \cdot 10^{-2}$	$7.88 \cdot 10^5$	$7.88 \cdot 10^5$	$1.23 \cdot 10^{-10}$	$3.09 \cdot 10^{-11}$	$3.46 \cdot 10^{-9}$	2	0.25	$4.0 \cdot 10^{-7}$	99	0.0125	75	100
8	$2.84 \cdot 10^9$	$2.04 \cdot 10^3$	$1.11 \cdot 10^{-2}$	$7.88 \cdot 10^5$	$7.88 \cdot 10^5$	$1.23 \cdot 10^{-10}$	$3.09 \cdot 10^{-11}$	$3.46 \cdot 10^{-9}$	2	0.25	$4.0 \cdot 10^{-7}$	99	0.00125	75	100
9	$2.84 \cdot 10^9$	$2.04 \cdot 10^3$	$1.11 \cdot 10^{-2}$	$7.88 \cdot 10^5$	$7.88 \cdot 10^5$	$1.23 \cdot 10^{-10}$	$7.72 \cdot 10^{-12}$	$3.46 \cdot 10^{-9}$	2	0.0625	$4.0 \cdot 10^{-7}$	99	0.00031	75	100
10	$2.84 \cdot 10^9$	$2.04 \cdot 10^3$	$1.11 \cdot 10^{-2}$	$7.88 \cdot 10^5$	$7.88 \cdot 10^5$	$1.23 \cdot 10^{-10}$	$7.72 \cdot 10^{-12}$	$3.46 \cdot 10^{-9}$	2	0.0625	$4.0 \cdot 10^{-7}$	999	0.00031	75	100
11	$2.84 \cdot 10^9$	$2.04 \cdot 10^3$	$1.11 \cdot 10^{-2}$	$7.88 \cdot 10^5$	$7.88 \cdot 10^5$	$1.23 \cdot 10^{-10}$	$7.72 \cdot 10^{-12}$	$3.46 \cdot 10^{-9}$	2	0.0625	$4.0 \cdot 10^{-7}$	499	0.00031	75	50
11 ($\Delta t = 0.01$ sec)	$2.84 \cdot 10^9$	$2.04 \cdot 10^3$	$1.11 \cdot 10^{-2}$	$7.88 \cdot 10^5$	$7.88 \cdot 10^5$	$1.23 \cdot 10^{-10}$	$7.72 \cdot 10^{-12}$	$3.46 \cdot 10^{-9}$	2	0.0625	$4.0 \cdot 10^{-7}$	499	0.00031	75	50

$$Q_{IB2} = C_1 \left[1 + C_2 \exp \frac{-(t-\tau)^2}{C_3} \right]$$

$$Q_{IB3} = C_5 \left[1 + C_6 \exp \frac{-(t-\tau)^2}{C_3} \right]$$

$$\dot{Q}_{IB2} = C_4 \, Q_{IB2}$$

$$\dot{Q}_{IB3} = C_7 \, Q_{IB3}$$

$$Kzsg = Kzsj = Kz = Kn2 = Kn3 = Kn3 = 0$$

Table 2. Mean Responses

Iteration	$\dfrac{\bar{\alpha}(T)}{\gamma_\alpha}$	$\dfrac{\bar{\dot{z}}(T)}{\gamma_{\dot{z}}}$	$\dfrac{\bar{z}(T)}{\gamma_z}$	Peak $\dfrac{\overline{IB1}}{\gamma_{IB1}}$	$T_p^{(a)}$	Peak $\dfrac{\overline{IB2}}{\gamma_{IB2}}$	T_p	Peak $\dfrac{\overline{IB3}}{\gamma_{IB3}}$	T_p	Peak $\dfrac{\bar{\beta}}{\gamma_\beta}$	T_p	J*
1	-0.86	0.034	0.13	0.037	80	-0.098	145	0.18	160	-0.33	160	0.20
2	-1.01	0.053	0.13	0.038	80	-0.095	145	0.17	160	-0.32	160	0.56
3	-0.45	0.28	0.16	0.035	80	0.14	160	0.32	160	-0.54	160	0.06
4	-0.11	0.47	0.23	0.059	5	-0.18	145	-0.21	140	0.35	160	0.06
5	-0.13	0.62	0.17	-0.13	50	-0.40	50	-0.81	50	-0.062	100	7.76
6	-0.12	0.44	0.22	0.060	160	-0.18	160	-0.21	145	0.51	160	0.027
7	-0.075	0.21	0.13	0.038	160	0.099	160	-0.11	145	0.15	160	0.0052
8	0.0078	0.033	0.055	0.046	70	0.091	70	0.027	160	0.10	80	0.0028
9	-0.0073	0.008	0.043	0.048	70	0.095	70	0.0097	160	0.11	80	0.0026
10	-0.050	0.076	0.075	0.043	70	0.084	70	0.063	160	0.098	80	0.0024
11	-0.019	0.027	0.053	0.047	70	0.092	70	0.025	160	0.10	80	0.0019
11 (Δt = 0.01 sec)	-0.0070	0.008	0.042	0.048	70	0.096	70	0.0090	90	0.11	80	0.0009
Limits (γ)	0.05934	70	30000	$9 \cdot 10^6$		$1.7 \cdot 10^6$		$5 \cdot 10^5$		0.0873		

(a) T_p = Time of occurrence of peak.

Table 3. Response Covariances

Iteration	$\left[\dfrac{\alpha(T)}{Y_\alpha}\right]^2$	$\left[\dfrac{\dot{z}(T)}{Y_{\dot{z}}}\right]^2$	$\left[\dfrac{z(T)}{Y_z}\right]^2$	Peak $\left[\dfrac{IB1}{Y_{IB1}}\right]^2$	T_p (a)	Peak $\left[\dfrac{IB2}{Y_{IB2}}\right]^2$	T_p	Peak $\left[\dfrac{IB3}{Y_{IB3}}\right]^2$	T_p	Peak $\left[\dfrac{\beta}{Y_\beta}\right]^2$	T_p
1	0.030	0.00005	0.00009	0.0027	75	0.019	75	0.096	75	0.0046	160
2	0.039	0.00012	0.00008	0.0027	75	0.019	75	0.096	75	0.0042	160
3	0.0054	0.0018	0.00013	0.0027	75	0.018	75	0.091	75	0.0072	160
4	0.00063	0.0030	0.00027	0.0027	75	0.018	75	0.090	75	0.0040	160
5	0.0034	0.044	0.00079	0.0093	145	0.095	145	0.190	75	0.0620	145
6	0.00055	0.0021	0.00021	0.0025	75	0.017	75	0.082	75	0.0039	160
7	0.00057	0.0020	0.00016	0.0023	75	0.015	75	0.065	75	0.0037	80
8	0.00096	0.0023	0.00020	0.0022	75	0.014	75	0.060	75	0.0038	80
9	0.0013	0.0024	0.00021	0.0022	75	0.013	75	0.059	75	0.0038	80
10	0.0013	0.0024	0.00021	0.0021	75	0.013	75	0.059	75	0.0039	80
11	0.0012	0.0023	0.00020	0.0021	75	0.013	75	0.057	75	0.0039	80
11 (Δt = 0.01 sec)	0.0017	0.0067	0.00025	0.0026	90	0.015	90	0.051	90	0.0037	80
Limits (γ^2)	$3.52 \cdot 10^{-3}$	$4.9 \cdot 10^{3}$	$9 \cdot 10^{8}$	$8.1 \cdot 10^{13}$		$2.89 \cdot 10^{12}$		$2.5 \cdot 10^{11}$		$7.62 \cdot 10^{-3}$	

(a) T_p = Time of occurrence of peak

The error was discovered during the course of simplifying controller A. After the error was discovered, the performance of controller A was re-evaluated with the corrected bending moment expression. The upper bound associated with the covariances for the correct model was about 0.4 times that for the incorrect model. The cost with an adjusted deterministic input and the mean input is about 1.02 times the cost produced by the covariances only.

Optimization with the correct model and the weights from the eleventh iteration yielded a controller, which will be denoted as controller A', with higher cost, but the cost was almost wholly due to gimbal deflection at burnout. One more iteration was performed in which the weights on gimbal deflection, and gimbal rate at burnout were increased by a factor of ten. The resulting controller, which will be denoted controller B, yielded the lowest value obtained for the upper bound. The cost of approximately 10^{-6} for controller B was again almost wholly due to gimbal deflection at burnout, and this could undoubtedly be reduced by further iterations. However, in view of the small value of $8 \cdot 10^{-4}$ obtained for the upper bound on the likelihood of mission failure with controller A, it was decided that the time and money remaining could be used more effectively in simplification analysis of controller A for the correct model.

The adjusted deterministic input was obtained as follows. It was assumed that the mean response with controller B was the desired mean response for controller A with the adjusted deterministic input. The mean responses of controller B will be achieved if the mean gimbal angle $\bar{\beta}(t)$, is equal to the mean gimbal angle $\bar{\beta}_B(t)$ for controller B. Since $\bar{\beta}(0)$ is zero for any controller, the mean gimbal angles will be equal if $\dot{\bar{\beta}}(t)$ is set equal to $\dot{\bar{\beta}}_B(t)$. Now

$$\dot{\bar{\beta}}_B(t) = 11.9 \, (K^B \, \bar{x}^B - \bar{\beta}_B + f_B)$$

for controller B, and

$$\dot{\bar{\beta}}(t) = 11.9 (K^A \, \bar{x} - \bar{\beta} + f)$$

for controller A. Setting $\tilde{\beta}$ and $\bar{x}$ equal to $\tilde{\beta}_B$ and $\bar{x}_B$ respectively yielded the adjusted deterministic input

$$f = (K^B - K^A) \bar{x}^B + f_B$$

The optimization results for the correct model are summarized in Table 4. The standard deviations of angle of attack, pitch rate, pitch attitude, drift rate, drift, gimbal angle, and IB3 are given in Figures 1 through 7 for controllers A and B. These figures display the significant difference in the character of the two controllers. The gains for the two controllers are displayed in Appendix D.

In comparison to controller B, controller A permits larger angle of attack, maintains smaller pitch attitude and pitch rate with smaller gimbal deflection during the interval of high dynamic pressure, and produces larger bending moments. Also the control activity to meet the terminal constraints is much less for controller A than for controller B.

Quality of Sensor Complements

The first measure of quality was tested on only the sensor complement described in the Controller Simplification Analysis of Section IV with the erroneous model. The performance of the controller was so bad that no quantitative results of value were obtained. Since the error in the model did not affect the states, using the corrected model would not significantly change the above results.

The second measure of quality was evaluated for a set of rate outputs and their integrals. The following six pairs of sensor outputs were considered:

1. $\dot{z} + (36.5 - x_{cg})\dot{\varphi} + \Sigma Y_i(36.5)\dot{\eta}_i$, $z + (36.5 - x_{cg})\varphi + \Sigma Y_i(36.5)\eta_i$

2. $\dot{z} + (65.7 - x_{cg})\dot{\varphi} + \Sigma Y_i(65.7)\dot{\eta}_i$, $z + (65.7 - x_{cg})\varphi + \Sigma Y_i(65.7)\eta_i$

50

Table 4. Mean Responses and Response Covariances

Mean Responses

Controller	$\dfrac{\bar{\alpha}(T)}{\gamma_\alpha}$	$\dfrac{\bar{\dot{z}}(T)}{\gamma_{\dot{z}}}$	$\dfrac{\bar{z}(T)}{\gamma_z}$	Peak $\dfrac{\overline{IB1}}{\gamma_{IB1}}$	T_p (a)	Peak $\dfrac{\overline{IB2}}{\gamma_{IB2}}$	T_p	Peak $\dfrac{\overline{IB3}}{\gamma_{IB3}}$	T_p	Peak $\dfrac{\bar{\beta}}{\gamma_\beta}$	T_p	J*
A	-0.0193	0.0272	0.0526	0.0814	80	0.1960	80	0.3748	80	0.1045	80	0.26751
A*	0.0002	-0.0068	0.0139	-0.0101	160	-0.0145	160	-0.0103	160	-0.0405	160	0.000819
A'	0.0066	-0.0045	0.0138	-0.0131	160	-0.0186	160	-0.0130	160	-0.0534	160	0.017305
B	0.0010	-0.0035	0.0138	-0.0081	160	-0.0110	160	-0.0078	150	-0.0352	160	0.000002

A* indicates controller A with adjusted deterministic input.

Response Covariances

Controller	$\left[\dfrac{\sigma_\alpha(T)}{\gamma_\alpha}\right]^2$	$\left[\dfrac{\sigma_{\dot{z}}(T)}{\gamma_{\dot{z}}}\right]^2$	$\left[\dfrac{\sigma_z(T)}{\gamma_z}\right]^2$	Peak $\left[\dfrac{\sigma_{IB1}}{\gamma_{IB1}}\right]^2$	T_p (a)	Peak $\left[\dfrac{\sigma_{IB2}}{\gamma_{IB2}}\right]^2$	T_p	Peak $\left[\dfrac{\sigma_{IB3}}{\gamma_{IB3}}\right]^2$	T_p	Peak $\left[\dfrac{\sigma_\beta}{\gamma_\beta}\right]^2$	T_p
A	0.0012	0.0023	0.0002	0.0023	75	0.0130	75	0.0476	75	0.0039	75
A'	0.0013	0.0003	0.0214	0.0039	160	0.0079	160	0.0113	160	0.0652	160
B	0.0004	0.0002	0.0209	0.0016	160	0.0042	160	0.0113	75	0.0291	75

(a) T_p = Time of occurrence of peak

51
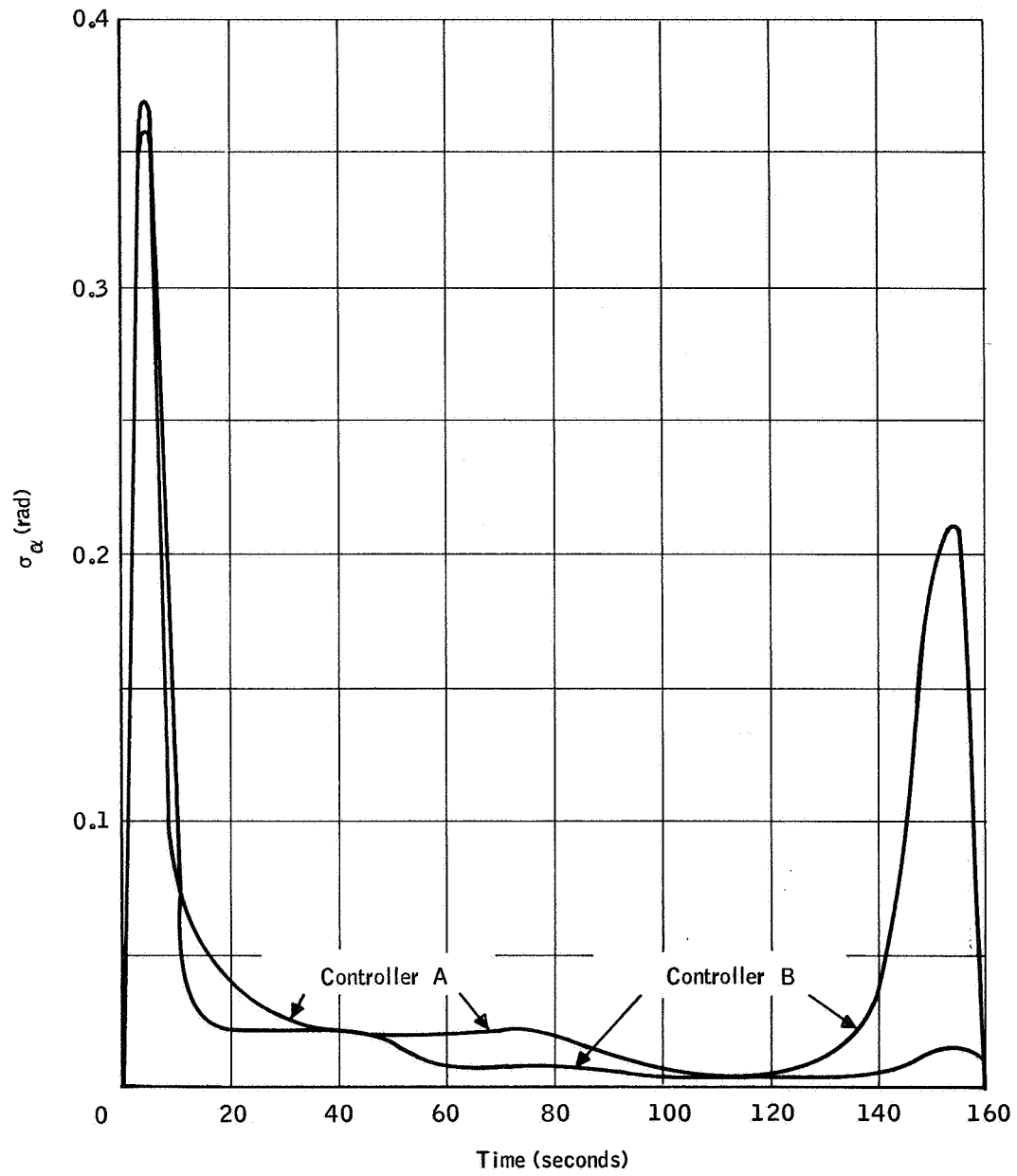
Figure 1. Standard Deviations of Angle of Attack
(for the corrected model)
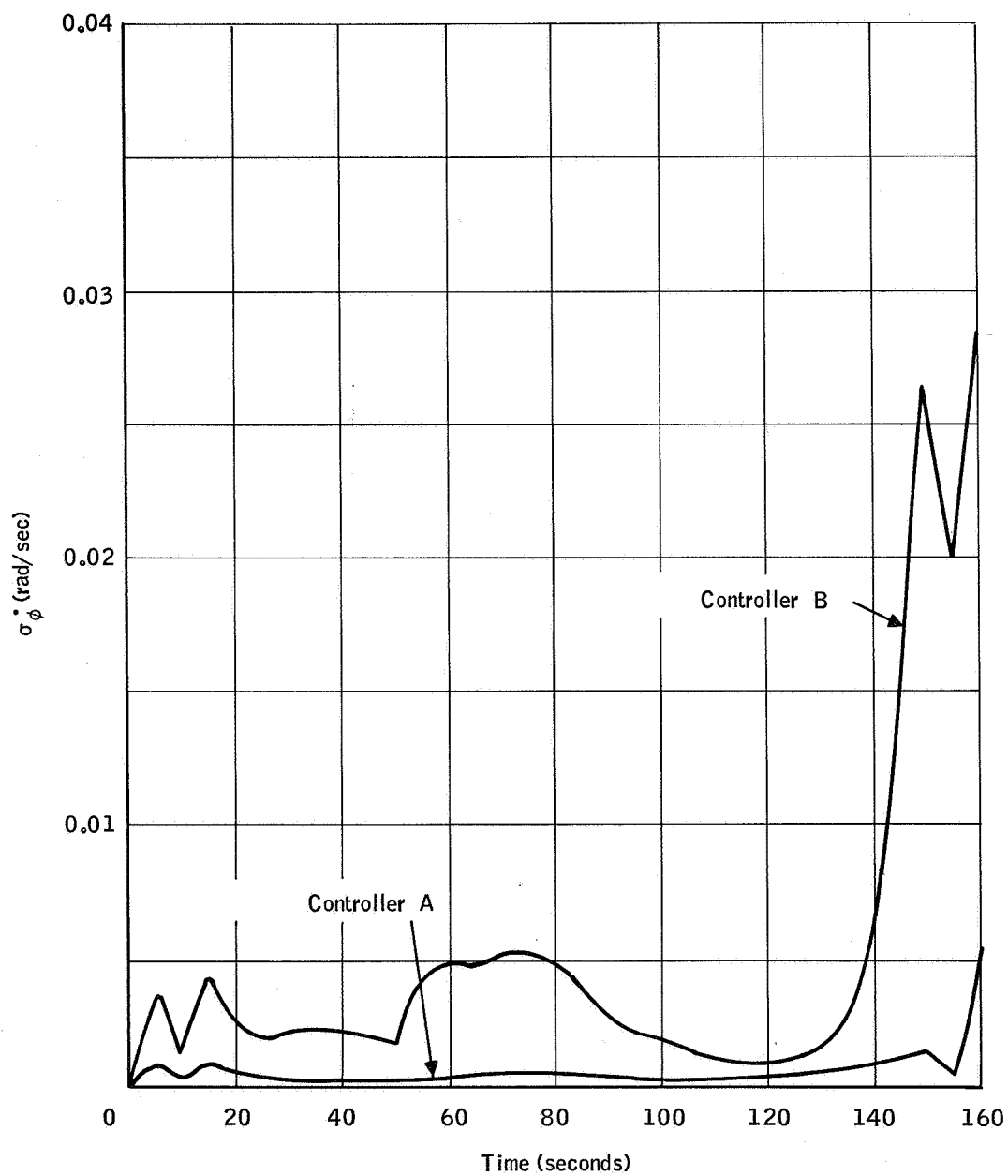
Figure 2. Standard Deviations of Attitude Rate
(for the corrected model)
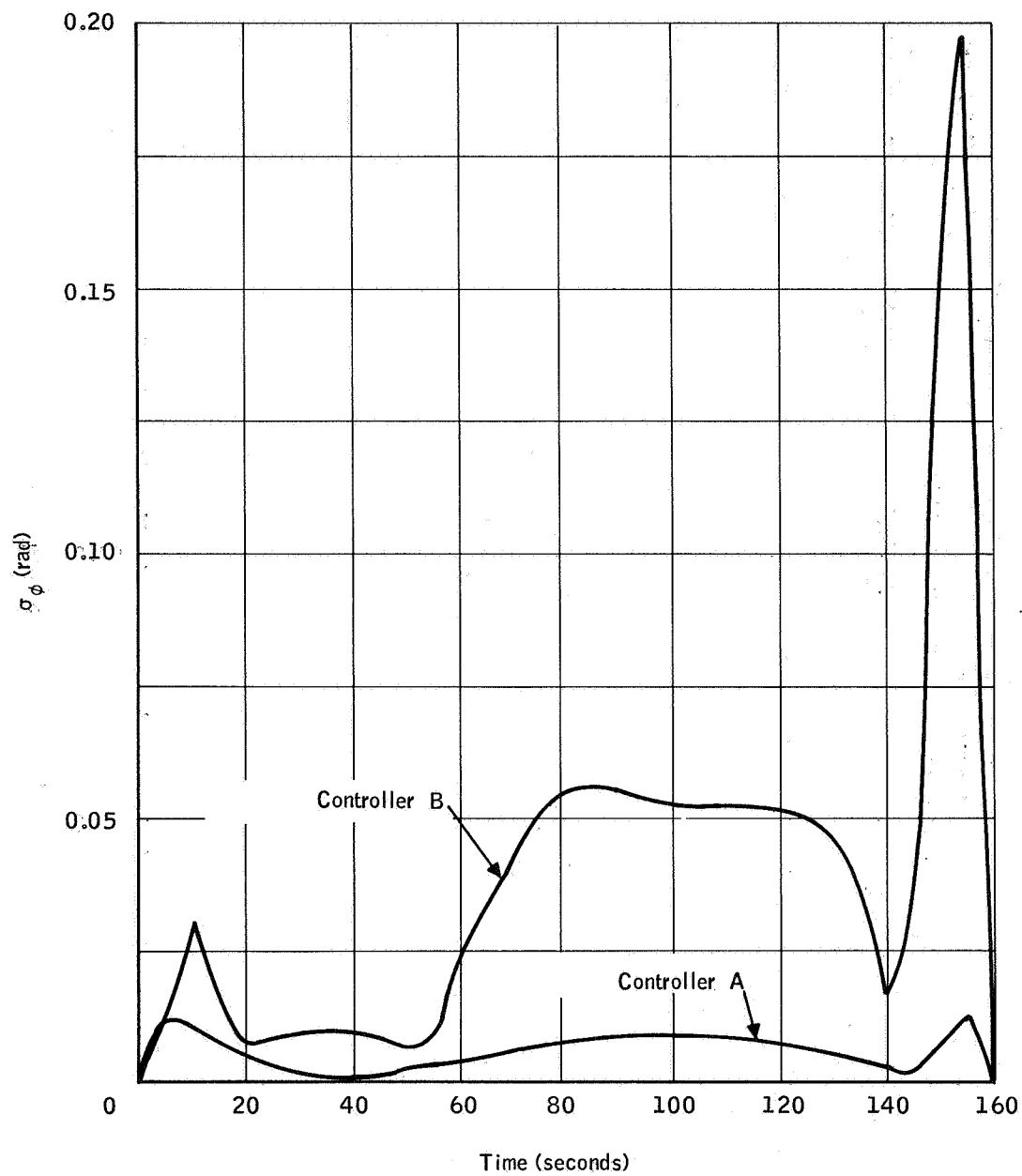
Figure 3. Standard Deviations of Attitude
(for the corrected model)

54
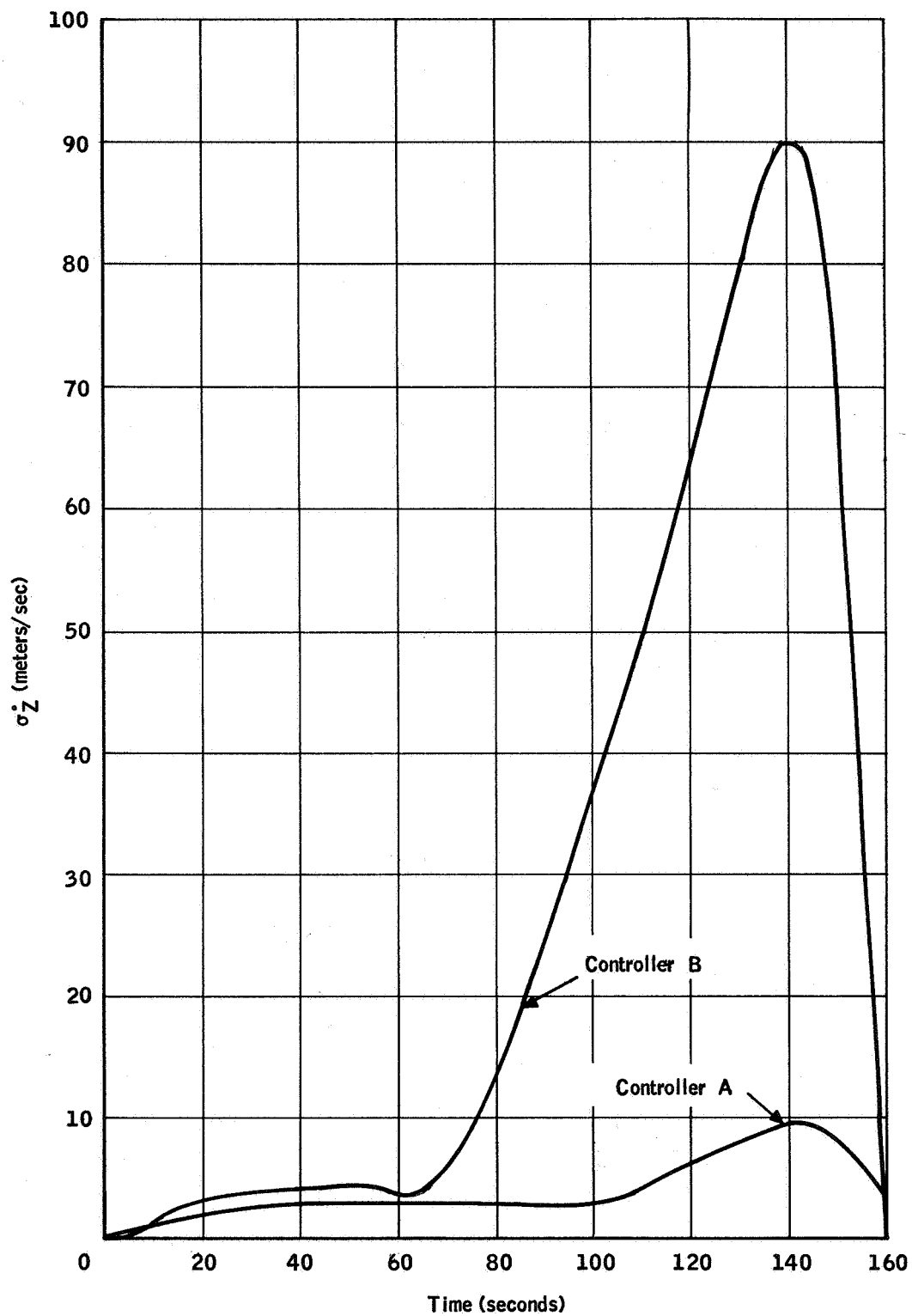
Figure 4. Standard Deviations of Drift Rate
(for the corrected model)
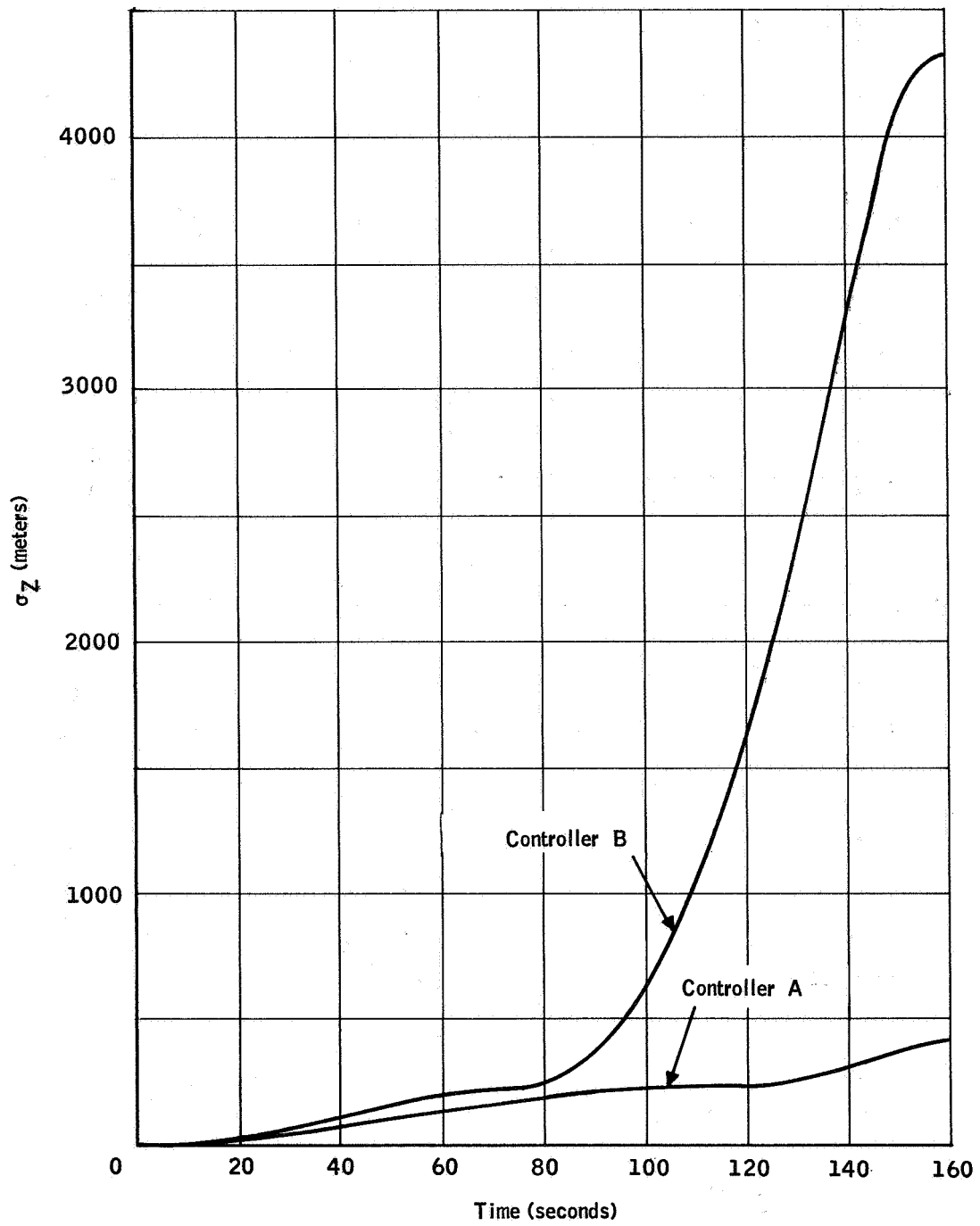
Figure 5. Standard Deviations of Drift
(for the corrected model)
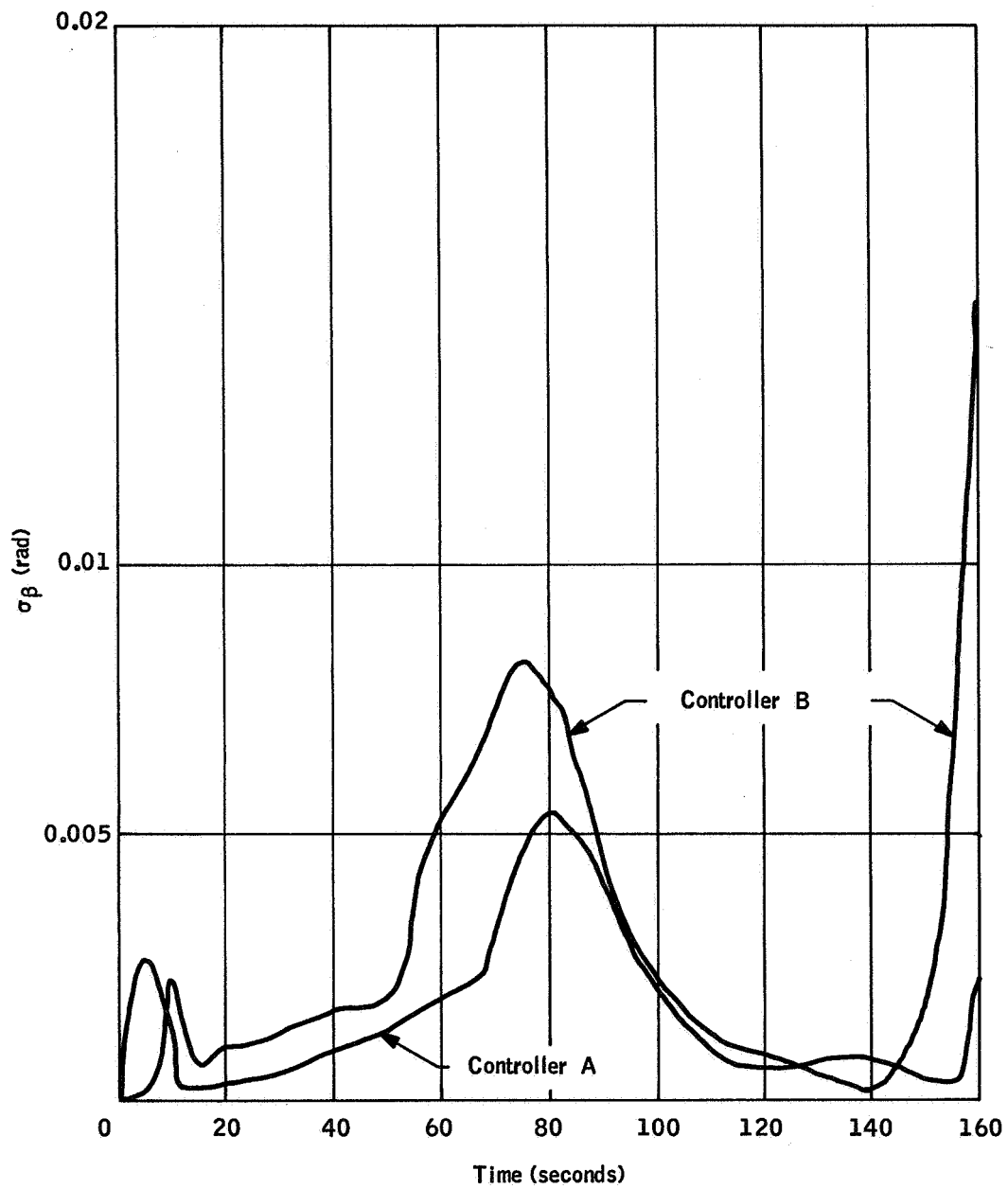
Figure 6. Standard Deviations of Gimbal Angle
(for the corrected model)
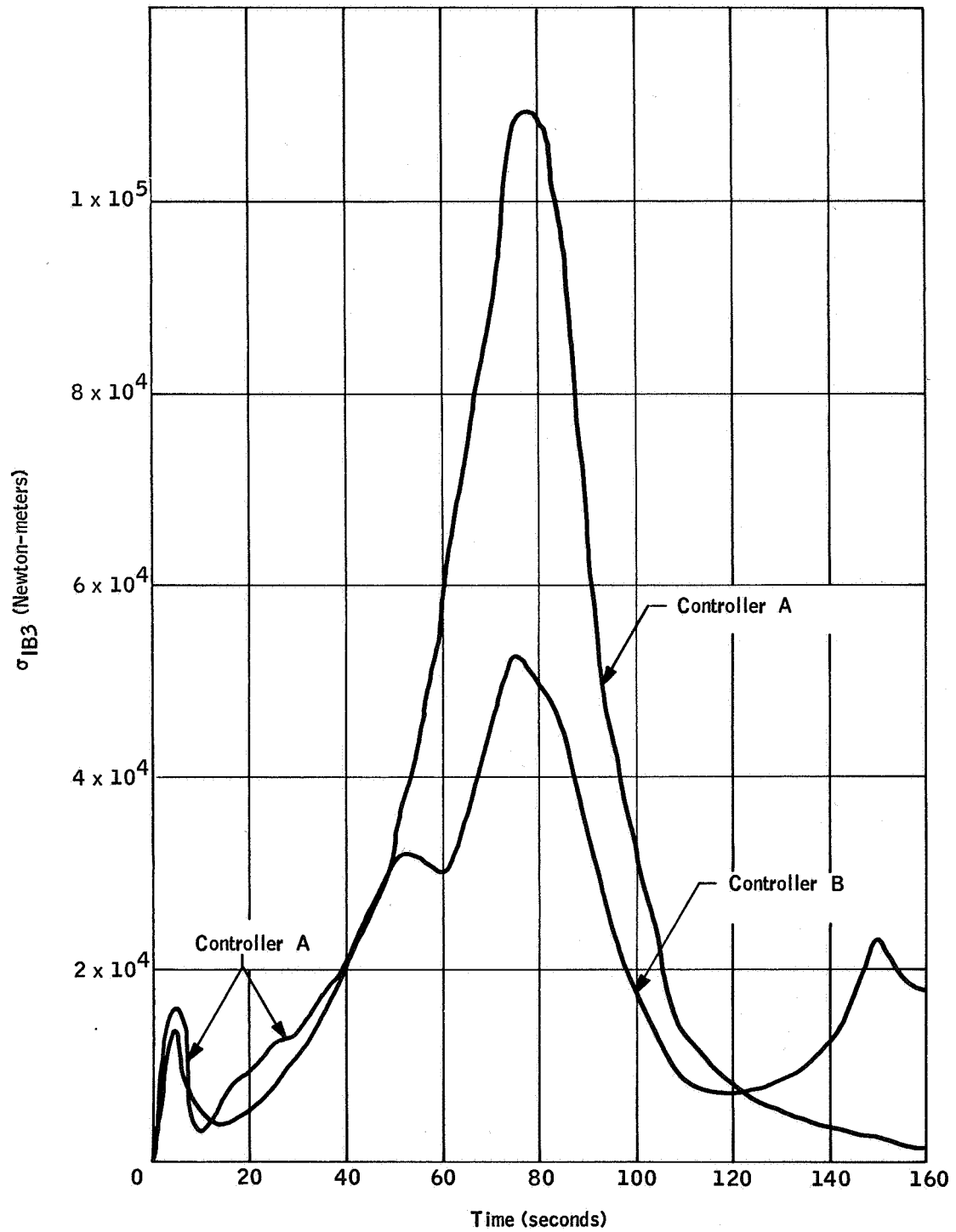
Figure 7. Standard Deviations of IB3 Response
(for the corrected model)

3. $\dot{z} + (80 - x_{cg})\dot{\varphi} + \Sigma\, Y_i(80)\dot{\eta}_i, \quad z + (80 - x_{cg})\varphi + \Sigma\, Y_i(80)\eta_i$

4. $\dot{\varphi} + \Sigma\, Y_i{}'(36.5)\dot{\eta}_i, \quad \varphi + \Sigma\, Y_i{}'(36.5)\eta_i$

5. $\dot{\varphi} + \Sigma\, Y_i{}'(65.7)\dot{\eta}_i, \quad \varphi + \Sigma\, Y_i{}'(65.7)\eta_i$

6. $\dot{\varphi} + \Sigma\, Y_i{}'(80)\dot{\eta}_i, \quad \varphi + \Sigma\, Y_i{}'(80)\eta_i$

Only the gains associated with $\dot{\varphi}$, $\dot{z}$, $\dot{\eta}_i$, φ, z, η_i can be approximated given this set of outputs, so the weighting matrix was chosen to give equal weights to these components of the difference, $KM - K^A$, and zero weights to the others. The evaluation was performed only at $t = 80$ seconds. The results are given in Table 5 for all combinations of sensors taken one, two, three, four, and five at a time.

This quality measure does not appear to be adequate since it fails to incorporate the known significance of the signs of gains. For example, the gains on $\dot{\eta}_1$, $\dot{\eta}_2$, z and η_2 in $\hat{K}M$ are opposite in sign to the gains of controller A in the best set of four pairs, the pairs 2, 3, 4, and 6. Also, equal weighting of errors does not take into account the differences in magnitudes of the gains of controller A. This could be remedied by modifying the weighting matrix, but this raises the question of what is the best weighting matrix. Time did not allow investigation of this question.

Controller Simplification

Experiments were performed to determine the degradation in performance caused by deleting the feedback of certain states from controller A. These experiments performed originally with the erroneous model, indicated that exclusion of the fuel-slosh displacement, fuel-slosh rate, drift, second flexure-mode displacement and rate states from the controller caused only minor deterioration during high dynamic pressure. The experimental results obtained for the correct model indicated that ω and x_3 feedbacks made significant

Table 5. Second Analytic Measure of Quality

One Pair		Two Pairs		Three Pairs		Four Pairs		Five Pairs	
Pair	$J_w(M)$	Pairs	$J_w(M)$	Pairs	$J_w(M)$	Pairs	$J_w(M)$	Pairs	$J_w(M)$
1	201.50	1,2	1.83	1,2,3	1.46	1,2,3,4	0.99	1,2,3,4,5	$0.13 \cdot 10^{-5}$
2	6.17	1,3	1.51	1,2,4	1.13	1,2,3,5	0.96	1,2,3,4,6	$0.18 \cdot 10^{-1}$
3	3.62	1,4	2.54	1,2,5	1.50	1,2,3,6	1.01	1,2,3,5,6	$0.12 \cdot 10^{-3}$
4	2.55	1,5	4.89	1,2,6	1.29	1,2,4,5	1.02	1,2,4,5,6	$0.21 \cdot 10^{-4}$
5	5.22	1,6	16.31	1,3,4	1.03	1,2,4,6	1.00	1,3,4,5,6	$0.32 \cdot 10^{-8}$
6	17.35	2,3	2.79	1,3,5	1.15	1,2,5,6	0.98	2,3,4,5,6	$0.74 \cdot 10^{-4}$
		2,4	1.97	1,3,6	1.47	1,3,4,5	1.02		
		2,5	3.69	1,4,5	1.06	1,3,4,6	0.99		
		2,6	4.13	1,4,6	2.48	1,3,5,6	0.95		
		3,4	1.68	1,5,6	3.44	1,4,5,6	1.03		
		3,5	2.96	2,3,4	1.49	2,3,4,5	1.02		
		3,6	3.36	2,3,5	2.52	2,3,4,6	0.97		
		4,5	1.07	2,3,6	2.30	2,3,5,6	0.61		
		4,6	2.48	2,4,5	1.05	2,4,5,6	1.02		
		5,6	3.58	2,4,6	1.89	3,4,5,6	1.02		
				2,5,6	2.78				
				3,4,5	1.05				
				3,4,6	1.66				
				3,5,6	2.63				
				4,5,6	1.04				

significant contributions to control. Qualitative descriptions of the experiments are given in Section IV. The quantitative descriptions for the correct model follow.

1. Controller: $K_\omega = K_x = K_{x_3} = 0$, other $K_i = K_i^A$.

   Total cost = IB3 cost + $\dot{z}(T)$ cost = 0.88 + 0.01

   IB3 cost significant only for 70-85 seconds.

   The motivation for this experiment was the fact that these gains were zero in both K*M and $\hat{K}$M. The conclusion drawn is that these states cannot be disregarded.

2. Controller: $K_\omega = K_x = 0$, other $K_i = K_i^A$.

   Total cost = β cost + IB3 cost + $\dot{z}$ cost + α cost = 1.293 + 0.472 + 0.165 + 0.026

   β cost significant only at 160 seconds.

   IB3 cost significant for 70-90 seconds.

   This experiment was performed to determine the significance of the wind states only. It demonstrates a significant degree of coupling of wind and load-distribution states.

3. Controller: $K_{\dot{z}_{sj}} = K_{z_{sj}} = 0$, other $K_i = K_i^A$

   Total cost = β cost + IB3 cost = 0.071 + 0.001

   β cost significant only for 140-145 seconds.

   IB3 cost significant only for 75-80 seconds.

   It was suspected that fuel-sloshing was of little significance during high dynamic pressure in the controller since these modes gave an insignificant contribution to the control. The supposition was confirmed. The drift contribution to the control was also small, which motivated experiment 4.

4. Controller: $K_{\dot{z}_{sj}} = K_{z_{sj}} = K_z = K_{\eta_2} = 0$, other $K_i = K_i^A$

   No significant change from 3 occurred.

   The η_2 contribution to the control was also small, which motivated experiment 5.

5. Controller: $K_{\dot{z}_{sj}} = K_{z_{sj}} = K_z = K_{\eta_2} = 0$, other $K_i = K_i^A$

Total cost = IB3 cost = 0.00143

IB3 cost significant only for 75-80 seconds.

IB3 cost for 75-80 second interval was approximately 1.75 times the corresponding cost for controller A with complete feedback.

6. Controller: $K_{\dot{z}_{sj}} = K_{z_{sj}} = K_z = K_{\eta_2} = K_{\eta_3} = 0$, other $K_i = K_i^A$

Total cost = 960, indicating the significance of the third bending mode to the controller. The major contributions to the cost were the IB3, β, IB2, and IB1 costs and these costs occurred in the interval from 115-150 seconds. This demonstrates the major significance of the high-frequency third bending mode late in the flight.

7. Controller: $K_{\dot{z}_{sj}} = K_{z_{sj}} = K_z = K_{\eta_2} = K_x = 0$, other $K_i = K_i^A$

No significant change from 5 occurred. The motivation for this experiment was that the contribution to the controller of the wind state x was small.

8. Controller: $K_{\dot{z}_{sj}} = K_{z_{sj}} = K_z = K_{\eta_2} = K_x = K_{x_3} = 0$, other $K_i = K_i^A$

Total cost = $\dot{z}$ cost + β cost + α cost = 0.0243 + 0.0003 + 0.0003

β cost significant only at 160 seconds.

This experiment was performed because the load distribution state, x_3, cannot be measured directly, and this state does not contribute directly to the bending moment responses. The relation of the feedback of x_3 to controller performance is not clear. In this experiment each bending-moment response was reduced sharply from the corresponding response in the previous experiment. In fact, the IB3 cost of $0.15 \cdot 10^{-4}$ for this experiment was much lower than IB3 cost of $8.0 \cdot 10^{-4}$ produced by controller A.

9. Controller: $K_{\dot{z}_{sj}} = K_{z_{sj}} = K_z = K_{\eta_2} = K_{\dot{\eta}_2} = 0$, other $K_i = K_i^A$

Total cost = IB3 cost = 0.0196

IB3 cost significant only for 70-85 seconds.

IB3 cost for 70-85 second interval was approximately 37 percent greater than the corresponding cost in the fifth experiment.

10. Controller: $K_{\dot{z}_{sj}} = K_{z_{sj}} = K_z = K_{\eta_2} = K_{\dot{\eta}_2} = K_{\eta_3} = K_{\dot{\eta}_3} = 0$, other $K_i = K_i^A$

Total cost = IB3 cost + IB2 cost + β cost + IB1 cost = 875 + 780 + 748 + 701

The response covariances were excessive after 70 seconds. The value of $[\text{IB3 covariance}]/(\text{IB3}_{MAX})^2$ at 75 seconds was 3.98 and at 160 seconds was $4.16 \cdot 10^{15}$.

The response covariances are summarized in Table 6. In the above controller definitions K^A denotes the gain vector for controller A. The remarks on significance of costs given above are with respect to the total cost. The simplification analysis of controller B was limited to determining the degradation in performance caused by deleting the fuel slosh, fuel slosh rate and drift feedbacks. The controller with these feedbacks deleted exhibited very poor performance; it produced a total cost of 911.9 consisting of contributions of 444.7 for β, 57.2 for IB1, 80.0 for IB2, 327.5 for IB3, 0.998 for $\alpha(160)$, 0.996 for $\dot{z}(160)$ and 0.57 for $z(160)$. The responses were unsatisfactory after 75 seconds. Thus, in contrast to controller A, these feedbacks very significantly affect the performance of controller B.

Simplified Controller

A simplified controller was designed based on the rationale given in Section IV. It was assumed that the rigid-body and the flexure states could be measured, and an estimator was designed to estimate the wind and load distribution states. The control input consists of feedback with the gains of

Table 6. Response Covariances

Experiments	$\left[\dfrac{\sigma_\alpha(T)}{Y_\alpha}\right]^2$	$\left[\dfrac{\sigma_{\dot z}(T)}{Y_{\dot z}}\right]^2$	$\left[\dfrac{\sigma_z(T)}{Y_z}\right]^2$	Peak $\left[\dfrac{\sigma_{IB1}}{Y_{IB1}}\right]^2$	$T_p^{(a)}$	Peak $\left[\dfrac{\sigma_{IB2}}{Y_{IB2}}\right]^2$	T_p	Peak $\left[\dfrac{\sigma_{IB3}}{Y_{IB3}}\right]^2$	T_p	Peak $\left[\dfrac{\sigma_\beta}{Y_\beta}\right]^2$	T_p	J^*
$K_\omega = K_x = K_{x_3} = 0$	0.041	0.099	0.014	0.0042	80	0.0236	80	0.0836	80	0.031	160	0.089
$K_\omega = K_x = 0$	0.203	0.519	0.076	0.0108	160	0.0339	80	0.1204	80	0.164	160	1.956
$K_{\dot z_{sj}} = K_{z_{sj}} = 0$	0.0006	0.001	0.0001	0.0146	140	0.0505	140	0.0680	140	0.080	140	0.072
$K_{\dot z_{sj}} = K_{z_{sj}} = K_z = 0$	0.0006	0.001	0.0001	0.0146	140	0.0505	140	0.0680	140	0.080	140	0.072
$K_{\dot z_{sj}} = K_{z_{sj}} = K_z = K_{\eta_2} = 0$	0.0012	0.001	0.0001	0.0041	140	0.0149	140	0.0504	75	0.019	140	0.0014
$K_{\dot z_{sj}} = K_{z_{sj}} = K_z = K_{\eta_2} = K_{\eta_3} = 0$	0.0014	0.001	0.0001	7.36	145	10.2	135	$4.1 \cdot 10^3$	140	31.1	140	960.2
$K_{\dot z_{sj}} = K_{z_{sj}} = K_z = K_{\eta_2} = K_x = 0$	0.0011	0.002	0.0004	0.0041	140	0.0149	140	0.0504	75	0.019	140	0.0015
$K_{\dot z_{sj}} = K_{z_{sj}} = K_z = K_{\eta_2} = K_x = K_{x_3} = 0$	0.086	0.197	0.0226	0.0045	140	0.0169	140	0.0346	75	0.044	160	0.025
$K_{\dot z_{sj}} = K_{z_{sj}} = K_z = K_{\eta_2} = K_{\eta_2}^\cdot = 0$	0.0010	0.001	0.0001	0.0057	140	0.0210	140	0.0524	75	0.026	140	0.0020
$K_{\dot z_{sj}} = K_{z_{sj}} = K_z = K_{\eta_2} = K_{\eta_3} = K_{\eta_3}^\cdot = 0$	$3 \cdot 10^5$	$3 \cdot 10^5$	14.5	$1.4 \cdot 10^{13}$	150	$1.8 \cdot 10^{14}$	160	$4.2 \cdot 10^{15}$	160	$4 \cdot 10^{10}$	145	3100
Simplified Controller	0.0079	0.012	0.0016	0.0044	140	0.0177	80	0.0670	75	0.020	140	0.0173
Limits (γ^2)	$3.52 \cdot 10^{-3}$	$4.9 \cdot 10^3$	$9 \cdot 10^8$	$8.1 \cdot 10^{13}$		$2.89 \cdot 10^{12}$		$2.5 \cdot 10^{11}$		$7.62 \cdot 10^{-3}$		

(a) T_p indicates time of occurrence of peak

controller A for the rigid-body and flexure states except that the z and η_2 gains were set to zero and the output of the estimator times the gains of controller A for the estimated states.

The estimator was designed with the assumptions that $E\{\xi \ \xi'\} = \frac{1}{10}$ $E\{\eta^2\} \begin{bmatrix} 1 & 0 \\ 0 & 1 \end{bmatrix}$ and $E\{\xi \eta'\} = \begin{bmatrix} 0 \\ 0 \end{bmatrix}$ where ξ is the noise vector associated with the measurements, equation (4.27) and η is the noise input to the wind filter, equation (2.13).

The estimator gains are shown in Figures 8a and 8b. Figure 9 shows the normalized error variances of the estimates of the wind states for the estimator defined by equation (4.28). The normalized error variances of the load distribution states are almost identical to the normalized error variance of w shown on Figure 9. It is evident from this figure that the quality of the estimates is very poor.

The controller exhibits fairly good performance considering the quality of the estimates obtained. The total cost is 0.0173, and this cost is completely due to the IB3 response during the interval from 70 to 85 seconds. The response covariances for this simplified controller are summarized in Table 6 for comparison with the results of the experiments.

It is believed, in view of the results of experiments 7 and 8, that the performance of this controller could be improved by setting the gain on the estimate of the wind state, x, to zero and modifying the gain on the estimate of the load-distribution state, x_3, during the interval of high dynamic pressure.
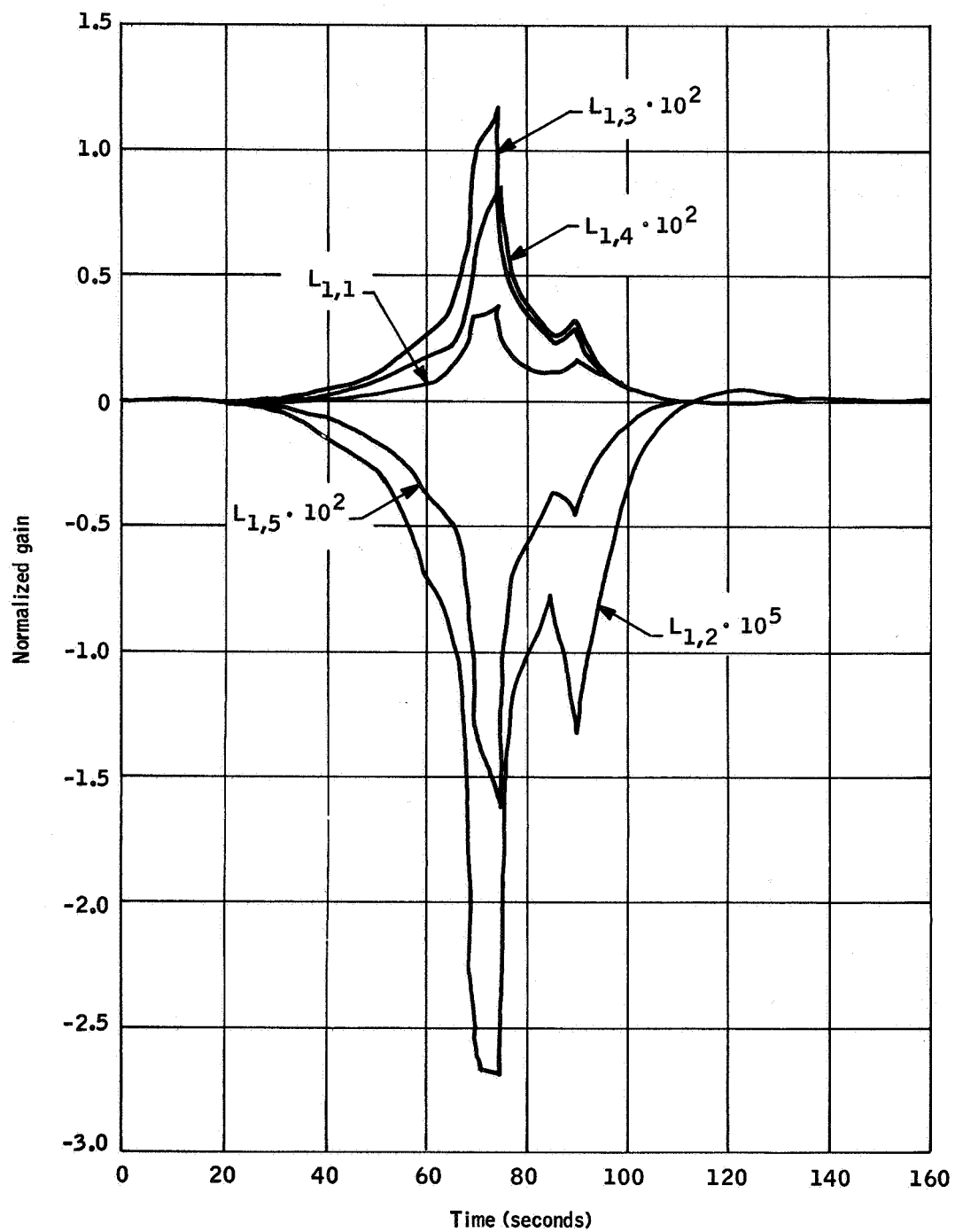
Figure 8a. Estimator Gains
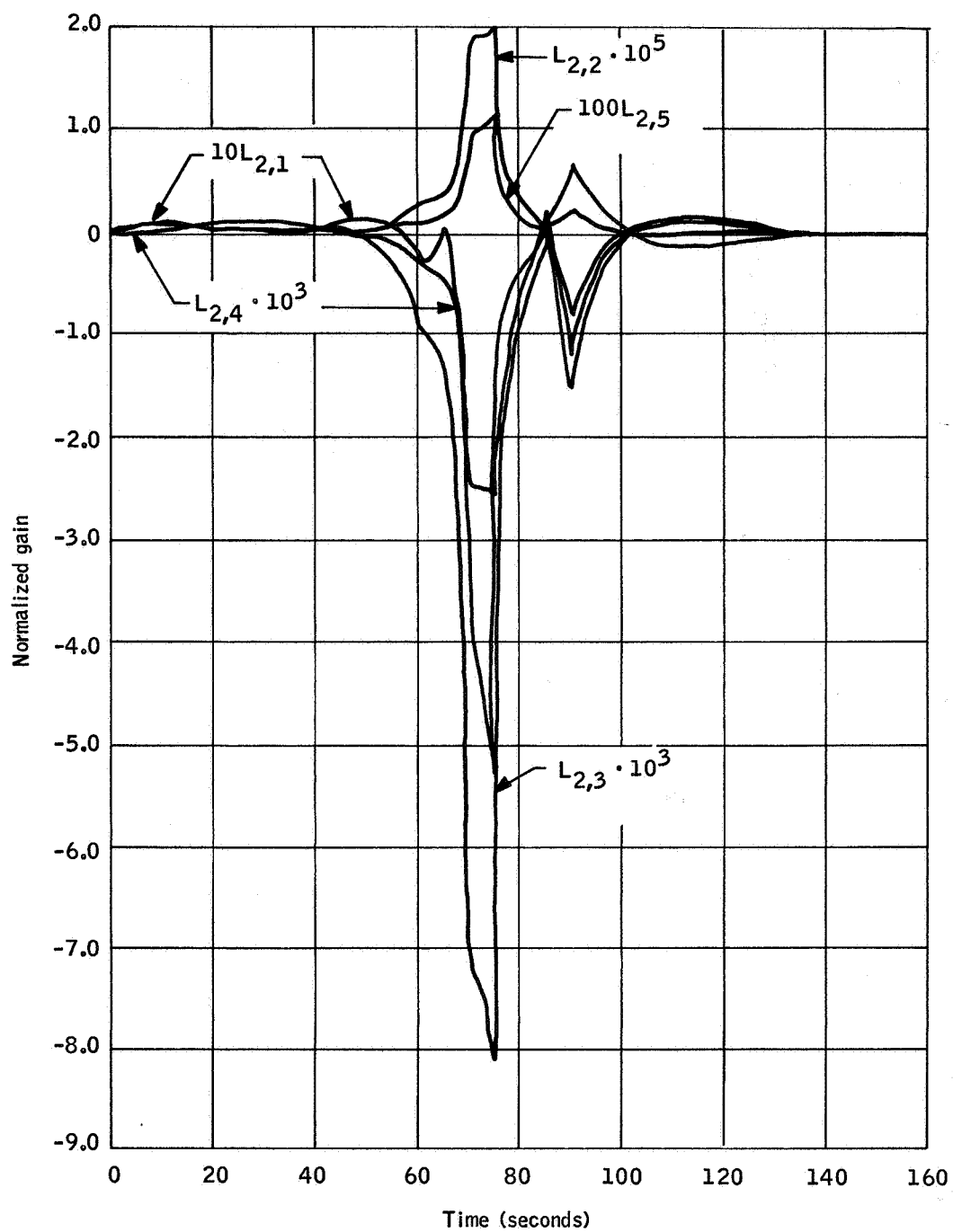
Figure 8b. Estimator Gains
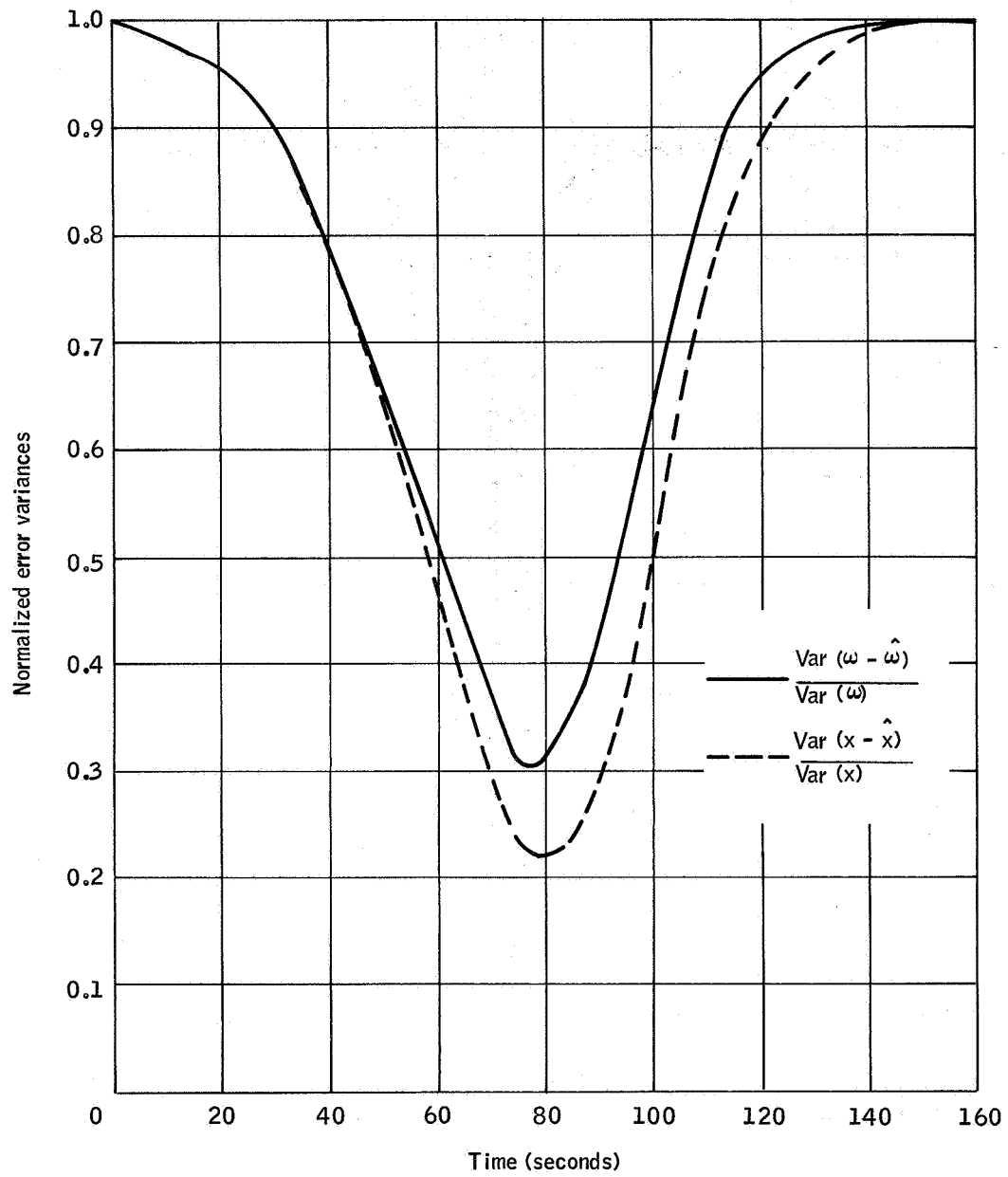
Figure 9. Normalized Error Variances of Estimated States

SECTION VI
CONCLUSIONS AND RECOMMENDATIONS

The first goal of this investigation was reached by demonstrating the applicability of the stochastic optimization theory to a vehicle model containing flexure and fuel slosh dynamics. The overall goal was only partially reached by demonstrating that the controller produced by the optimization theory could be simplified to a physically realizable, practical controller. The second goal was not met in that no satisfactory technique was developed to determine the minimum number of sensors, the kinds of sensors, and the sensor location required for good controller performance. Some insight was gained on the question of sensor choice and location, but a complete answer was not obtained.

The specific conclusions and recommendations for future study in the areas of optimization, sensor choice, and controller simplification are presented below.

Optimization

Optimization with complete measurement capability was easily performed for the model vehicle studied using essentially a direct iterative procedure on the quadratic weights. No attempt was made to achieve complete convergence in that iterations were stopped when a satisfactory controller was obtained.

Improved convergence of the iterative procedure could probably be achieved using results privately communicated to Dr. G.B. Skelton from Prof. J.Y.S. Luh and Mr. M. Lukas of Purdue University. The iteration procedure described in Section III would be modified as follows:

a) Find initial R_o and S_o matrices corresponding to an initial controller obtained by application of the quadratic theory to minimize J** with an initial choice of Q and V matrices.

b)   Given R_i and S_i compute the matrices $\frac{\partial f}{\partial R}$ and $\frac{\partial f}{\partial S}$ evaluated at $R = R_i$, $S = S_i$.

c)   Set $Q_i = \frac{\partial f}{\partial S}$ and $V = \frac{\partial f}{\partial R}$ and find the minimizing control for J^{**} by application of the quadratic theory.

d)   Compute the corresponding R and S matrices and denote them by $\hat{R}_i$ and $\hat{S}_i$.

e)   Compute $J^*(\lambda) = f_1[\lambda S_i(T) + (1-\lambda)\hat{S}_i(T), \; \lambda R_i(T) + (1-\lambda)\hat{R}_i(T)]$

$$+ \int_0^T f_2[\lambda S_i(t) + (1-\lambda)\hat{S}_i(t), \; \lambda R_i(t) + (1-\lambda)\hat{R}_i(t)]dt$$

and find the $\lambda_o \in [0, 1]$ that minimizes $J^*(\lambda)$ for $0 \le \lambda \le 1$.

f)   Set $R_{i+1} = \lambda_o R_i + (1-\lambda_o)\hat{R}_i$ and $S_{i+1} + (1-\lambda_o)\hat{S}_i$ and repeat steps (b) through (e) until condition (3.13) is satisfied.

For the study vehicle considered there were no significant problems associated with the iterative procedure used. These iterations indicated that the terminal constraints could easily be met. The bending moments during the interval of high dynamic pressure were the difficult responses to control during the iterations, using the model containing the error in the pitch rate coefficient of the bending-moment equation. With the correct pitch-rate coefficient, the gimbal angle near burnout became the dominant response requiring control. The resulting controller exhibited remarkable load-relief capability, but apparently this capability is highly dependent on accurate knowledge of the fuel-sloshing motion. Thus, developing a means of accurately measuring or estimating fuel-slosh motion could pay great dividends in load-relief capability.

Sensor Choice

The analytic measures of quality defined in this study and discussed in Section IV were not satisfactory means of predicting the quality of sensor complements for control purposes. These measures of quality were based on the premise that the optimal controller for any given sensor complement with which satisfactory performance could be achieved would closely approximate the optimal controller using complete state feedback. This apparently was not true for the sensor complements considered.

The first measure of quality was evaluated for only one sensor complement with such dismal results that it was not investigated further. In retrospect, this was not a fair evaluation of the measure because all of the information available from the sensor complement was not utilized; that is, the integrals of some of the sensor signals were not included in the measurement or observation vector. Better results could probably have been obtained if these integrals had been included in the measurement vector. However, the question of whether the basic premise upon which the measures of quality were derived is true or not could not be answered in the present study.

A method for determining the answer to this question is to solve the optimization problem with the controller constrained to be a linear controller with a fixed set of feedback sensors and then compare the resulting controller with the optimal controller using complete state feedback. A procedure which makes the optimization problem with a controller of fixed form amenable to digital computer solution is given in reference 3.

Controller Simplification

The optimal controller with complete measurement capability provided insights as to possible controller simplification. Generally those states which made minor contributions to the controller could be neglected without causing major deterioration in performance. This was also true for those states which directly contribute to the IB3 response.

71

Empirical results indicate that:

- The wind state, ω, and load-distribution states are significant feedbacks and probably require estimation for good controller performance.

- The fuel-slosh and second-flexure-mode degrees of freedom and the drift feedbacks may be simultaneously deleted from controller A without severe deterioration in performance.

- The simplified controller which involves a fifth-order estimator and the outputs of five accelerometers and their integrals gives fairly good performance in spite of rather poor quality estimates.

It is believed that the performance of this simplified controller could be improved and that the controller could be further simplified with more simulation studies. However, digital simulation is a very expensive means of experimentation, and it is recommended that an analog or hybrid simulation be utilized in controller simplification studies.

A basic question which became evident but was unanswered from this analysis is: What interaction in the form of coupling or cancellation takes place between particular state feedbacks? The existence of such interactions was clearly demonstrated between the wind states and a load-distribution state and between fuel-sloshing states and the second-flexure-mode states. One way to seek the answer to this question is by costly simulation analyses. Another approach which may be fruitful is to utilize frequency domain analysis techniques for constant coefficient representations of the model at particular times during the launch interval, since these techniques can provide information concerning interaction that is difficult to obtain from time domain analysys techniques.

In summary the fundamental goal of the sensor choice and controller simplification approach was not reached. Although, for the study vehicle considered, this investigation did lead to a practical simplified controller, a general technique was not developed. It is felt that the analysis performed

did give some clues but did not give a complete answer to the problems of controller simplification and sensor choice. Techniques described in this section are suggested for further study of these problems.

REFERENCES

1. L. D. Edinger, et al., "Design of a Load-Relief Control System", NASA Contractor Report CR-61169, April 21, 1967.

2. Honeywell Final Report 21171-SR1, "Data Base Report for Saturn V/ Voyager Load Relief Study", 15 September 1967 (updated 30 January 1968), prepared for NASA-MSFC, Contract NAS 8-21171.

3. Sven Axsäter, "Sub-optimal Time-variable Feedback Control of Linear Dynamic Systems with Random Inputs", Int. J. Control, 1966, Vol. 4, No. 6, pp. 549-566.

4. MSFC Memo, "Static Aerodynamic Characteristics of the Saturn V/ Voyager (45' shroud length)", December 20, 1966.

APPENDIX A

DISTRIBUTED AERODYNAMIC LOADING APPROXIMATIONS

APPENDIX A
DISTRIBUTED AERODYNAMIC LOADING APPROXIMATIONS

This appendix presents the distribution of aerodynamic forces along the length of the vehicle and the approximations of the distributed loading used in this study. The model developed here is a modification of the model developed in reference 1. The major changes consist of a modification of the formulae for the side force per unit length per unit angle of attack, because of the different vehicle used in this study, and incorporating distributed effects in the flexure modes.

As stated in reference 1, the objective is to develop a model that will yield qualitatively correct trends for the study. The model is the simplest that can be conceived, and results obtained from synthesizing controls for the model should be interpreted with caution.

Formulae for the estimated side force per unit length per unit angle of attack are presented first. Then the derivation of the coefficients for distributing wind effects is described.

Approximation of $d\tilde{t}/d\alpha$

An approximation of $d\tilde{t}/d\alpha$ is derived in Appendix C of reference 1 for "Model Vehicle No. 2 for Advanced Control Studies". The Saturn V/Voyager with a 45-foot length shroud is assumed to differ from Model Vehicle No. 2 only forward of station 63.97 meters. Thus the same approximation is used for x < 63.97, namely:

$$\frac{1}{q}\frac{d\tilde{t}}{d\alpha} = 21.223 - 2.45\,x \qquad 0.63 \le x \le 1.63$$

$$= F_1\,(9.17,\ M,\ x) \qquad 1.63 < x \le 2.54$$

$$= F_1\,(19.22,\ M,\ x) \qquad 2.54 < x \le 3.14$$

$$= F_2 (M, x) \qquad\qquad 3.14 < x \le 5.05$$

$$= 21.6056 - 2.455x \qquad 5.05 < x \le 8.32$$

$$= 1.1850 \qquad\qquad 8.32 < x \le 63.97$$

where x denotes distance in meters along vehicle measured from a point 2.54 meters behind the engine gimbal location, M denotes Mach number, q denotes dynamic pressure in kg/m^2, α denotes angle of attack in radians and

$$F_1(C, M, x) = 4\, C (1-M^2)^{-1/2} \qquad\qquad M < \sqrt{3}/2$$

$$= 8\left[C - 2(3.14-x)\, \frac{2M - \sqrt{3}}{\sqrt{5} - \sqrt{3}} \right] \qquad \sqrt{3}/2 \le M \le \sqrt{5}/2$$

$$= \frac{4}{M^2 - 1}\, C\, \sqrt{M^2 - 1} - (3.14-x) \qquad \sqrt{5}/2 < M$$

$$F_2(M, x) = 4(31.26 - 3.805x)(1-M^2)^{-1/2} \qquad M < \sqrt{3}/2$$

$$= 8(31.26 - 3.805x) \qquad\qquad \sqrt{3}/2 \le M \le \sqrt{5}/2$$

$$= 4(31.26 - 3.805x)(M^2 - 1)^{-1/2} \qquad \sqrt{5}/2 < M.$$

The following estimate for the forward section of the vehicle was obtained using the method described in reference 1:

$$\frac{1}{q}\, \frac{d\tilde{t}}{d\alpha} = (80.67-x)\, \frac{32}{3}\, \sin^2 \theta_2 \cos \theta_2 \qquad 63.97 < x \le 69.70$$

$$= 0.2477\pi \qquad\qquad 69.70 < x \le 96.46$$

$$= (114.2-x)\, \frac{32}{3}\, \sin^2 \theta_1 \cos \theta_1 \qquad 96.46 < x \le 100.7$$

$$= (105.0-x)\, \frac{32}{3}\, \sin^2 \theta_0 \cos \theta_0 \qquad 100.7 < x \le 105.0$$

where $\tan \theta_o = \dfrac{25}{43}$, $\tan \theta_1 = \dfrac{31}{0.42(396)}$, and $\tan \theta_2 = \dfrac{68}{0.57(396)}$.

The estimates above were not consistent with the data given in Figures 14-18 of reference 4. To obtain better consistency with this data the estimate forward of 63.97 meters was changed to

$$\frac{1}{q} \frac{d\tilde{t}}{d\alpha} = (80.67 - x)\frac{32}{3}\sin^2 \theta_2 \cos \theta_2 + 7.0 \qquad 63.97 < x \le 69.70$$

$$= 0.2477\pi \qquad 69.70 < x \le 89.92$$

$$= 5.0 + 0.2477\pi \qquad 89.92 < x \le 96.46$$

$$= (114.2 - x)\frac{32}{3}\sin^2 \theta_1 \cos \theta_1 + c(t) \qquad 96.46 < x \le 100.7$$

$$= (105.0 - x)\frac{32}{3}\sin^2 \theta_o \cos \theta_o \qquad 100.7 < x \le 105.0$$

where θ_o, θ_1, θ_2 are unchanged and $c(t) = 12$ for $60 \le t \le 70$ and $c(t) = 7$ otherwise.

Distributed Load Coefficients

The integrals to be approximated are of the form

$$\int_o^{x_N} \frac{d\tilde{t}}{d\alpha} \frac{v_w(x, t)}{V(t)} g_i(x, t)\, dx$$

and the approximations are obtained by setting

$$\frac{d\tilde{t}}{d\alpha} g_i = a_{2i-1}(t) h_1(x_N - x) + a_{2i} h_2(x_N - x)$$

where x_N denotes the length of the vehicle and $h_1(r)$ and $h_2(r)$, the impulse responses of a first-order filter and a second-order Pade type filter, are given by

$$h_1(r) = \frac{1}{2\pi j} \int_{-j\infty}^{j\infty} e^{sr} \frac{1}{sX_1+1} \, ds,$$

and

$$h_2(r) = \frac{1}{2\pi j} \int_{-j\infty}^{-\infty} e^{sr} \frac{-5X_2 s + 6}{(X_2 s)^2 + 4X_2 s + 6} \, ds$$

Then

$$\int_0^{x_N} \frac{d\tilde{t}}{d\alpha} \frac{v_\omega(x,t)}{V} g_i(x,t) \, dx = \int_0^{x_N} [a_{2i-1} h_1(x_N - x) + a_{2i} h_2(x_N - x)] \frac{v_\omega(x,t)}{V} \, dx$$

$$= a_{2i-1} \int_0^{x_N} h_1(x_N - x) v_\omega\left[x_N, t - \frac{x_N - x}{V}\right] \frac{dx}{V} + a_{2i} \int_0^{x_N} h_2(x_N - x) v_\omega\left[x_N, t\right.$$

$$\left. - \frac{x_N - x}{V}\right] \frac{dx}{V}$$

$$= a_{2i-1} \int_0^{x_N} h_1(rV) v_\omega(x_N, t-r) \frac{dr}{V} + a_{2i} \int_0^{x_N} h_2(rV) v_\omega(x_N, t-r) \frac{dr}{V}$$

$$\approx a_{2i-1} x_1 + a_{2i} x_2$$

Thus the coefficients $a_{2i-1}(t)$, $a_{2i}(t)$ must be determined for $i = 1, 2, \ldots, 8$ where $g_1 = 1$, $g_2 = x - x_{cg}$, $g_3 = Y_1(x)$, $g_4 = Y_2(x)$, $g_5 = Y_3(x)$, $g_{5+j} = (x - x_{cg})$ $Y_1 + Y_2 + (x_j - x) \chi(x_j - x)$ for $j = 1, 2, 3$ and x_j denote the locations for which bending moment responses are being considered.

First, the coefficients were normalized by requiring

$$a_1 + a_2 = N$$

A4

$$a_3 + a_4 = N\ell_{cp}$$

$$a_{3+2i} + a_{4+2i} = N_{\dot{\eta}_i}, \quad i = 1, 2, 3$$

$$a_{9+2j} + a_{10+2j} = M_\alpha'(x_j), \quad j = 1, 2, 3$$

where the terms on the right are the steady aerodynamic terms. This normalization is intended to enforce consistency with the data for constant loading, i.e.,

$$\int_o^{x_N} [a_1 h_1(x) + a_2 h_2(x)]\, dx = N \text{ since } \int_o^{x_N} h_i(x)\, dx \approx 1.$$

The integrals, $w_i(x, t) = \int_x^{x_N} \dfrac{d\tilde{t}}{d\alpha}\, g_i(y, t)\, dy$, were computed and the corresponding $a_{2i-1}(t)$ and $a_{2i}(t)$ were chosen so that

$$\int_o^{x_N} [a_{2i-1}(t)\, h_1(x_N - x) + a_{2i}(t)\, h_2(x_N - x)]\, dx$$

approximated $w_i(x, t)$ qualitatively.

APPENDIX B

COEFFICIENT MATRICES

APPENDIX B
COEFFICIENT MATRICES

The coefficient matrices for the continuous state and response equations are presented in this appendix. Certain properties of these matrices are also derived.

For simplicity in displaying the results the state vector and coefficient matrices will be partitioned as follows:

$$x = \begin{bmatrix} x^1 \\ x^2 \\ x^3 \\ x^4 \end{bmatrix}, \quad x^1 = \begin{bmatrix} \dot{\varphi} \\ \dot{z} \\ \dot{\eta}_1 \\ \dot{\eta}_2 \\ \dot{\eta}_3 \end{bmatrix}, \quad x^2 = \begin{bmatrix} \dot{z}_{s1} \\ \dot{z}_{s2} \\ \dot{z}_{s3} \end{bmatrix}, \quad x^3 = \begin{bmatrix} \varphi \\ z \\ \eta_1 \\ \eta_2 \\ \eta_3 \\ z_{s1} \\ z_{s2} \\ z_{s3} \end{bmatrix}, \quad x^4 = \begin{bmatrix} \beta \\ \omega \\ x \\ x_1 \\ x_2 \\ x_3 \end{bmatrix}$$

$$A = \begin{bmatrix} A_{11} & A_{12} & A_{13} & A_{14} \\ A_{21} & A_{22} & A_{23} & A_{24} \\ A_{31} & A_{32} & A_{33} & A_{34} \\ A_{41} & A_{42} & A_{43} & A_{44} \end{bmatrix} \qquad B = \begin{bmatrix} B_{11} & B_{12} & B_{13} & B_{14} \\ B_{21} & B_{22} & B_{23} & B_{24} \\ B_{31} & B_{32} & B_{33} & B_{34} \\ B_{41} & B_{42} & B_{43} & B_{44} \end{bmatrix}$$

$$C = \begin{bmatrix} C_1 \\ C_2 \\ C_3 \\ C_4 \end{bmatrix}, \quad D = \begin{bmatrix} D_1 \\ D_2 \\ D_3 \\ D_4 \end{bmatrix}, \quad E = \begin{bmatrix} E_1 \\ E_2 \\ E_3 \\ E_4 \end{bmatrix}$$

where the A_{ij}, B_{ij}, C_i, D_i, E_i are of appropriate dimensions to be consistent with the partitioning of x. Also set

$$\tilde{r} = \begin{bmatrix} \tilde{r}^1 \\ \tilde{r}^2 \\ \tilde{r}^3 \end{bmatrix} \quad \text{where } \tilde{r}^1 = \begin{bmatrix} \beta \\ \dot{\beta} \end{bmatrix}, \quad \tilde{r}^2 = \begin{bmatrix} IB1 \\ IB2 \\ IB3 \end{bmatrix}, \quad \tilde{r}^3 = \begin{bmatrix} \alpha \\ \dot{\phi} \\ \dot{z} \\ \phi \\ z \end{bmatrix}$$

and

$$H_i = \begin{bmatrix} H_{11}{}^i & H_{12}{}^i & H_{13}{}^i & H_{14}{}^i \\ H_{21}{}^i & H_{22}{}^i & H_{23}{}^i & H_{24}{}^i \\ H_{31}{}^i & H_{32}{}^i & H_{33}{}^i & H_{34}{}^i \end{bmatrix} \quad \text{for } i = 1, \ 2 \text{ with } H_{jk}{}^i$$

of appropriate dimensions and partition $\tilde{C}$ and $\tilde{E}$ in the form $\tilde{C} = \begin{bmatrix} \tilde{C}_1 \\ \tilde{C}_2 \\ \tilde{C}_3 \end{bmatrix}$, $E = \begin{bmatrix} \tilde{E}_1 \\ \tilde{E}_2 \\ \tilde{E}_3 \end{bmatrix}$

With I_n denoting the n x n identity matrix, A and B may be written as

$$A = \begin{bmatrix} I_5 & A_{12} & 0 & 0 \\ A_{21} & I_3 & 0 & 0 \\ 0 & 0 & I_8 & 0 \\ 0 & 0 & 0 & I_6 \end{bmatrix} \quad \text{and B} = \begin{bmatrix} B_{11} & 0 & B_{13} & B_{14} \\ 0 & B_{22} & B_{23} & 0 \\ B_{31} & B_{32} & 0 & 0 \\ 0 & 0 & 0 & B_{44} \end{bmatrix}$$

B2

where

$$A_{12} = \begin{bmatrix} (x_{s1}-x_{cg})M_{s1}/I_{yy} & (x_{s2}-x_{cg})M_{s2}/I_{yy} & (x_{s3}-x_{cg})M_{s3}/I_{yy} \\ M_{s1}/M & M_{s2}/M & M_{s3}/M \\ Y_1(x_{s1})M_{s1}/M_1 & Y_1(x_{s2})M_{s2}/M_1 & Y_1(x_{s3})M_{s3}/M_1 \\ Y_2(x_{s1})M_{s1}/M_2 & Y_2(x_{s2})M_{s2}/M_2 & Y_2(x_{s3})M_{s3}/M_2 \\ Y_3(x_{s1})M_{s1}/M_3 & Y_3(x_{s2})M_{s2}/M_3 & Y_3(x_{s3})M_{s3}/M_3 \end{bmatrix}$$

$$A_{21} = \begin{bmatrix} x_{s1}-x_{cg} & 1 & Y_1(x_{s1}) & Y_2(x_{s1}) & Y_3(x_{s1}) \\ x_{s2}-x_{cg} & 1 & Y_1(x_{s2}) & Y_2(x_{s2}) & Y_3(x_{s2}) \\ x_{s3}-x_{cg} & 1 & Y_1(x_{s3}) & Y_2(x_{s3}) & Y_3(x_{s3}) \end{bmatrix}$$

$$A_{11} = -\begin{bmatrix} T_{\dot{\varphi}}/VI_{yy} & N\ell_{cp}/VI_{yy} & T_{\dot{\eta}_1}/VI_{yy} & T_{\dot{\eta}_2}/VI_{yy} & T_{\dot{\eta}_3}/VI_{yy} \\ N\ell_{cp}/MV & N/MV & N_{\dot{\eta}_1}/MV & N_{\dot{\eta}_2}/MV & N_{\dot{\eta}_3}/MV \\ T_{\dot{\eta}_1}/M_1 V & N_{\dot{\eta}_1}/M_1 V & (N_{\dot{\eta}_{11}}/M_1 V)-2\zeta_1\omega_1 & 0 & 0 \\ T_{\dot{\eta}_2}/M_2 V & N_{\dot{\eta}_2}/M_2 V & 0 & (N_{\dot{\eta}_{22}}/M_2 V)-2\zeta_2\omega_2 & 0 \\ T_{\dot{\eta}_3}/M_3 V & N_{\dot{\eta}_3}/M_3 V & 0 & 0 & (N_{\dot{\eta}_{33}}/M_3 V)-2\zeta_3\omega_3 \end{bmatrix}$$

$$B_{13} = \begin{bmatrix} \dfrac{N\ell_{cp}}{I_{yy}} & 0 & \dfrac{\tilde{T}\eta_1}{I_{yy}} & \dfrac{\tilde{T}\eta_2}{I_{yy}} & \dfrac{\tilde{T}\eta_3}{I_{yy}} & \dfrac{M_{s1}A_x}{I_{yy}} & \dfrac{M_{s2}A_x}{I_{yy}} & \dfrac{M_{s3}A_x}{I_{yy}} \\[2mm] \dfrac{T-D+N}{M} & 0 & \dfrac{\tilde{N}\eta_1}{M} & \dfrac{\tilde{N}\eta_2}{M} & \dfrac{\tilde{N}\eta_3}{M} & 0 & 0 & 0 \\[2mm] \dfrac{N\eta_1}{M_1 V} & 0 & \dfrac{N\eta_{11}}{M_1}-\omega_1^2 & 0 & 0 & \dfrac{M_{s1}A_x Y_1'(x_{s1})}{M_1} & \dfrac{M_{s2}A_x Y_1'(x_{s2})}{M_1} & \dfrac{M_{s3}A_x Y_1'(x_{s3})}{M_1} \\[2mm] \dfrac{N\eta_2}{M_1 V} & 0 & 0 & \dfrac{N\eta_{22}}{M_2}-\omega_2^2 & 0 & \dfrac{M_{s1}A_x Y_2'(x_{s1})}{M_2} & \dfrac{M_{s2}A_x Y_2'(x_{s2})}{M_2} & \dfrac{M_{s3}A_x Y_2'(x_{s3})}{M_2} \\[2mm] \dfrac{N\eta_3}{M_1 V} & 0 & 0 & 0 & \dfrac{N\eta_{33}}{M_3}-\omega_3^2 & \dfrac{M_{s1}A_x Y_3'(x_{s1})}{M_3} & \dfrac{M_{s2}A_x Y_3'(x_{s2})}{M_3} & \dfrac{M_{s3}A_x Y_3'(x_{s3})}{M_3} \end{bmatrix}$$

where $\tilde{T}_{\eta_i} = T_{\eta_i} - T Y_i(x_\beta) - T(x_{cg}-x_\beta)Y_i'(x_\beta)$, $A_x = (T-D)/M$ and $\tilde{N}_{\eta_i} = N_{\eta_i} + (T-D)Y_i(x_\beta)$,

$$B_{14} = \begin{bmatrix} R'(x_{cg}-x_\beta)/I_{yy} & 0 & 0 & a_1 & a_2 & 0 \\[2mm] R'/M & 0 & 0 & a_3 & a_4 & 0 \\[2mm] R'Y_1(x_\beta)/M_1 & 0 & 0 & a_5 & a_6 & 0 \\[2mm] R'Y_2(x_\beta)/M_2 & 0 & 0 & a_7 & a_8 & 0 \\[2mm] R'Y_3(x_\beta)/M_3 & 0 & 0 & a_9 & a_{10} & 0 \end{bmatrix}$$

B4

$$B_{22} = \begin{bmatrix} -2\zeta_{s1}\omega_{s1} & 0 & 0 \\ 0 & -2\zeta_{s2}\omega_{s2} & 0 \\ 0 & 0 & -2\zeta_{s3}\omega_{s3} \end{bmatrix}$$

$$B_{23} = \begin{bmatrix} A_x & 0 & A_xY_1'(x_{s1}) & A_xY_2'(x_{s1}) & A_xY_3'(x_{s1}) & -\omega_{s1}^2 & 0 & 0 \\ A_x & 0 & A_xY_1'(x_{s2}) & A_xY_2'(x_{s2}) & A_xY_3'(x_{s2}) & 0 & -\omega_{s2}^2 & 0 \\ A_x & 0 & A_xY_1'(x_{s3}) & A_xY_2'(x_{s3}) & A_xY_3'(x_{s3}) & 0 & 0 & -\omega_{s3}^2 \end{bmatrix}$$

$$B_{31} = \begin{bmatrix} I_5 \\ 0 \end{bmatrix} \;, \quad B_{32} = \begin{bmatrix} 0 \\ I_3 \end{bmatrix}$$

$$B_{44} = \begin{bmatrix} -11.9 & 0 & 0 & 0 & 0 & 0 \\ 0 & 0 & c_3\dot{h} & 0 & 0 & 0 \\ 0 & -c_5\dot{h} & -c_4\dot{h} & 0 & 0 & 0 \\ 0 & \sigma_{v_\omega}/X_1 & 0 & -V/X_1 & 0 & 0 \\ 0 & -5\sigma_{v_\omega}/X_2 & 0 & 0 & -4V/X_2 & -6V/X_2 \\ 0 & \sigma_{v_{(\eta)}}/X_2 & 0 & 0 & V/X_2 & 0 \end{bmatrix}$$

The vectors C_i, D_i, and E_i are all zero for $i = 1$, 2, and 3.

$$C_4 = \begin{bmatrix} 11.9 \\ 0 \\ 0 \\ 0 \\ 0 \\ 0 \end{bmatrix}, \quad D_4 = \begin{bmatrix} 0 \\ C_1 \\ C_2 \\ 0 \\ 0 \\ 0 \end{bmatrix} \sqrt{h}, \quad E_4 = \begin{bmatrix} 0 \\ 0 \\ 0 \\ (X_1)^{-1} \\ -5(X_2)^{-1} \\ (X_2)^{-1} \end{bmatrix}$$

The inverse of A is (partitioned in the same manner)

$$A^{-1} = \begin{bmatrix} I_5 + A_{12}(I_3 - A_{21}A_{12})^{-1}A_{21} & -A_{12}(I_3 - A_{21}A_{12})^{-1} & 0 & 0 \\ -(I_3 - A_{21}A_{12})^{-1}A_{12} & (I_3 - A_{21}A_{12})^{-1} & 0 & 0 \\ 0 & 0 & I_8 & 0 \\ 0 & 0 & 0 & I_6 \end{bmatrix}$$

Thus $A^{-1}C = C$, $A^{-1}D = D$, $A^{-1}E = E$ and $A^{-1}B$ is

$$A^{-1}B = \begin{bmatrix} B_{11}A_{12}\Delta A_{21}B_{11} & -A_{12}\Delta B_{22} & B_{13} + A_{12}\Delta(A_{21}B_{13} - B_{23}) & B_{14} + A_{12}\Delta A_{21}B_{14} \\ -\Delta A_{12}B_{11} & \Delta B_{22} & \Delta(B_{23} - A_{12}B_{13}) & -\Delta A_{12}B_{14} \\ B_{31} & B_{32} & 0 & 0 \\ 0 & 0 & 0 & B_{44} \end{bmatrix}$$

where $\Delta = (I_3 - A_{21}A_{12})^{-1}$.

B6

The coefficients in the response equations are of the form

$$H_1 = \begin{bmatrix} 0 & 0 & 0 & H_{14}{}^1 \\ H_{21}{}^1 & 0 & H_{23}{}^1 & H_{24}{}^1 \\ H_{31}{}^1 & 0 & H_{33}{}^1 & H_{34}{}^1 \end{bmatrix}, \quad H_2 = \begin{bmatrix} 0 & 0 & 0 & 0 \\ H_{21}{}^2 & 0 & 0 & 0 \\ 0 & 0 & 0 & 0 \end{bmatrix}$$

$$\widetilde{C} = \begin{bmatrix} \widetilde{C}_1 \\ 0 \\ 0 \end{bmatrix}, \quad \widetilde{E} = \begin{bmatrix} 0 \\ 0 \\ \widetilde{E}_3 \end{bmatrix} \quad \text{where}$$

$$H_{14}{}^1 = \begin{bmatrix} 1 & 0 & 0 & 0 & 0 & 0 \\ -11.9 & 0 & 0 & 0 & 0 & 0 \end{bmatrix}, \quad \widetilde{C}_1 = \begin{bmatrix} 0 \\ 11.9 \end{bmatrix}$$

$$H_{21}{}^1 = \begin{bmatrix} M_\varphi{}^{\prime}(x_1) & -M_\alpha{}^{\prime}(x_1)/V & 0 & 0 & 0 \\ M_\varphi{}^{\prime}(x_2) & -M_\alpha{}^{\prime}(x_2)/V & 0 & 0 & 0 \\ M_\varphi{}^{\prime}(x_3) & -M_\alpha{}^{\prime}(x_3)/V & 0 & 0 & 0 \end{bmatrix}$$

$$H_{23}{}^1 = \begin{bmatrix} M_\alpha{}^{\prime}(x_1) & 0 & 0 & 0 & 0 & 0 & 0 & 0 \\ M_\alpha{}^{\prime}(x_2) & 0 & 0 & 0 & 0 & 0 & 0 & 0 \\ M_\alpha{}^{\prime}(x_3) & 0 & 0 & 0 & 0 & 0 & 0 & 0 \end{bmatrix}$$

$$H_{24}{}^1 = \begin{bmatrix} M_\beta{}^{\prime}(x_1) & 0 & 0 & a_{11} & a_{12} & 0 \\ M_\beta{}^{\prime}(x_2) & 0 & 0 & a_{13} & a_{14} & 0 \\ M_\beta{}^{\prime}(x_3) & 0 & 0 & a_{15} & a_{16} & 0 \end{bmatrix}$$

$$
H_{21}{}^2 = \begin{bmatrix} 0 & 0 & M^{'}_{\ddot{\eta}_1}(x_1) & M^{'}_{\ddot{\eta}_2}(x_1) & M^{'}_{\ddot{\eta}_3}(x_1) \\ 0 & 0 & M^{'}_{\ddot{\eta}_1}(x_2) & M^{'}_{\ddot{\eta}_2}(x_2) & M^{'}_{\ddot{\eta}_3}(x_2) \\ 0 & 0 & M^{'}_{\ddot{\eta}_1}(x_3) & M^{'}_{\ddot{\eta}_2}(x_3) & M^{'}_{\ddot{\eta}_3}(x_3) \end{bmatrix}
$$

$$
H_{31}{}^1 = \begin{bmatrix} 0 & -V^{-1} & 0 & 0 & 0 \\ 1 & 0 & 0 & 0 & 0 \\ 0 & 1 & 0 & 0 & 0 \\ 0 & 0 & 0 & 0 & 0 \\ 0 & 0 & 0 & 0 & 0 \end{bmatrix}
$$

$$
H_{33}{}^1 = \begin{bmatrix} 1 & 0 & 0 & 0 & 0 & 0 & 0 & 0 \\ 0 & 0 & 0 & 0 & 0 & 0 & 0 & 0 \\ 0 & 0 & 0 & 0 & 0 & 0 & 0 & 0 \\ 1 & 0 & 0 & 0 & 0 & 0 & 0 & 0 \\ 0 & 1 & 0 & 0 & 0 & 0 & 0 & 0 \end{bmatrix}
$$

$$
H_{34}{}^1 = \begin{bmatrix} 0 & \sigma_{v_w}/V & 0 & 0 & 0 & 0 \\ 0 & 0 & 0 & 0 & 0 & 0 \\ 0 & 0 & 0 & 0 & 0 & 0 \\ 0 & 0 & 0 & 0 & 0 & 0 \\ 0 & 0 & 0 & 0 & 0 & 0 \end{bmatrix} \quad \text{and} \quad \widetilde{E}_3 = \begin{bmatrix} V^{-1} \\ 0 \\ 0 \\ 0 \\ 0 \end{bmatrix}
$$

The only nonzero element of the partitioned H_2 is in the first column. But the first row of each of the partitioned, C, D, and E and hence of $A^{-1}C$, $A^{-1}D$ and $A^{-1}E$ are zero. Therefore, the products $H_2 A^{-1}C$, $H_2 A^{-1}D$, and $H_2 A^{-1}E$ are zero. Thus

B8

$$\tilde{r}^2 = [H_{21}{}^1 + H_{21}{}^2 (B_{11} + A_{12} \Delta A_{21} B_{11})] x^1 - H_{21}{}^2 A_{12} \Delta B_{22} x^2$$

$$+ \left\{ H_{23}{}^1 + H_{21}{}^2 [B_{13} + A_{12} \Delta (A_{21} B_{13} - B_{23})] \right\} x^3$$

$$+ [H_{24}{}^1 + H_{21}{}^2 (B_{14} + A_{12} \Delta A_{21} B_{14})] x^4$$

$$= [\tilde{H}_{21}, \ \tilde{H}_{22}, \ \tilde{H}_{23}, \ \tilde{H}_{24}] \ [(x^1)^T, \ (x^2)^T, \ (x^3)^T, \ (x^4)^T]^T$$

To obtain the response equation in the form of equation (2.22) of Section II, it remains to be shown that

$$[\tilde{H}_{21}, \ \tilde{H}_{22}, \ \tilde{H}_{23}, \ \tilde{H}_{24}] \ [D_1{}^T, \ D_2{}^T, \ D_3{}^T, \ D_4{}^T]^T = 0$$

But $D_1 = D_2 = D_3 = 0$ so the above product is equal to

$$\tilde{H}_{24} D_4 = [H_{24}{}^1 + H_{21}{}^2 (I_5 + A_{12} \Delta A_{21}) B_{14}] D_4$$

But $H_{24}{}^1 D_4 = B_{14} D_4 = 0$ which gives the desired result.

APPENDIX C

DERIVATION OF THE OPTIMUM FIXED-FORM CONTROLLER

APPENDIX C
DERIVATION OF THE OPTIMUM FIXED-FORM CONTROLLER

Given

$$J = TR[Q(T)S(T) + \int_{o}^{T} Q(t)S(t)]dt \qquad (C-1)$$

$$\dot{X} = (F+G_1KM)X + X(F+G_1KM)' + G_2NG_2' \qquad (C-2)$$

and

$$r(t) = [H(t) + D(t)K(t)M(t)]x(t) \qquad (C-3)$$

so that

$$S(t) = (H+DKM)X(H+DKM)' \qquad (C-4)$$

the problem is to minimize J by choice of K, given the $\dot{X}$ equation as a constraint.

The Hamiltonian for this problem is

$$H = TR(QS) + TR(P[(F+G_1KM)X + X(F+G_1KM)' + G_2NG_2']) \qquad (C-5)$$

where we have introduced the costate matrix P, one costate for each term in X. The Maximum Principle then leads us to

$$\frac{\partial H}{\partial P} = \dot{X} = (F+G_1KM)X + X(F+G_1KM)' + G_2NG_2' \qquad (C-6)$$

$$\frac{\partial H}{\partial X} = -\dot{P} = (F+G_1KM)'P + P(F+G_1KM) + (H+DKM)'Q(H+DKM) \qquad (C-7)$$

$$\frac{\partial H}{\partial K} = 0 = 2D'Q(H+DKM)XM' + 2G_1'PXM' \qquad \text{(C-8)}$$

The latter produces the stated gain equation

$$K = -(D'QD)^{-1}(D'QH+G_1'P)XM'(MXM')^{-1} \qquad \text{(C-9)}$$

In the launch booster problem, at the final time

$$Q(T)D(T) = 0 \qquad \text{(C-10)}$$

so the final gain value K(T) has no affect on the cost J. The transversatility condition at the final time then gives

$$\frac{\partial TR[Q(T)S(T)]}{\partial X(T)} = P(T) = H(T)'Q(T)H(T) \qquad \text{(C-11)}$$

completing the derivation.

The costate matrix P can be interpreted as measuring the contribution of the initial state covariance X_o and the noise covariance G_2NG_2' to the cost J. With the minimized Hamiltonian equal to zero, there results

$$H = 0 = TR[QS + P\dot{X}] \qquad \text{(C-12)}$$

$$= TR[QS + P(F+G_1KM)X + PX(F+G_1KM)' + PG_2NG_2']$$

$$= TR[-\dot{P}X + PG_2NG_2'] .$$

whence

$$TR[QS] = \frac{-d}{dt}TR[PX] + TR[PG_2NG_2'] \qquad \text{(C-13)}$$

With

$$Q(T)D(T) = 0 \qquad \text{(C-14)}$$

then

$$TR[Q(T)S(T)] = TR[Q(T)H(T)'X(T)H(T)] \qquad\qquad (C-15)$$

$$= TR[P(T)X(T)]$$

so that

$$J = TR[P(T)X(T)] + \int_0^T (-\frac{d}{dt} TR[PX] + TR[PG_2NG_2'])dt$$

$$= TR[P(T)X(T)] + TR[P(0)X(0)] - TR[P(T)X(T)] + \int_0^T TR[PG_2NG_2']dt$$

$$= \int_0^T TR[PG_2NG_2']dt + TR[P(0)X(0)] \qquad\qquad (C-16)$$

Further, writing J(t) as the "cost-to-go"

$$J(t) = TR[Q(T)S(T) + \int_t^T Q(t)S(t)dt] \qquad\qquad (C-17)$$

the above manipulation gives

$$J(t) = \int_t^T TR[PG_2NG_2']dt + TR[P(t)X(t)] \qquad\qquad (C-18)$$

The ij^{th} term of P(t) may thus be regarded as a measure of the contribution of the ij^{th} term of the noise input G_2NG_2' to the cost, or the contribution of the ij^{th} term of the covariance X(t) to the "cost-to-go", providing future noise inputs G_2NG_2 are zero. Both interpretations are meaningful and both are useful for obtaining insights into the physics of the control problem.

Derivation of Least-Mean-Square-Error State Estimator

Let x be a vector, and suppose we measure m = Mx. We wish to construct K and the estimate $\hat{x}$ = Km such that $\hat{x}$ is as close as possible to x. To be specific, let us choose K to minimize the mean-square error J

$$J = TR[E\{(\hat{x}-x)(\hat{x}-x)'\}] \qquad\qquad (C-19)$$

$$= E\{(\hat{x}-x)'(\hat{x}-x)\}$$

With

$$\hat{x} - x = (KM-I)x \qquad\qquad (C-20)$$

and

$$E\{x\,x'\} = I \qquad\qquad (C-21)$$

Then

$$J = TR[(KM-I)\,X(KM-I)'] \qquad\qquad (C-22)$$

Then

$$\frac{\partial J}{\partial K} = 0 = 2(KM-I)XM' \qquad\qquad (C-23$$

so that

$$K = XM'(MXM')^{-1} \qquad\qquad (C-24)$$

Comparing this K with the optimal gain given by equation (C-9) we see that the optimal gain employs a least-mean-square-error state estimator. Defining L to be $-(D_1'QD_1)^{-1}(D_1'QH+G_1'P)$, the optimal control is $u = L\hat{x}$.

With this gain the error covariance is

$$E\{(\hat{x}-x)(\hat{x}-x)'\} = (KM-I)X(KM-I)' \qquad\qquad (C-25)$$

$$= (I-KM)X$$

$$= X - XM'(MXM')^{-1}MX$$

C4

Noting that for M invertible,

$$KM = I$$

and

$$E\left\{(\hat{x}-x)\,(\hat{x}-x)\right\} = 0$$

the states orthogonal to the rows of M (the null space of the domain of M) are not directly observable, and it is these states that make up the error covariance matrix.

APPENDIX D

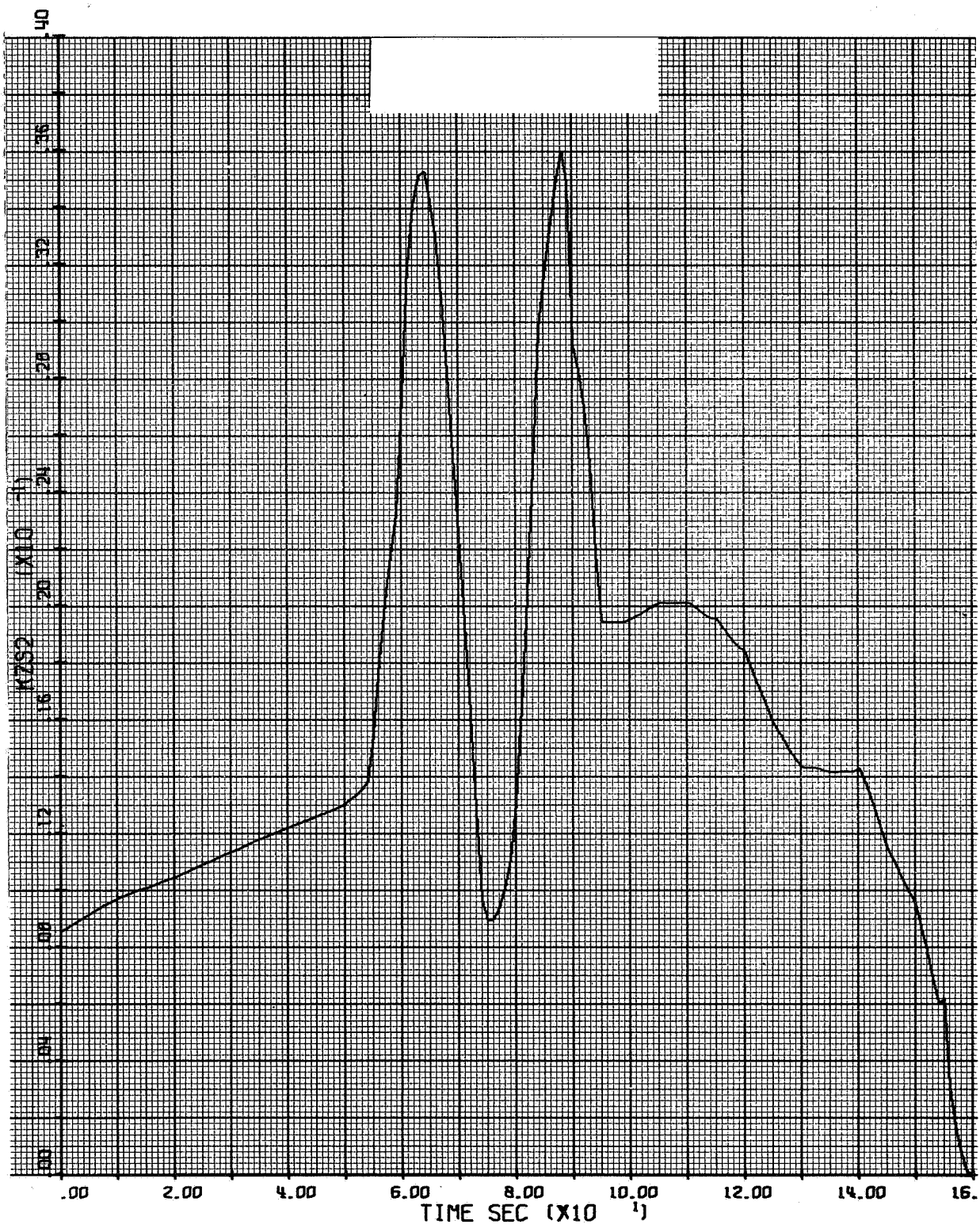# CONTROLLER GAINS
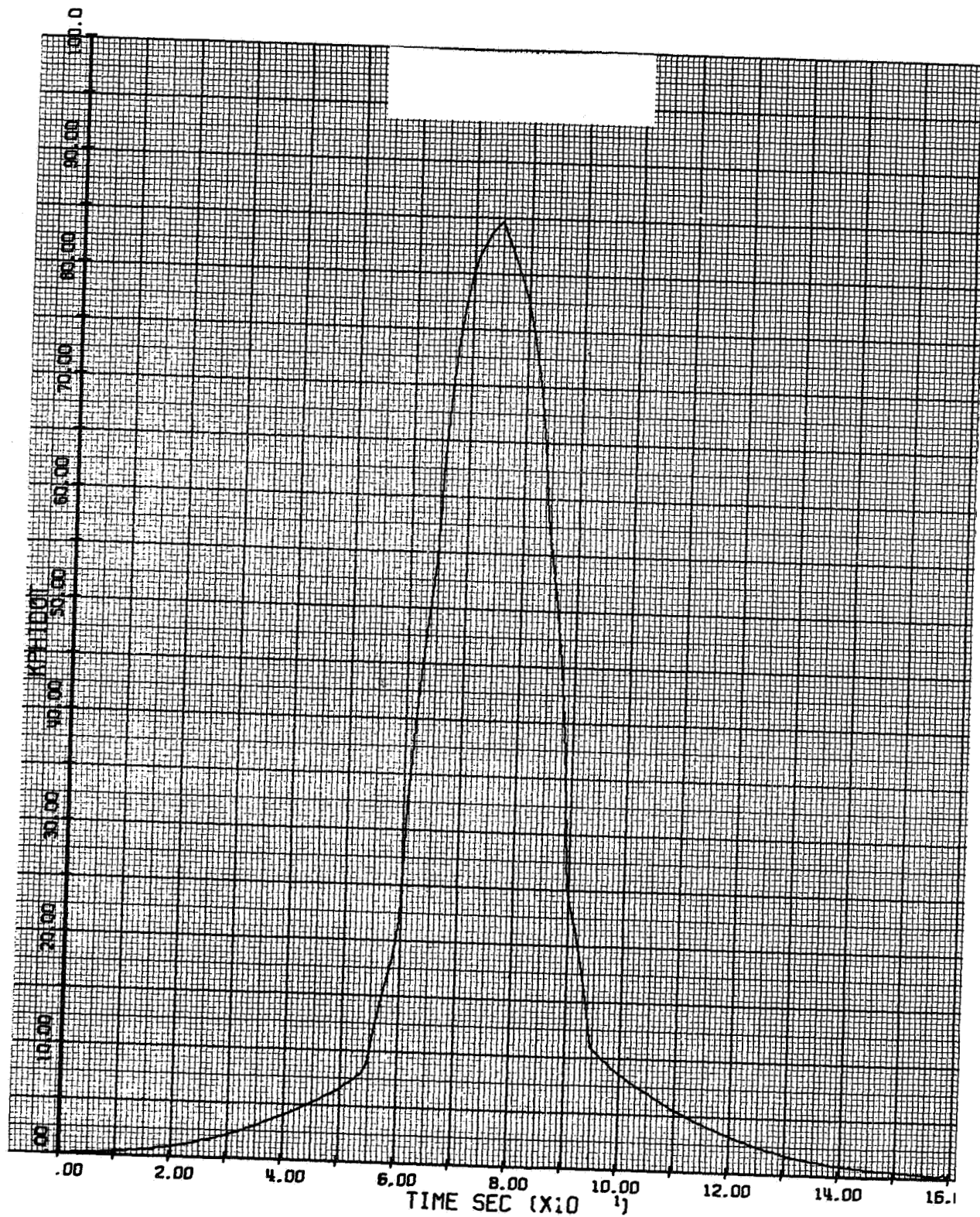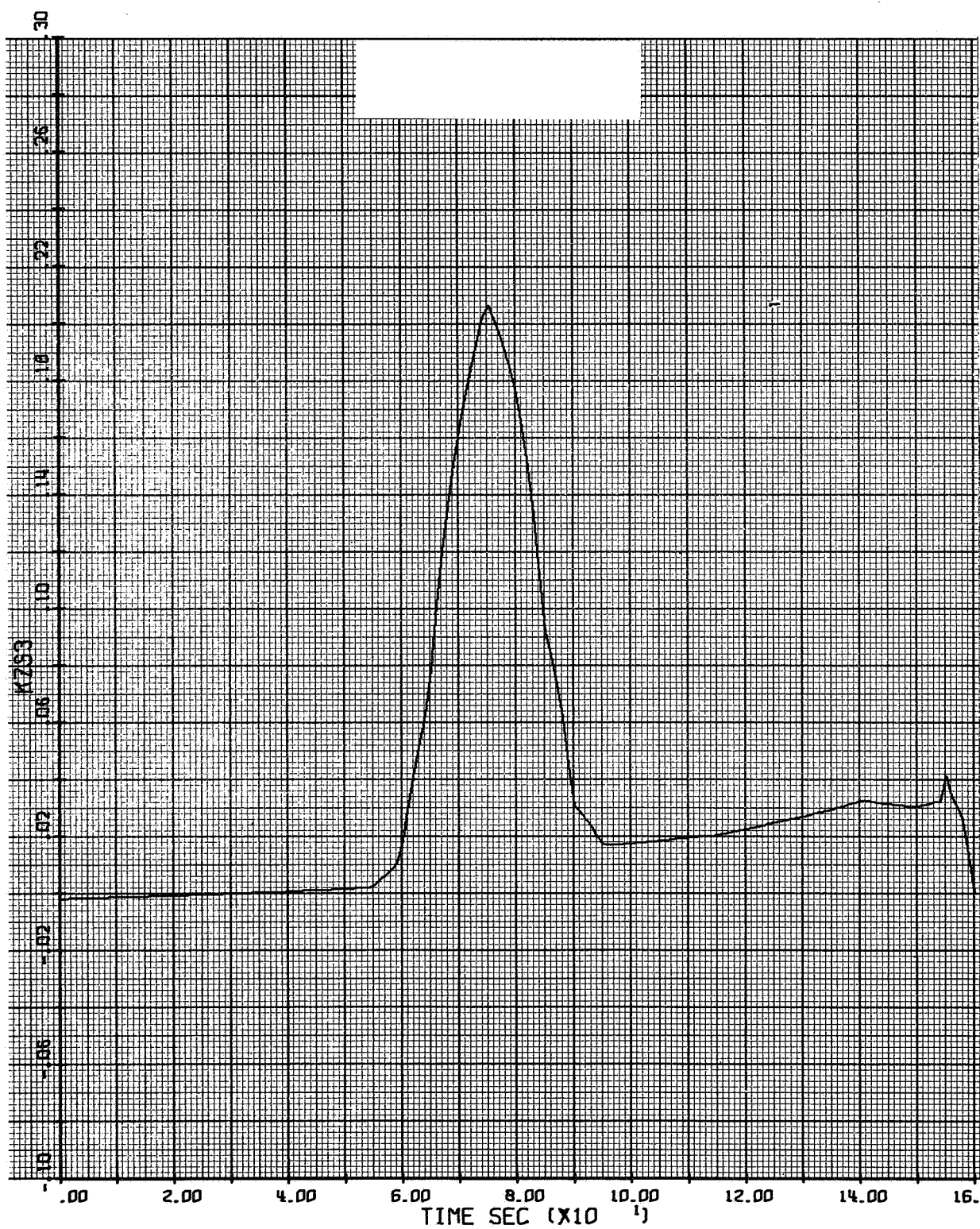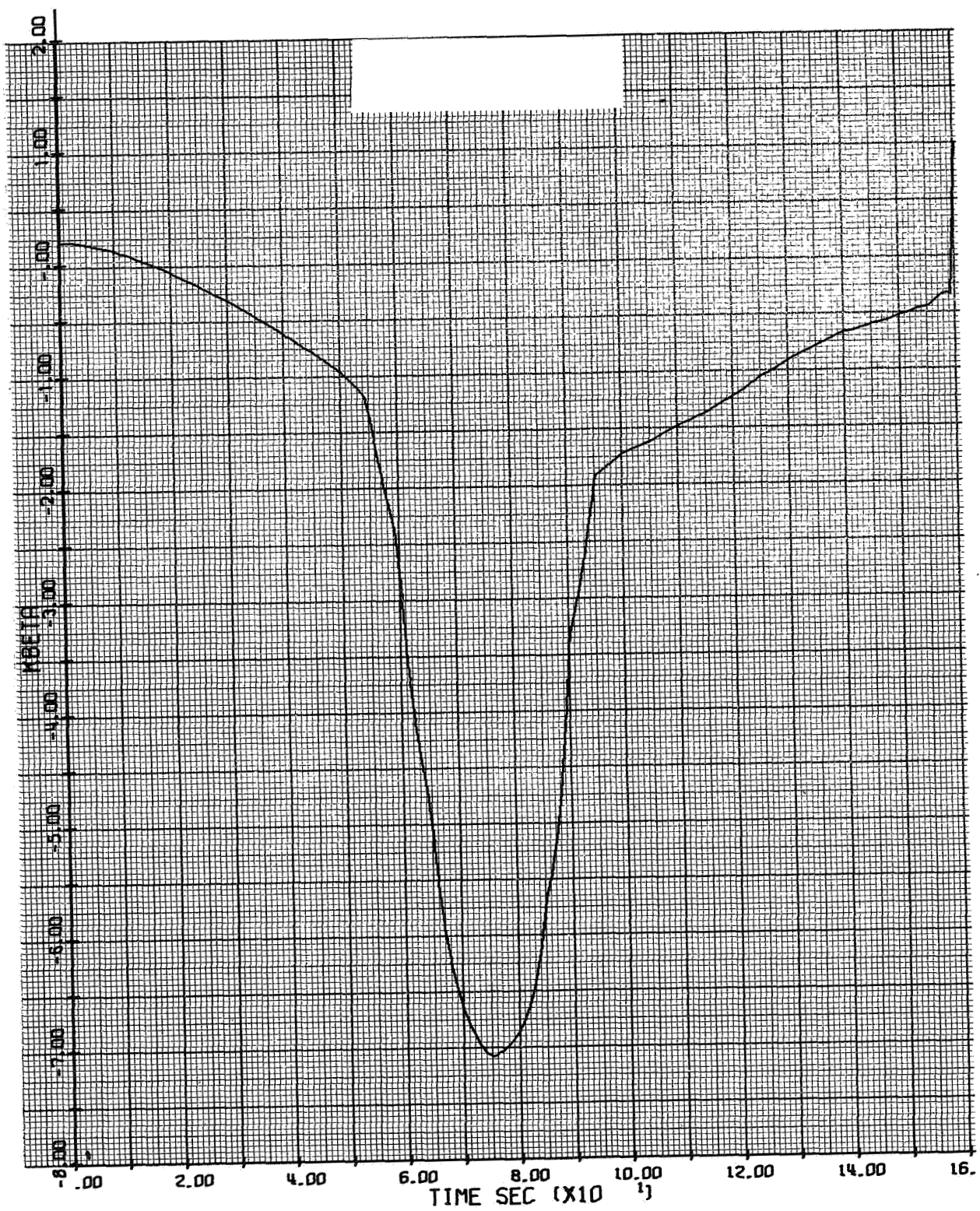
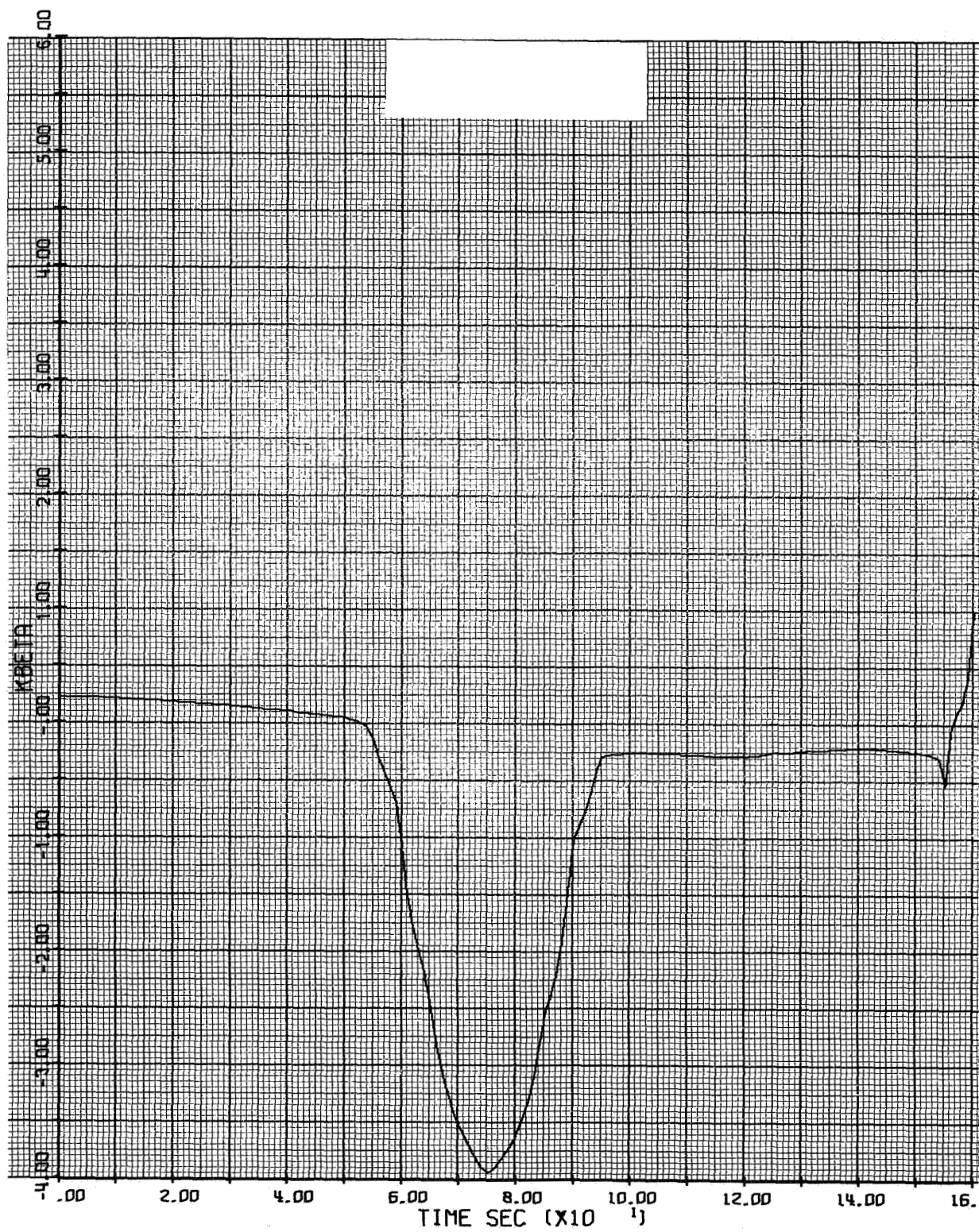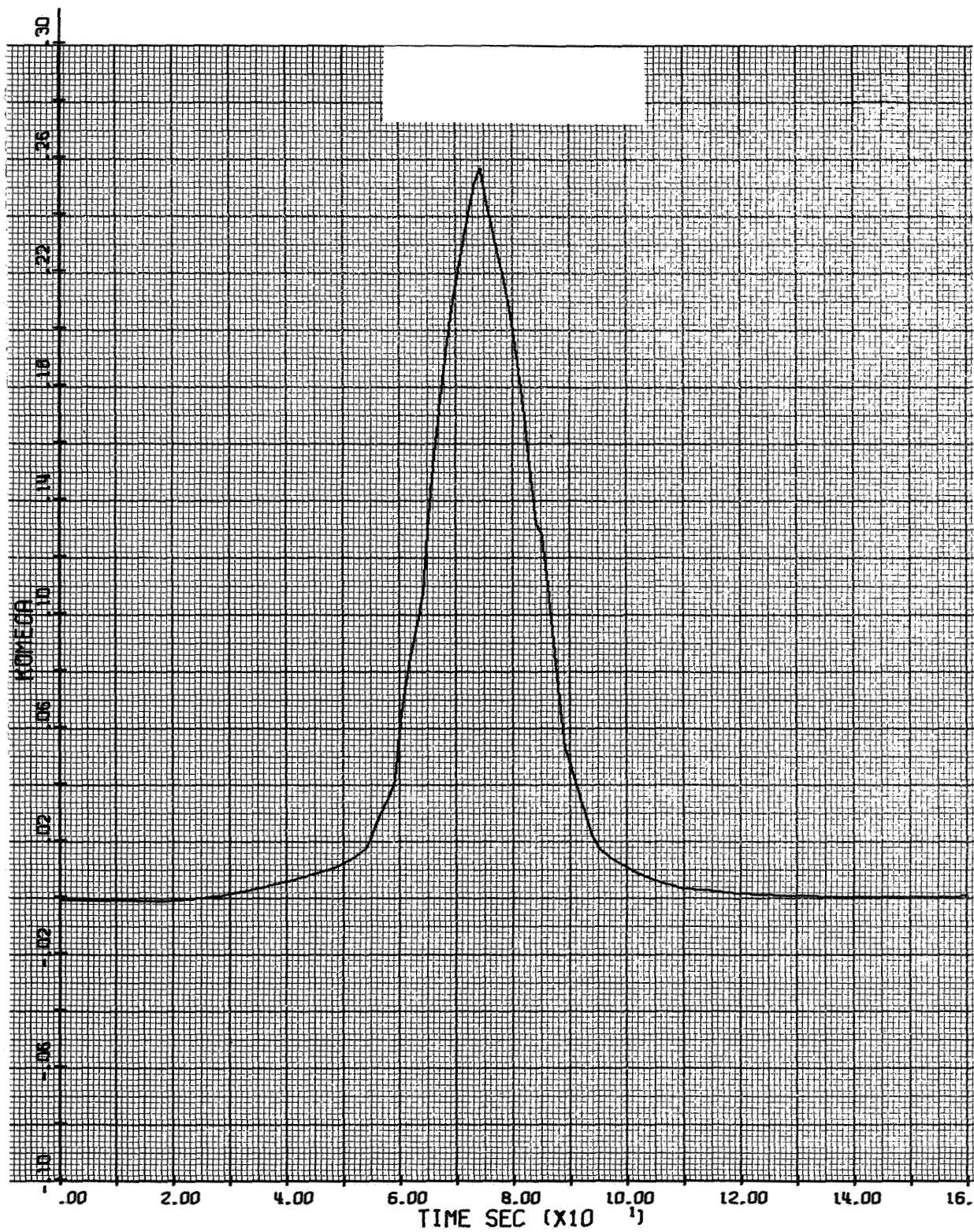Figure D-1a. $\dot{\varphi}$ Gain for Controller A
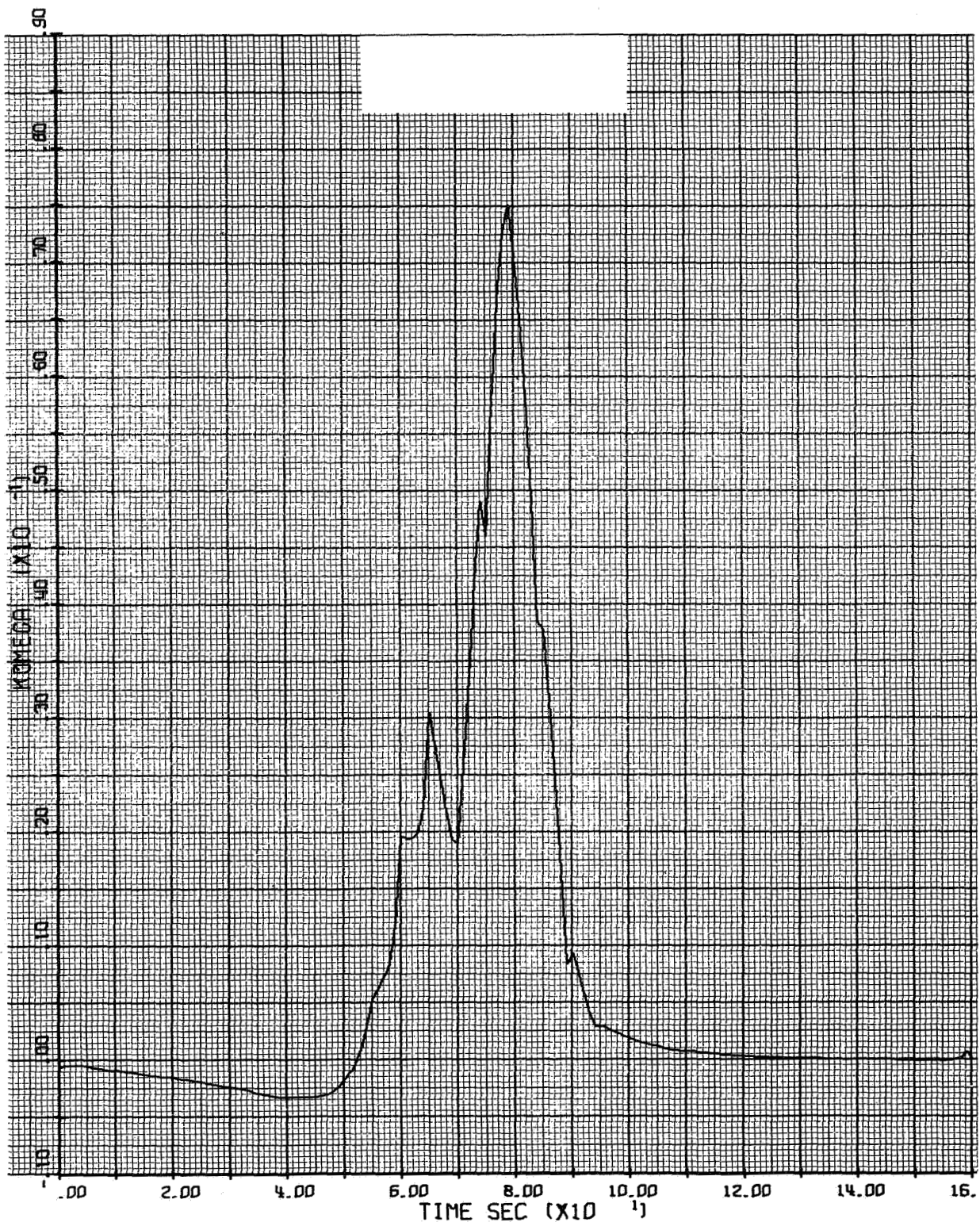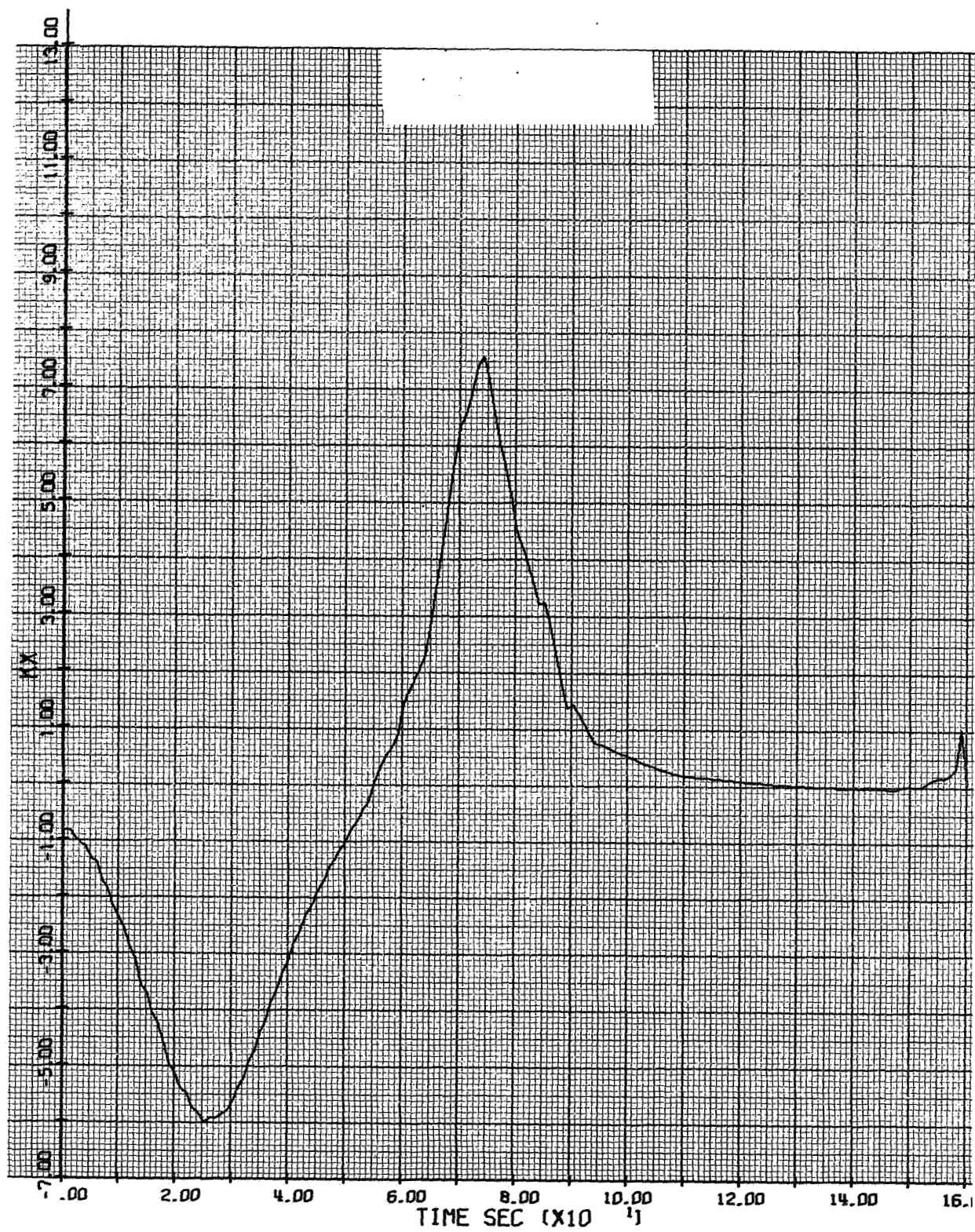
Figure D-1b. φ Gain for Controller B

D2
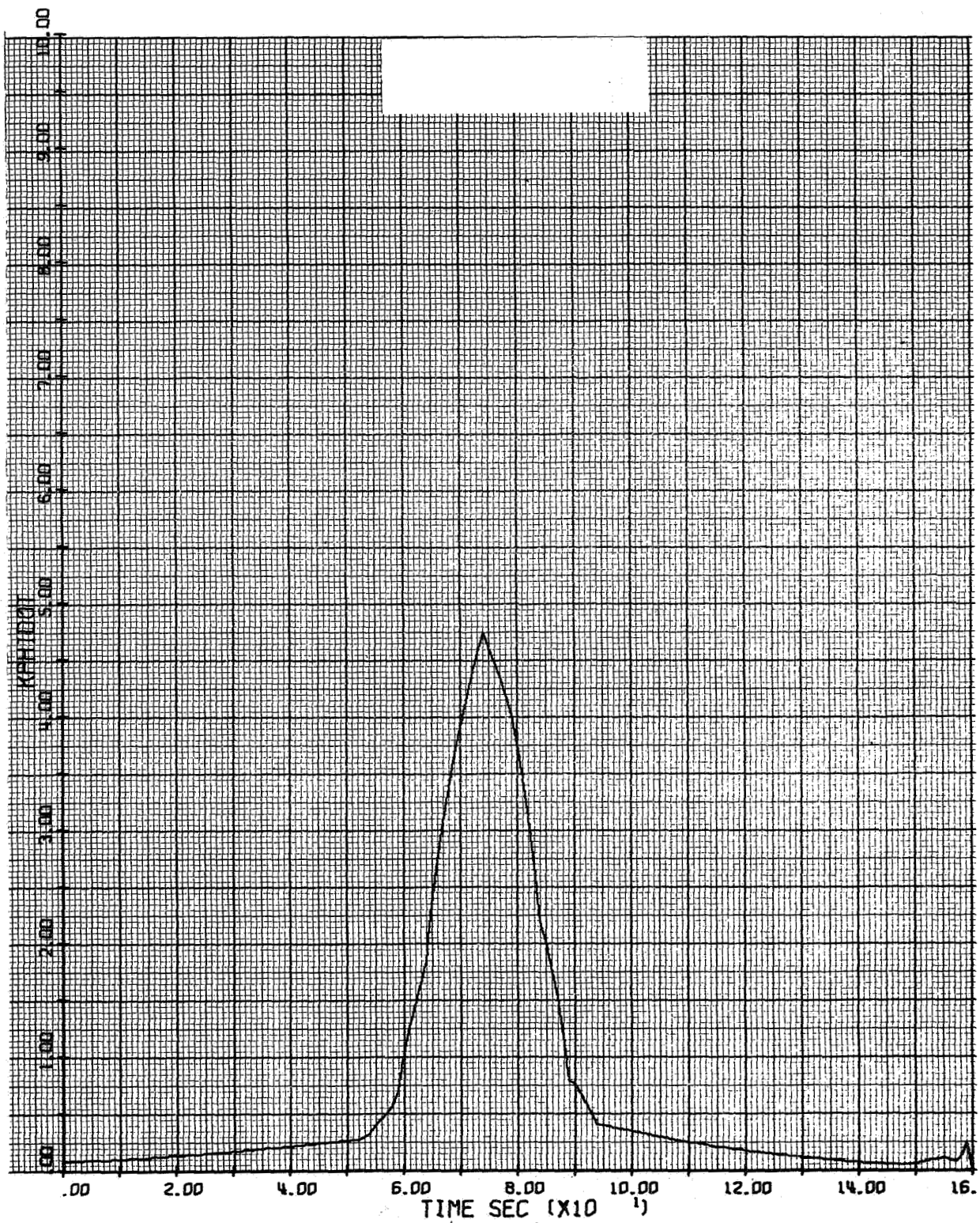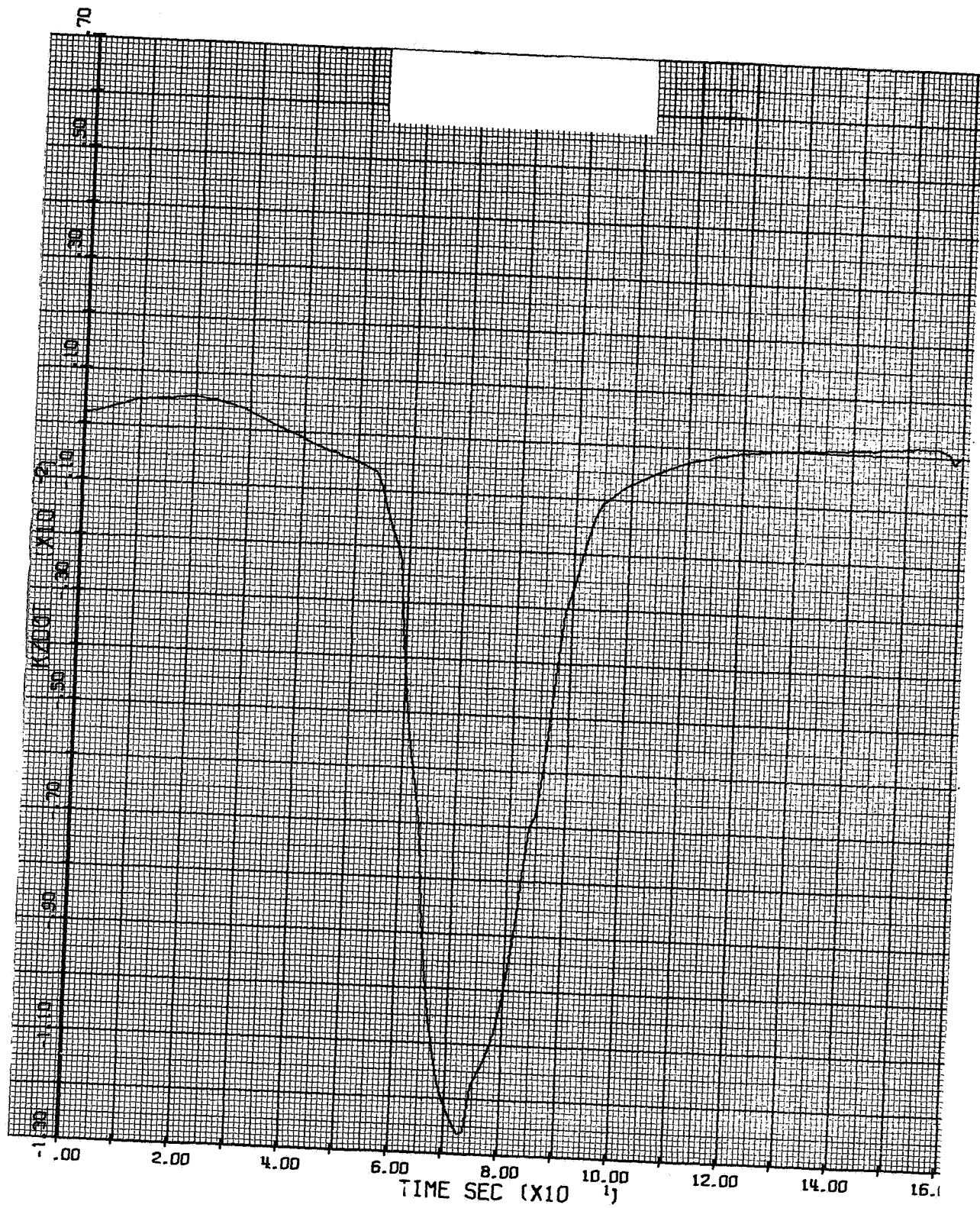
Figure D-2a. Ż Gain for Controller A
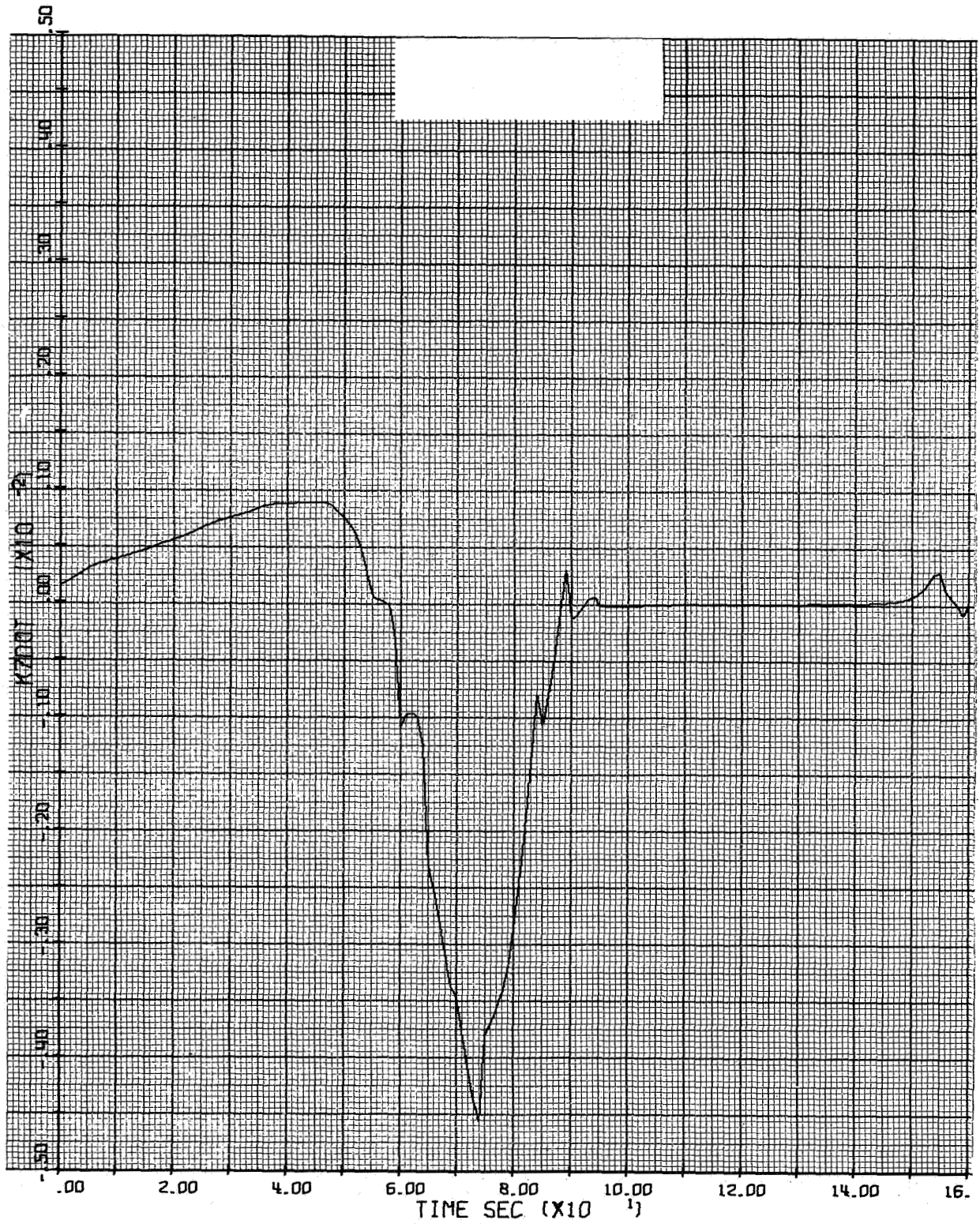
Figure D-2b. Ż Gain for Controller B

D4
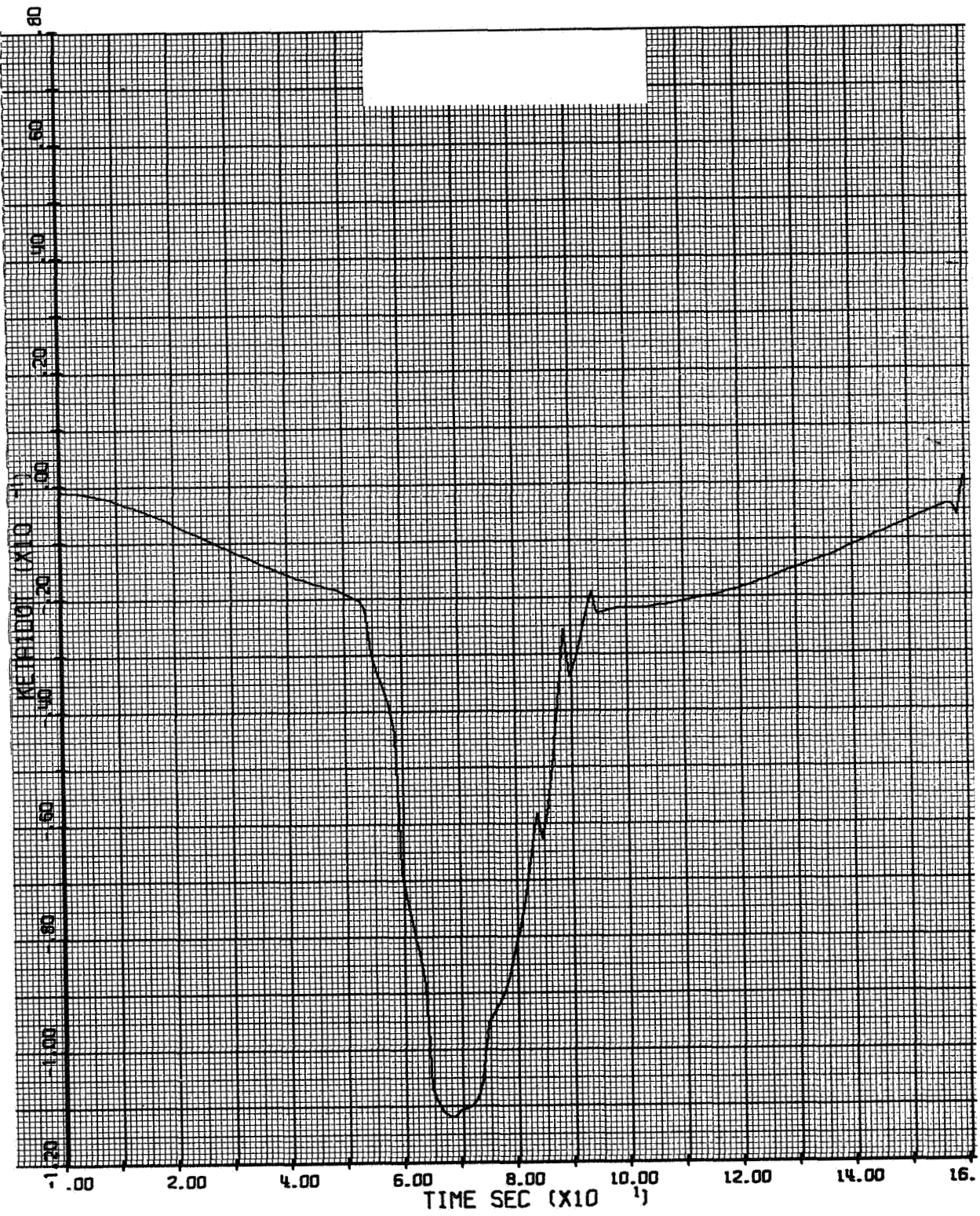
Figure D-3a. $\dot{\eta}_1$ Gain for Controller A
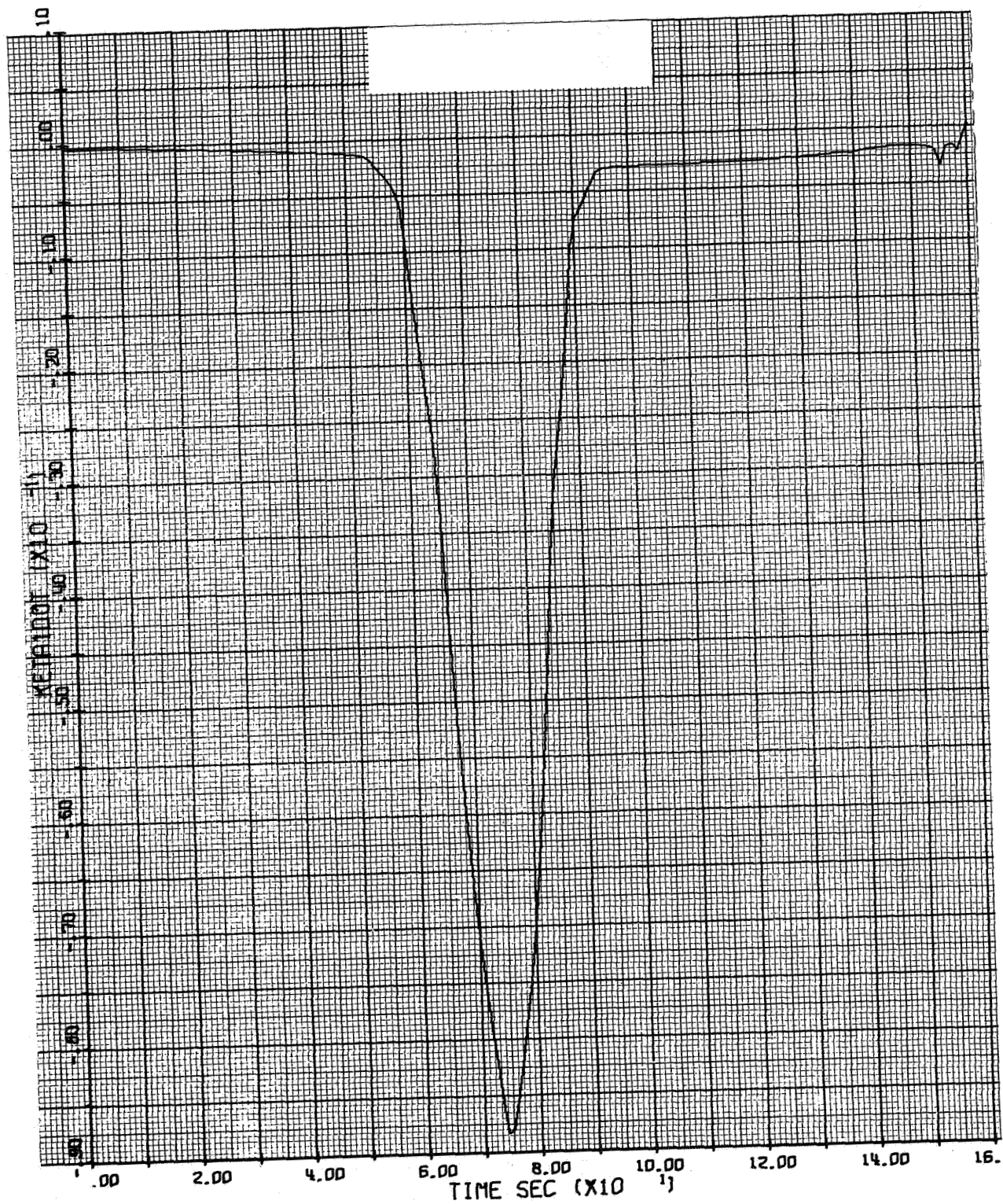
Figure D-3b. $\dot{\eta}_1$ Gain for Controller B

D6
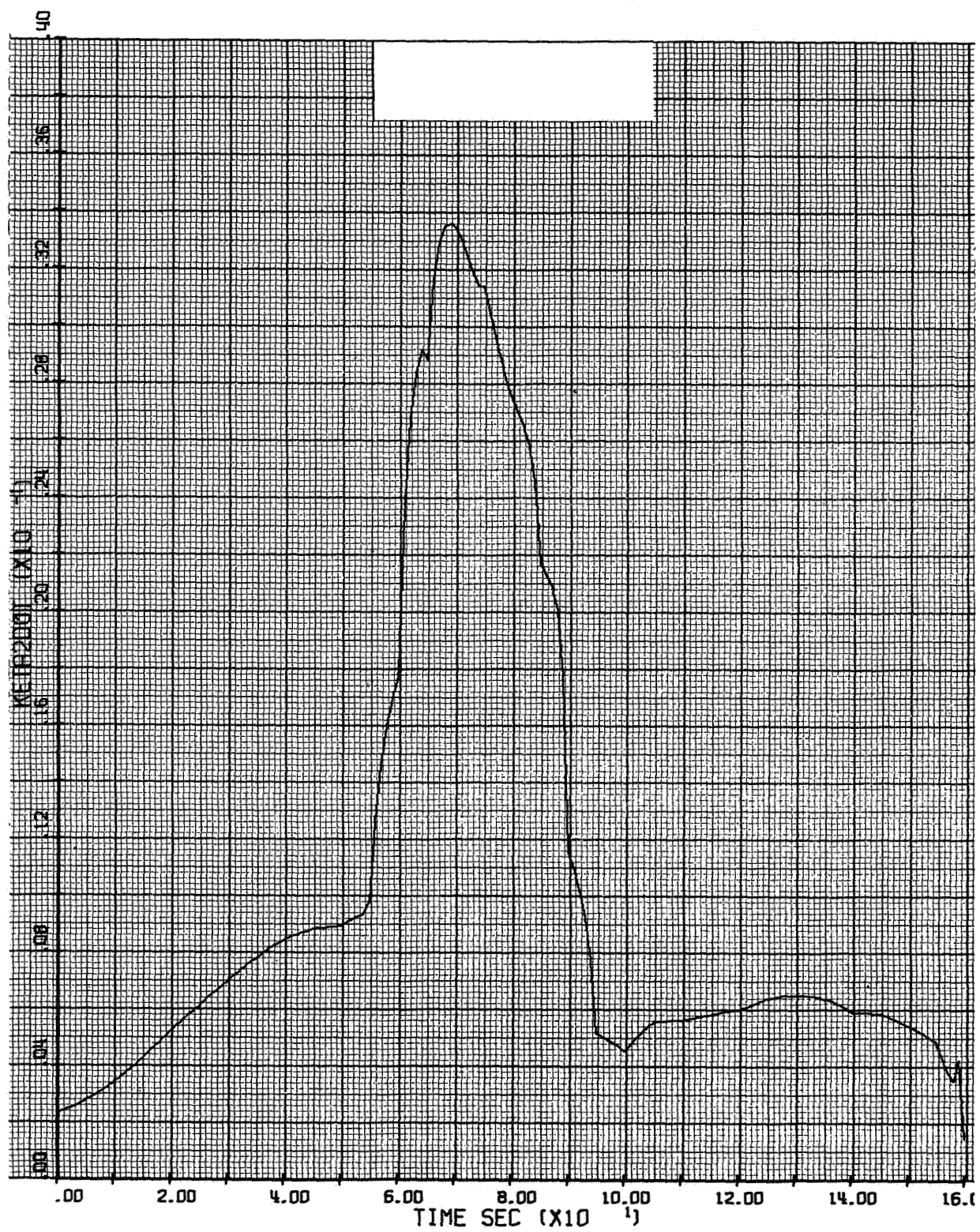
Figure D-4a. $\dot{\eta}_2$ Gain for Controller A
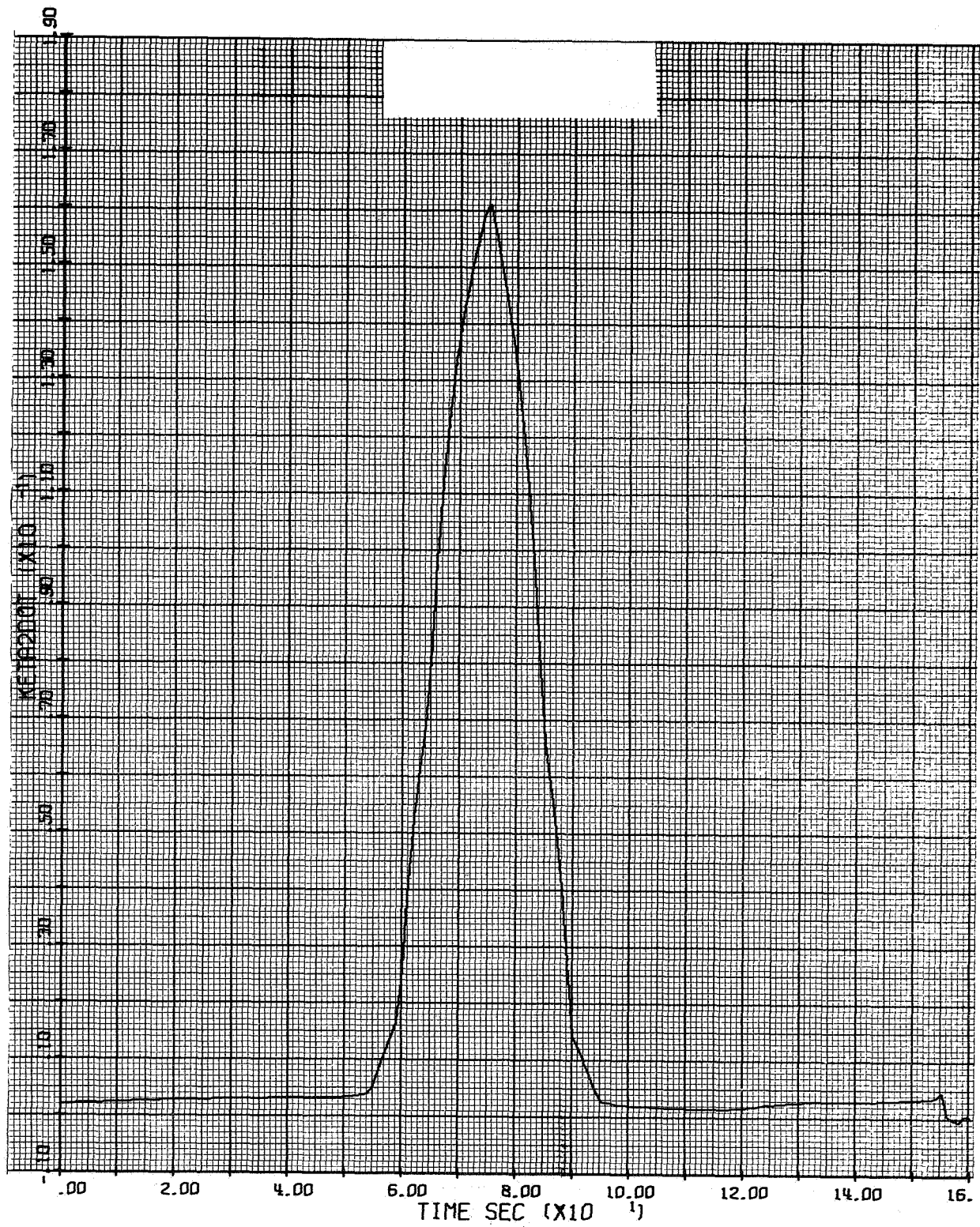
Figure D-4b. $\dot{\eta}_2$ Gain for Controller B
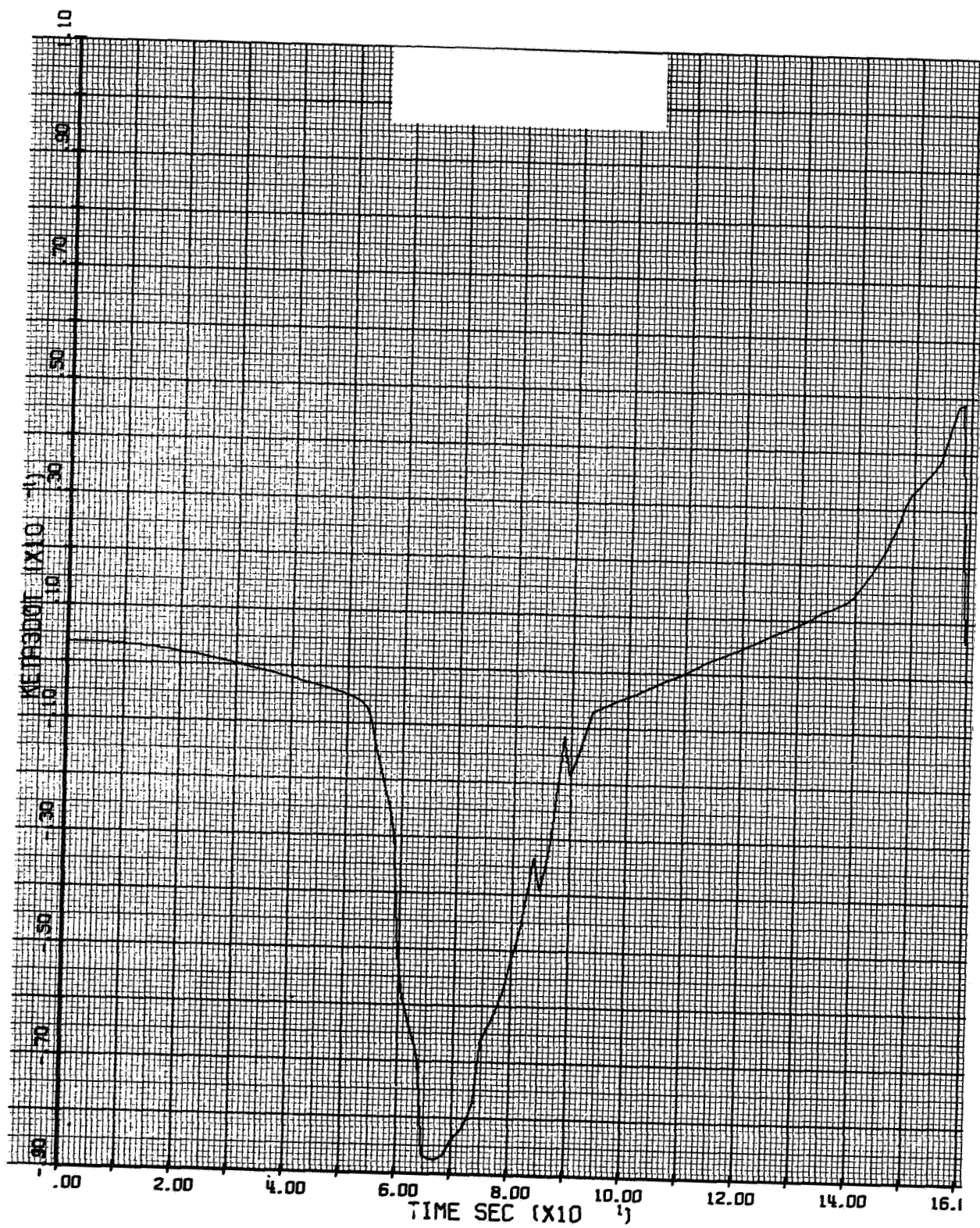
Figure D-5a. $\dot{\eta}_3$ Gain for Controller A

D9
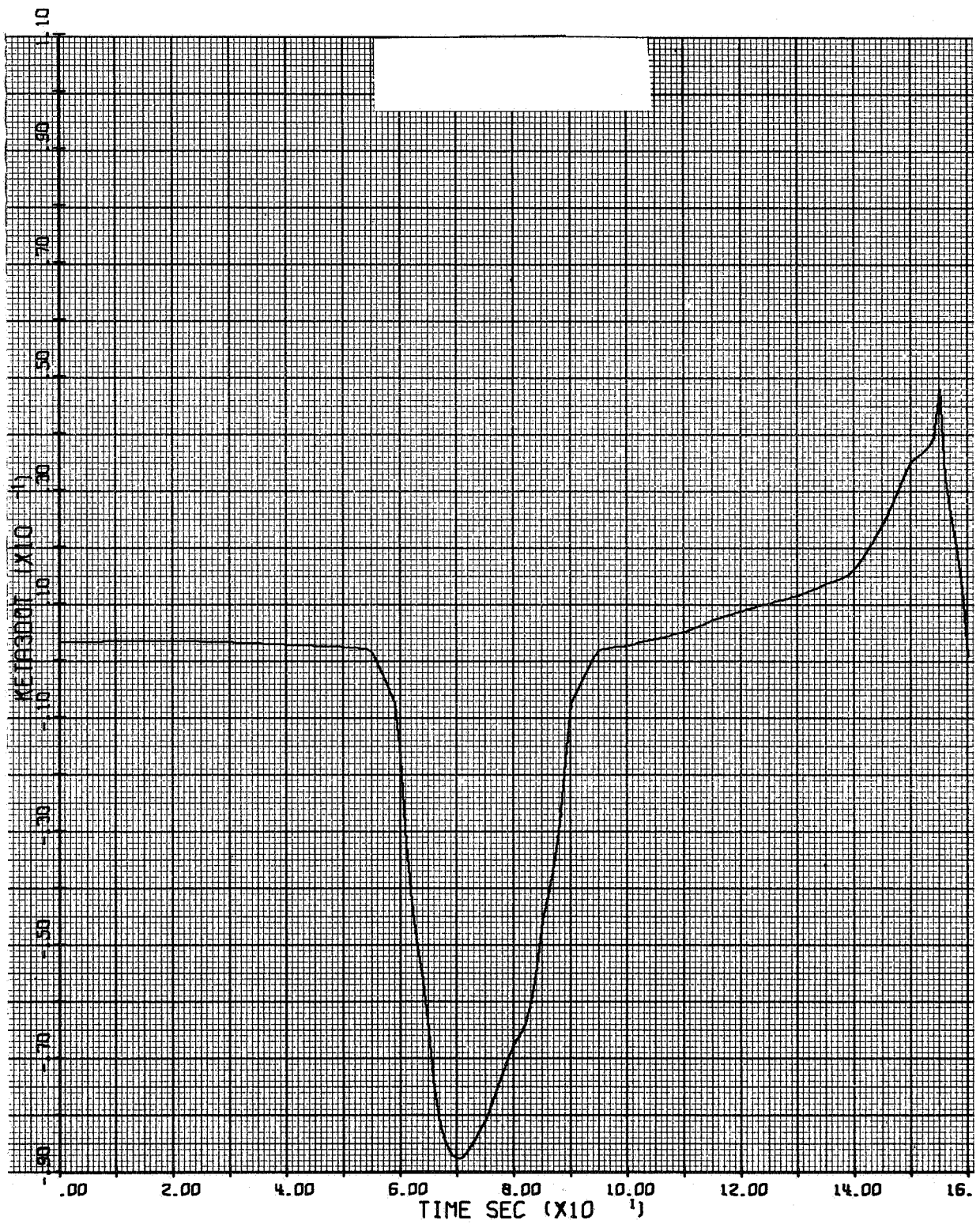
Figure D-5b. $\dot{\eta}_3$ Gain for Controller B

D10
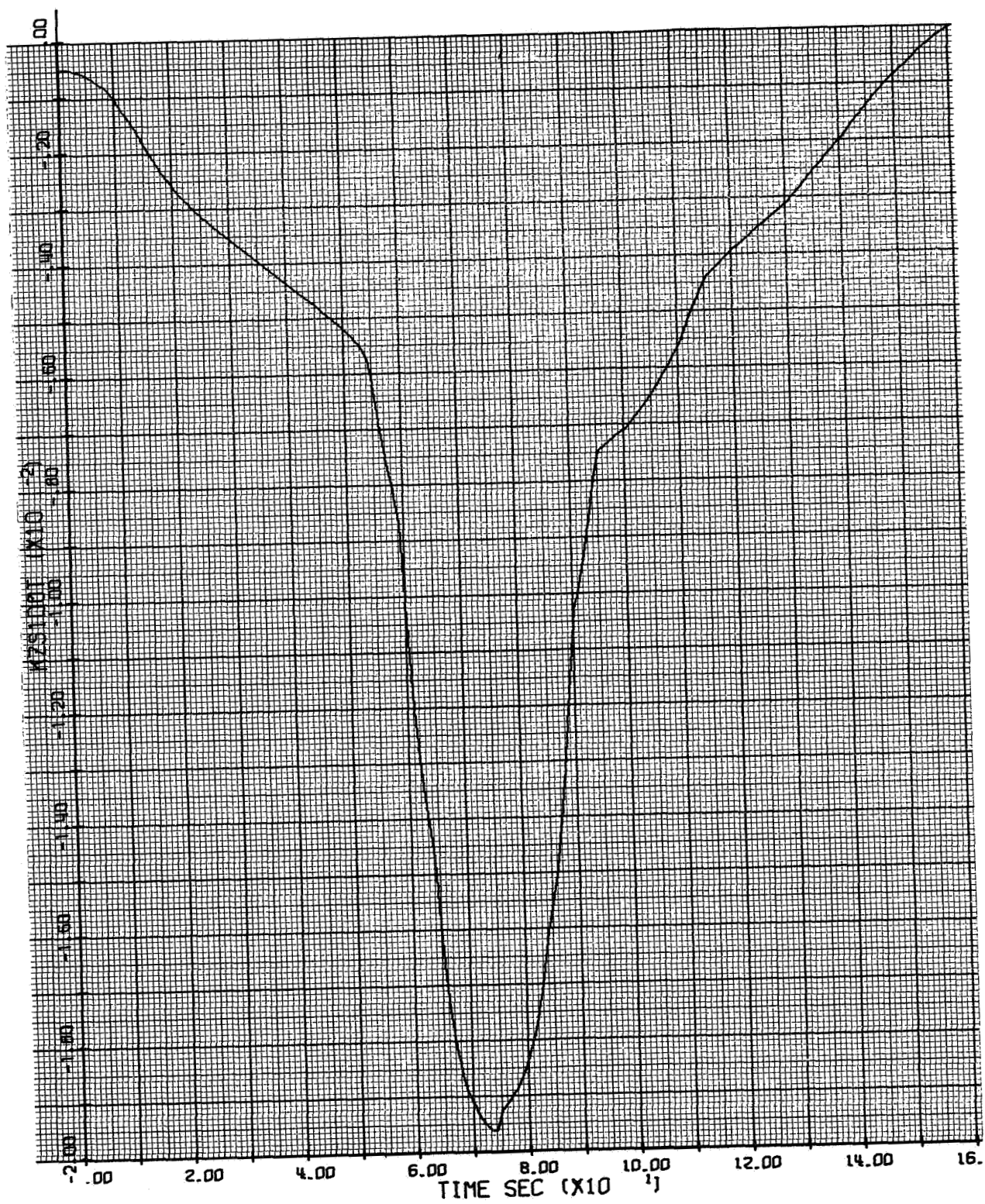
Figure D-6a. $\dot{Z}_{s1}$ Gain for Controller A
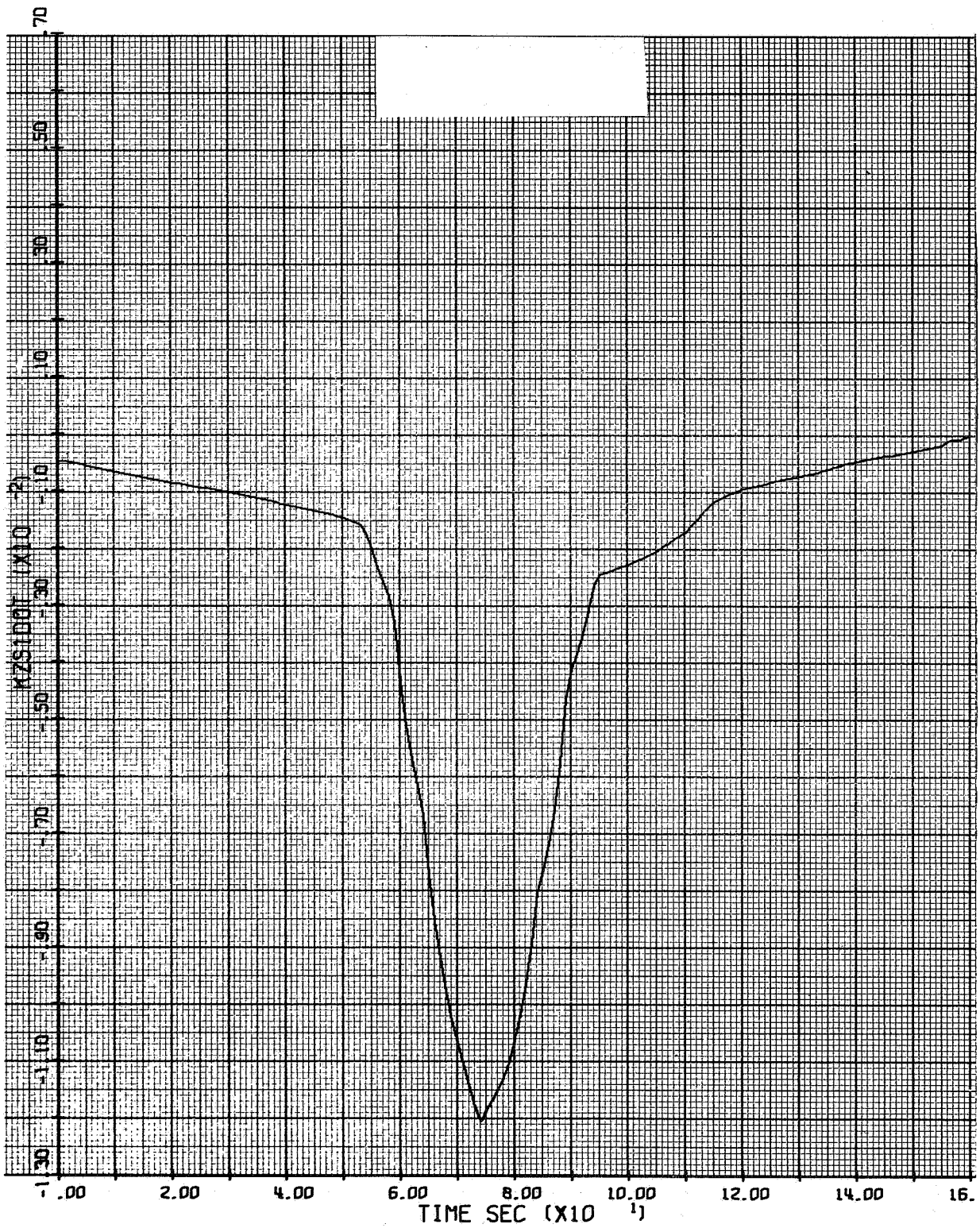
Figure D-6b. $\dot{Z}_{s1}$ Gain for Controller B
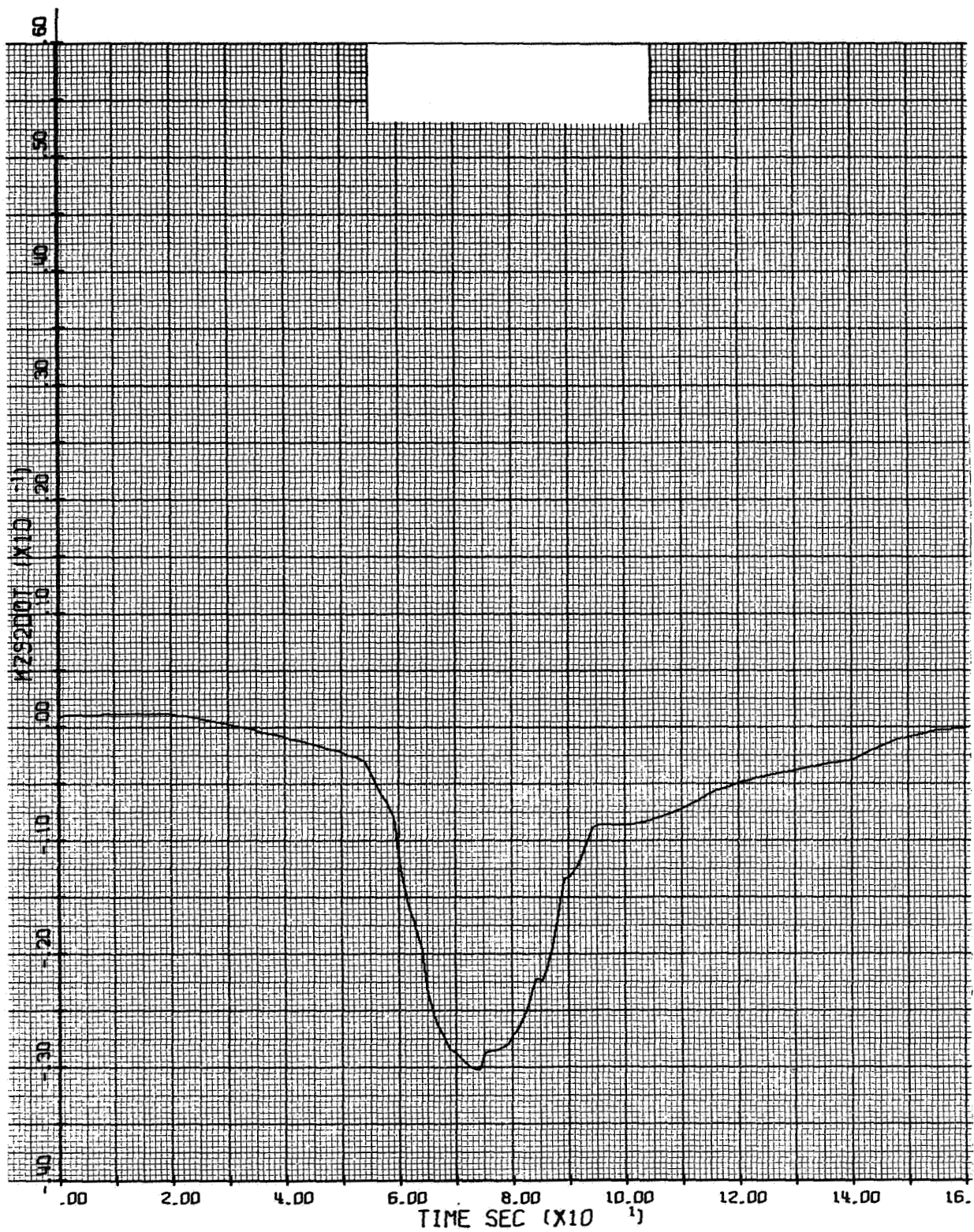
Figure D-7a. $\dot{Z}_{s2}$ Gain for Controller A
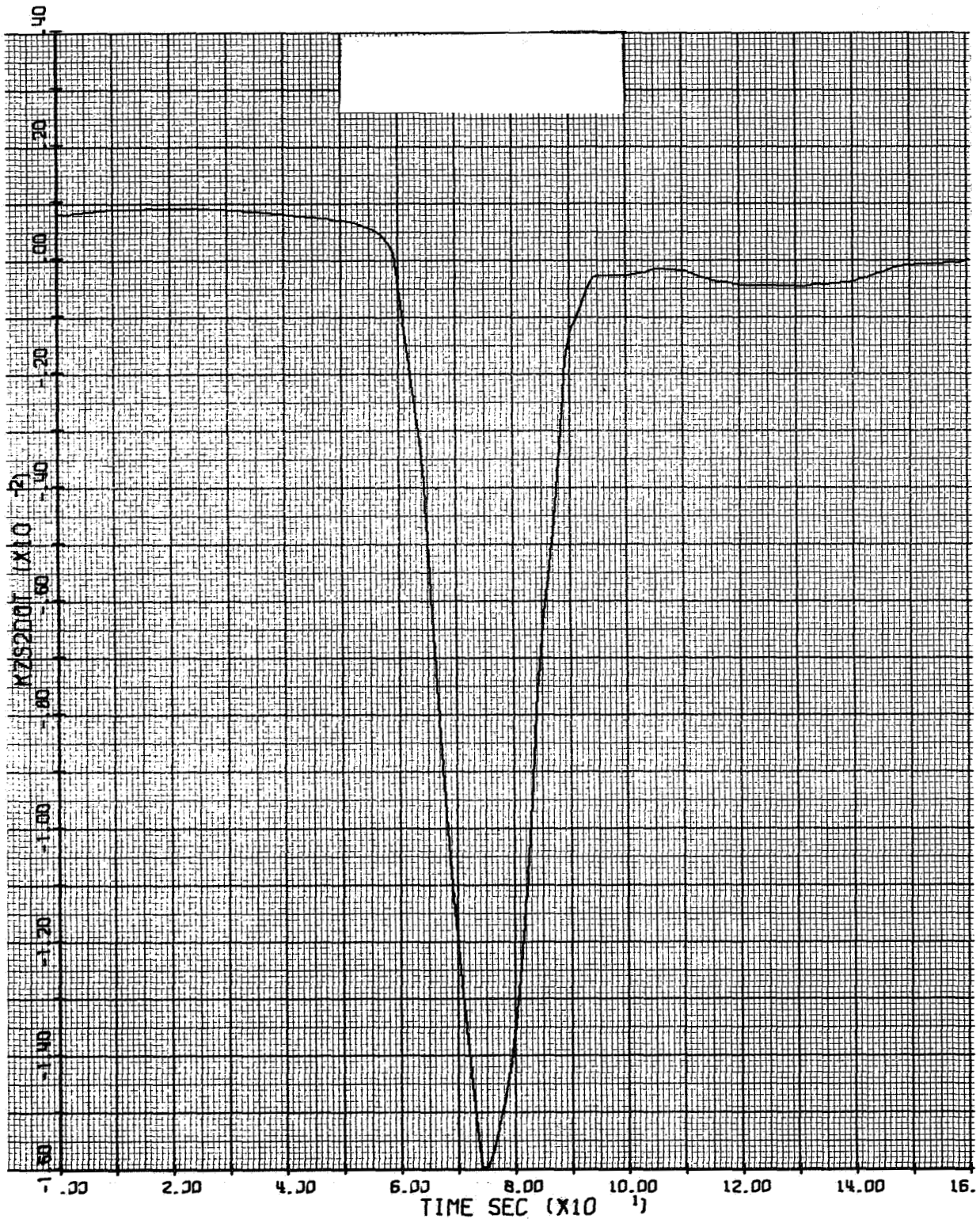
Figure D-7b. $\dot{Z}_{s2}$ Gain for Controller B

D14
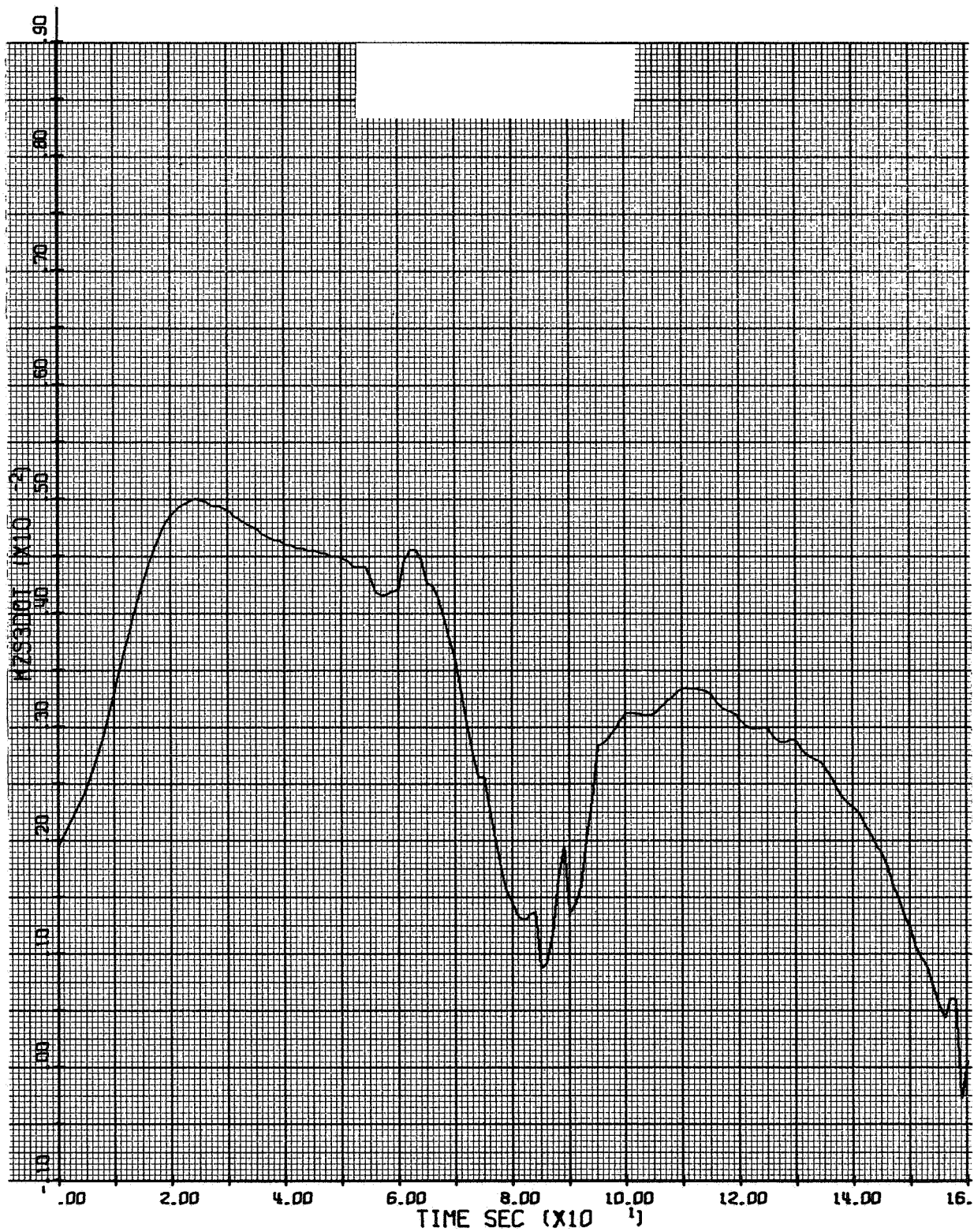
Figure D-8a. $\dot{Z}_{s3}$ Gain for Controller A
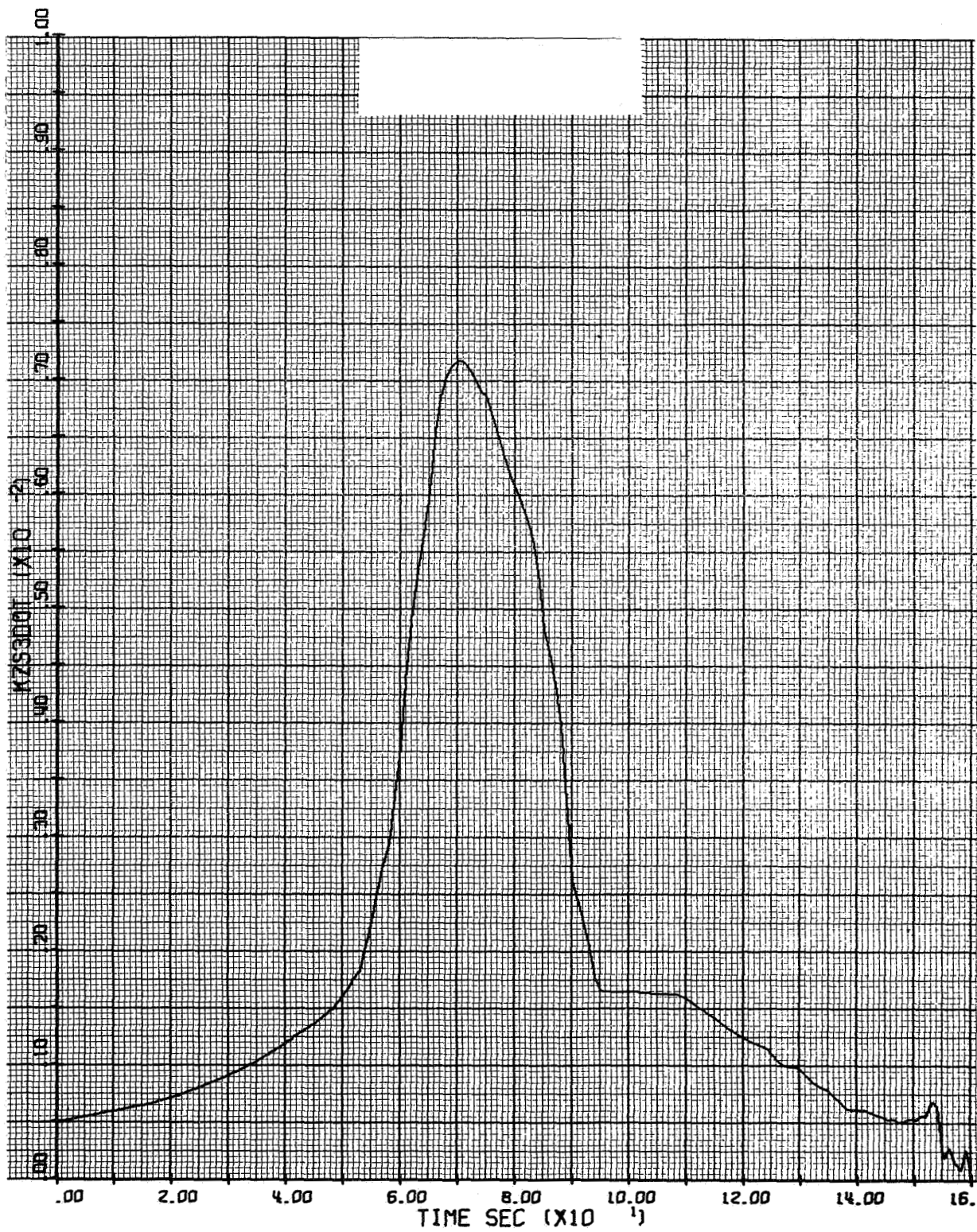
Figure D-8b. $\dot{Z}_{s3}$ Gain for Controller B

D16

Figure D-9a. φ Gain for Controller A
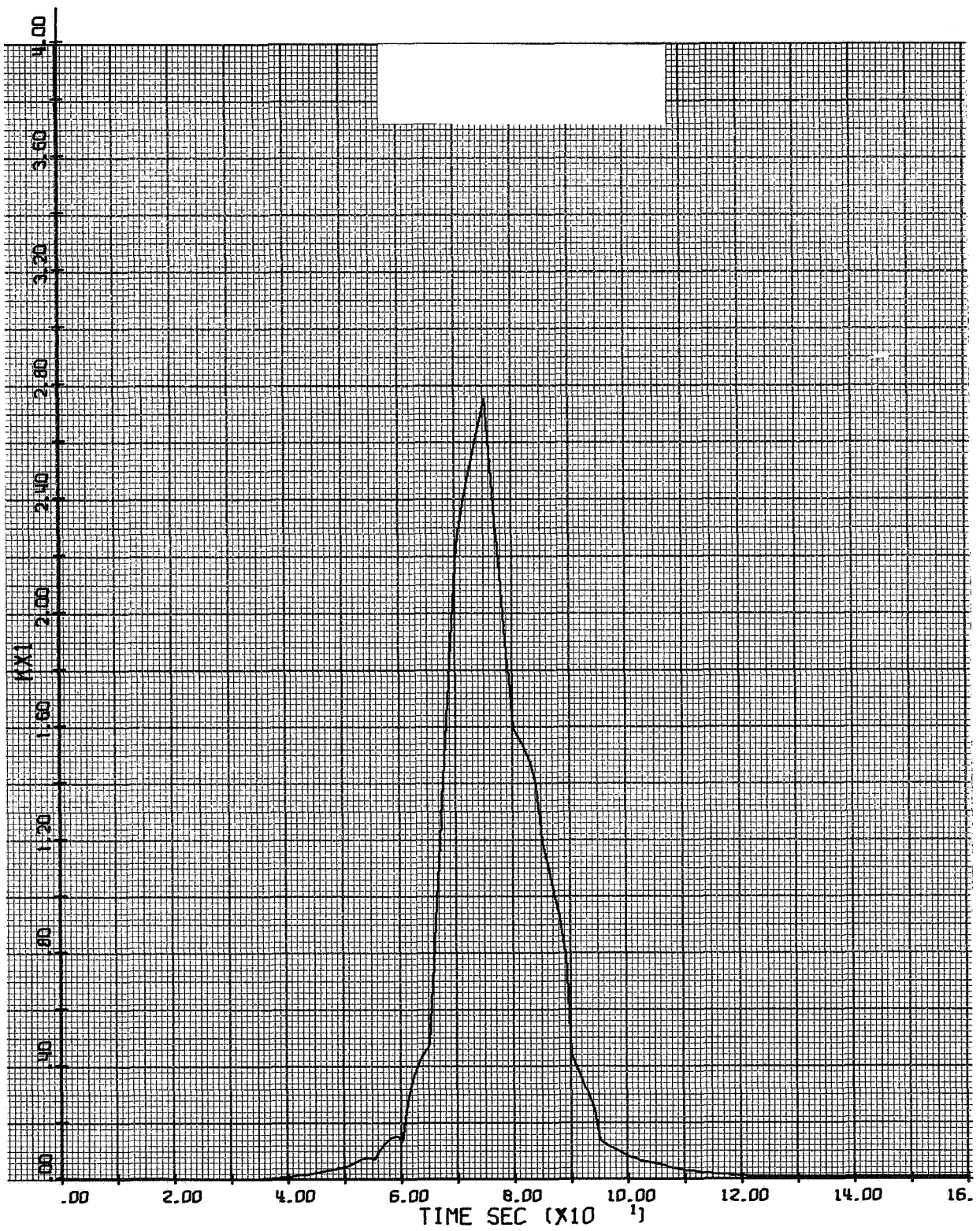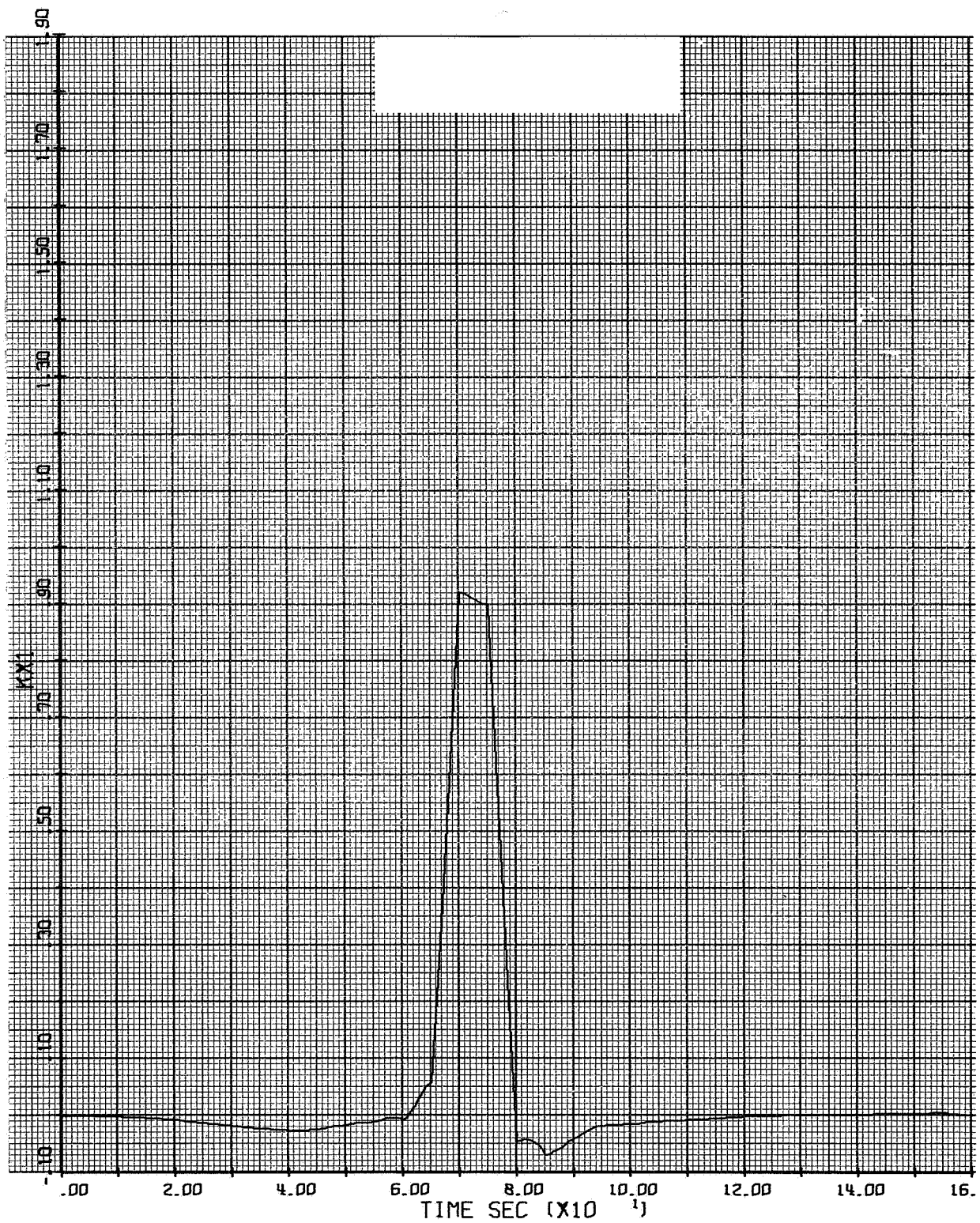
D17
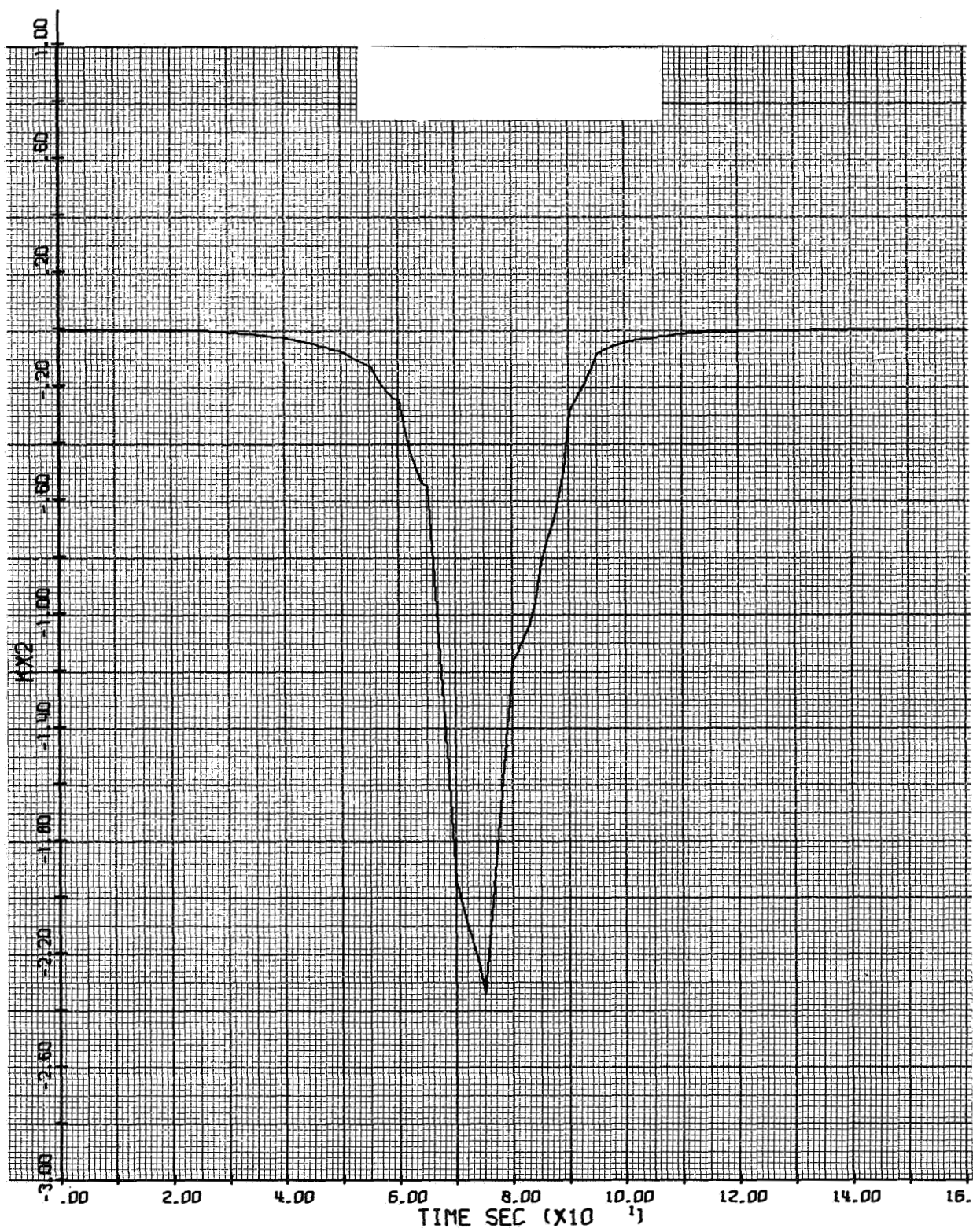
Figure D-9b. φ Gain for Controller B

D18
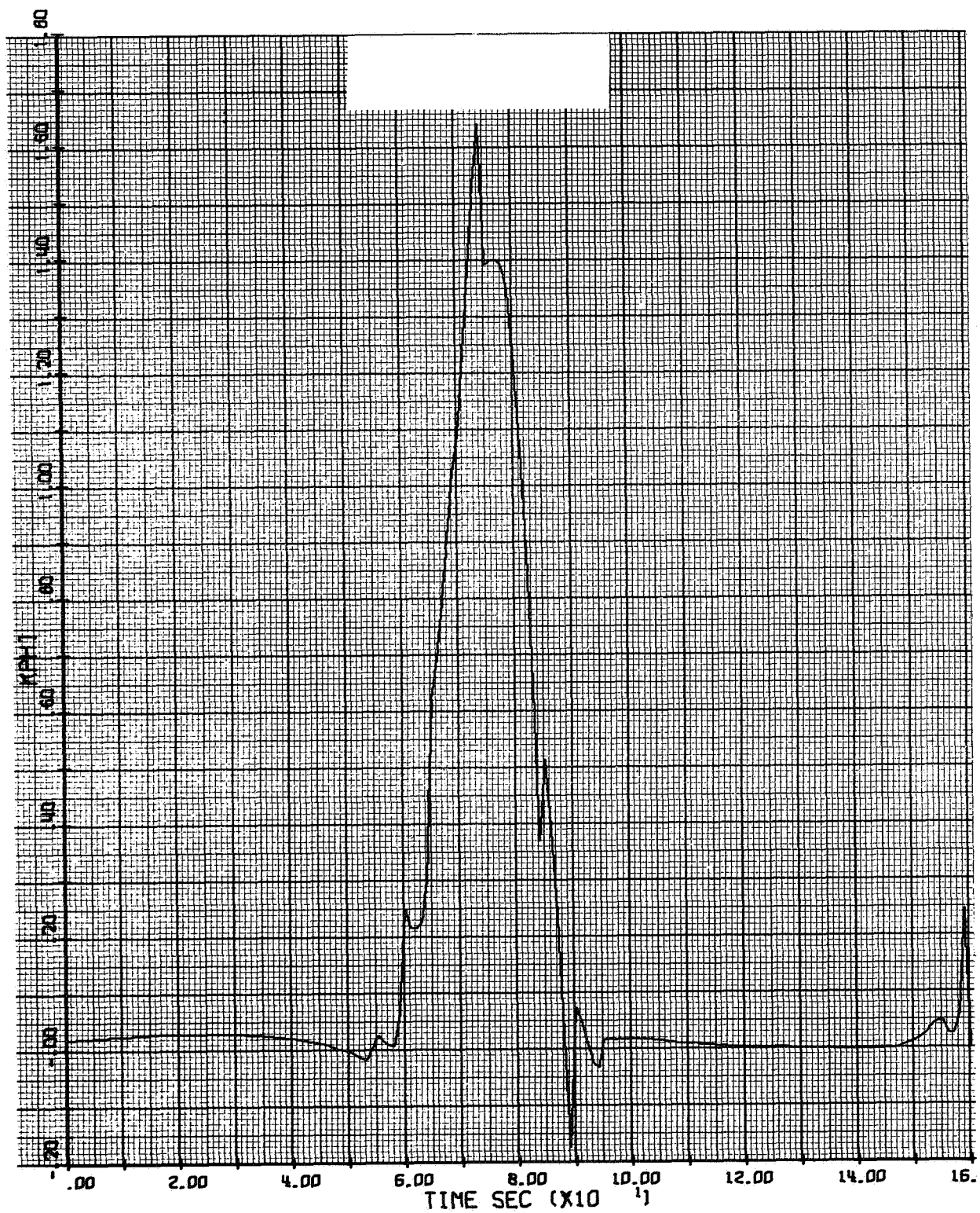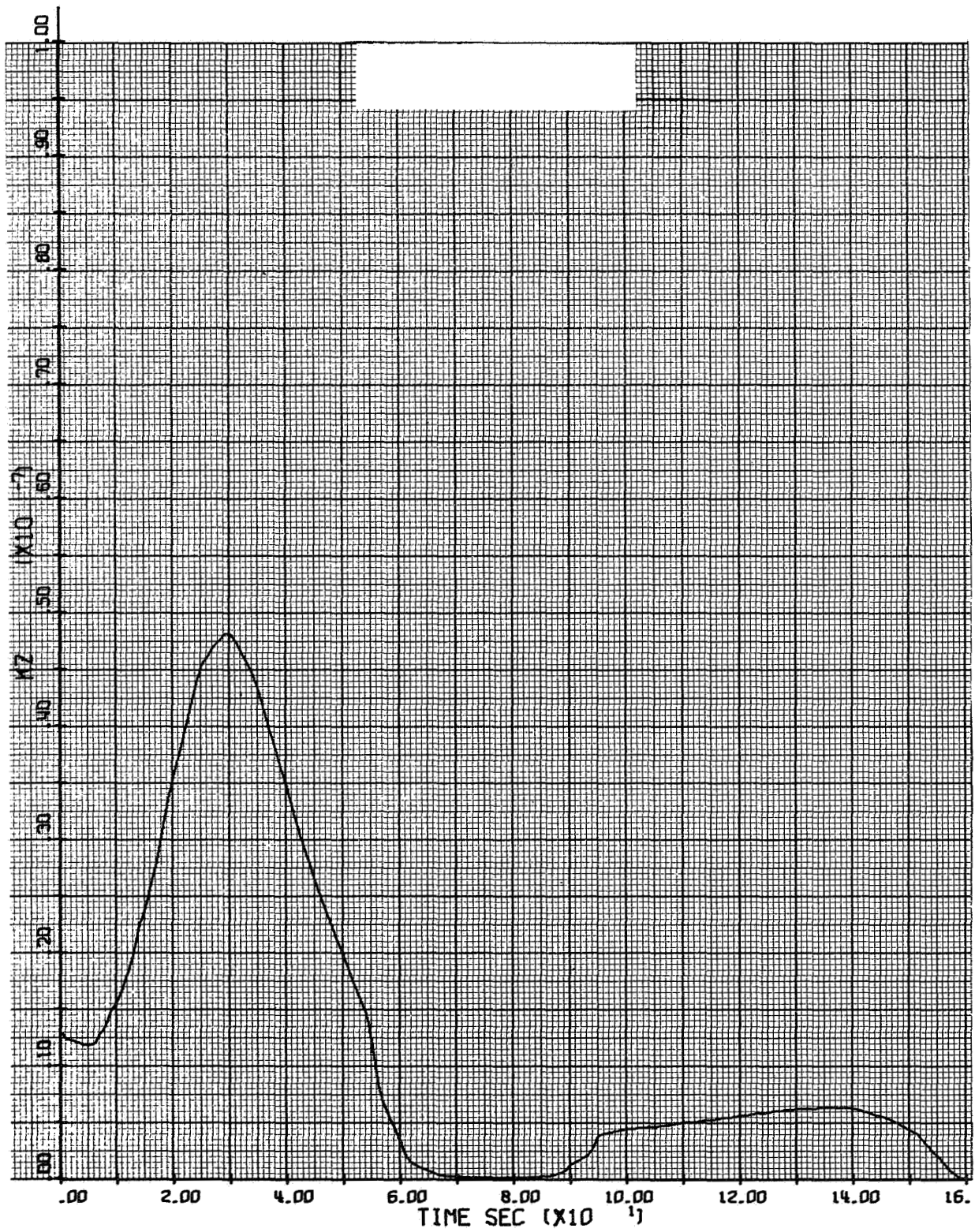
Figure D-10a. Z Gain for Controller A
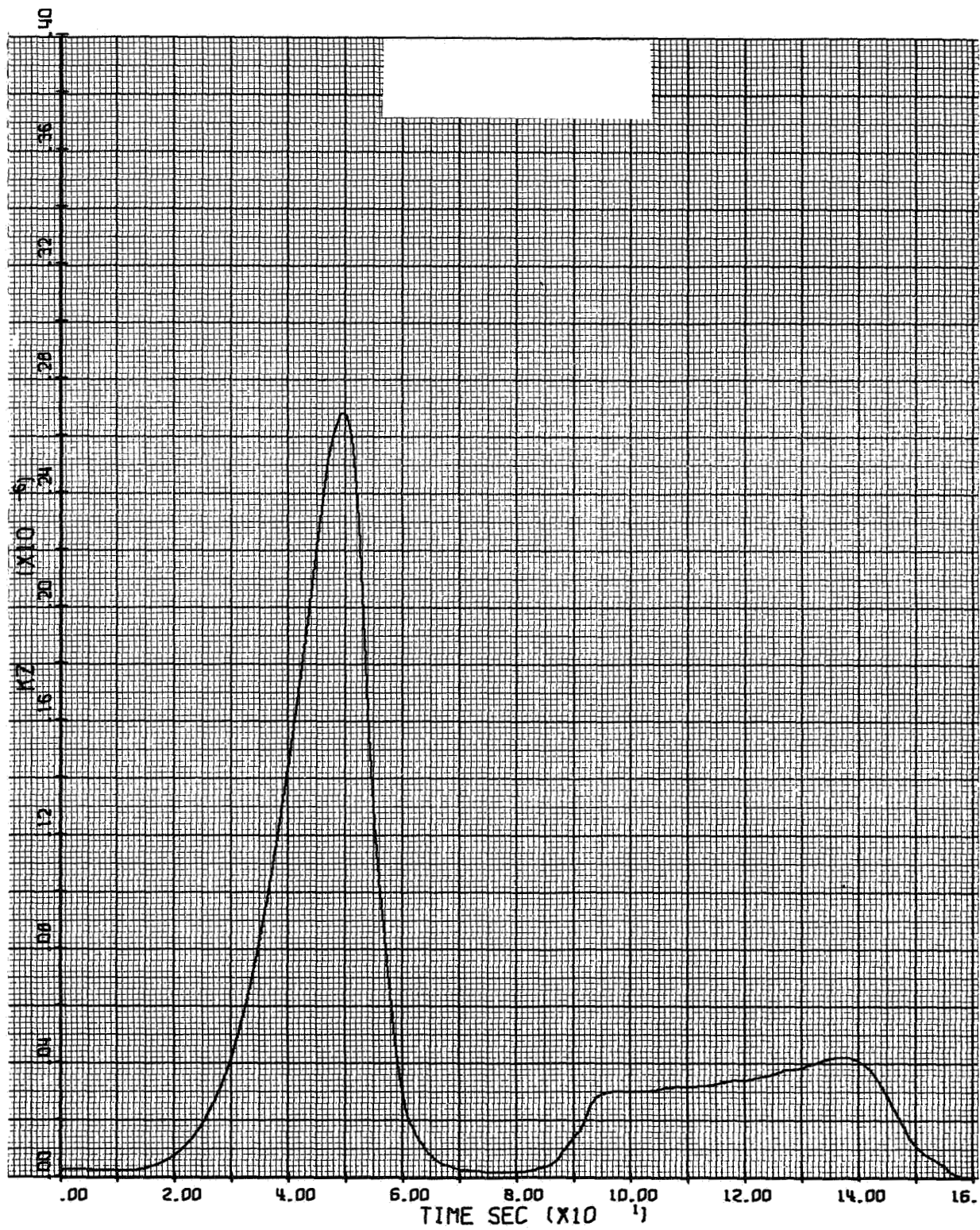
Figure D-10b. Z Gain for Controller B

Figure D-11a. η_1 Gain for Controller A
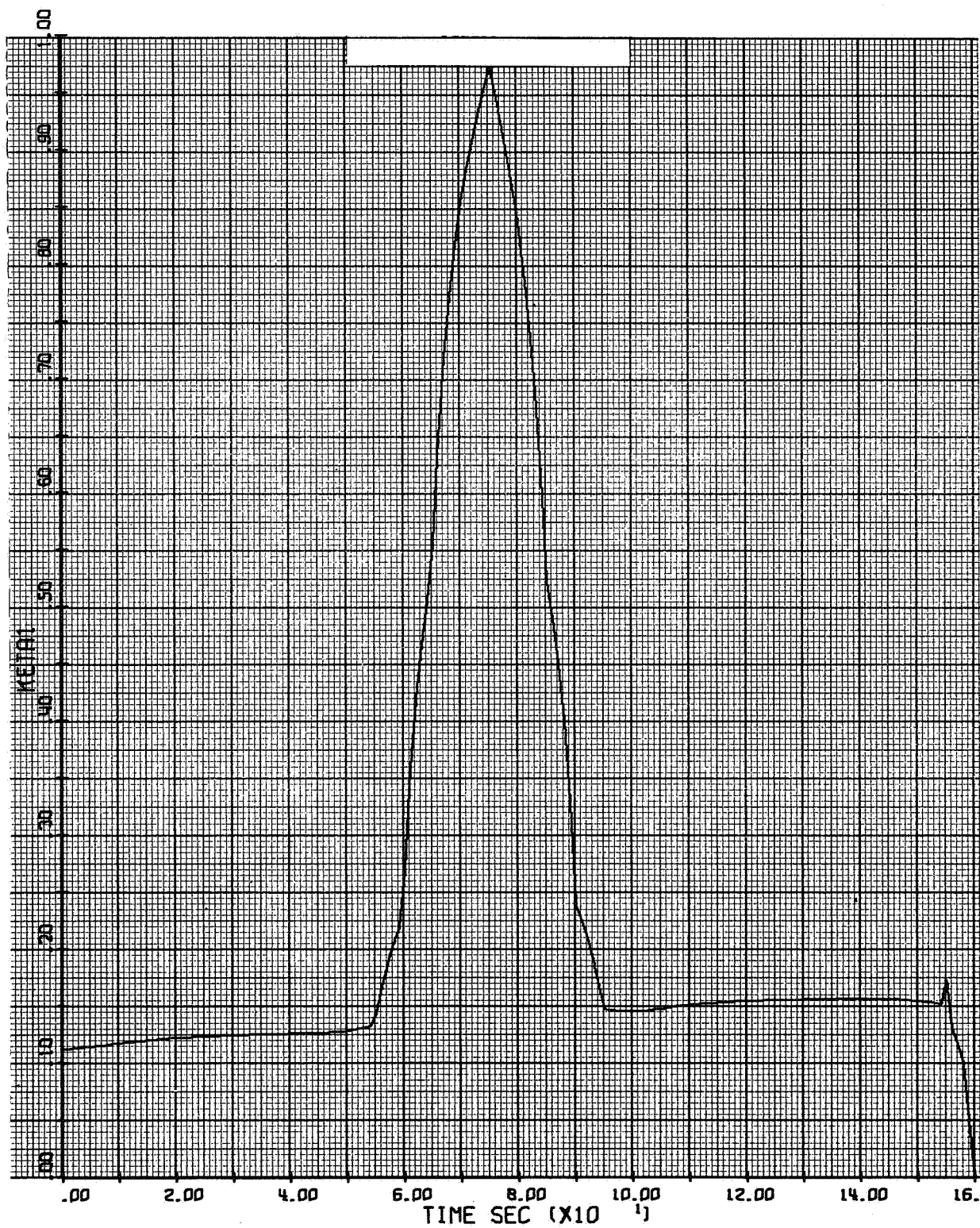
Figure D-11b. η_1 Gain for Controller B
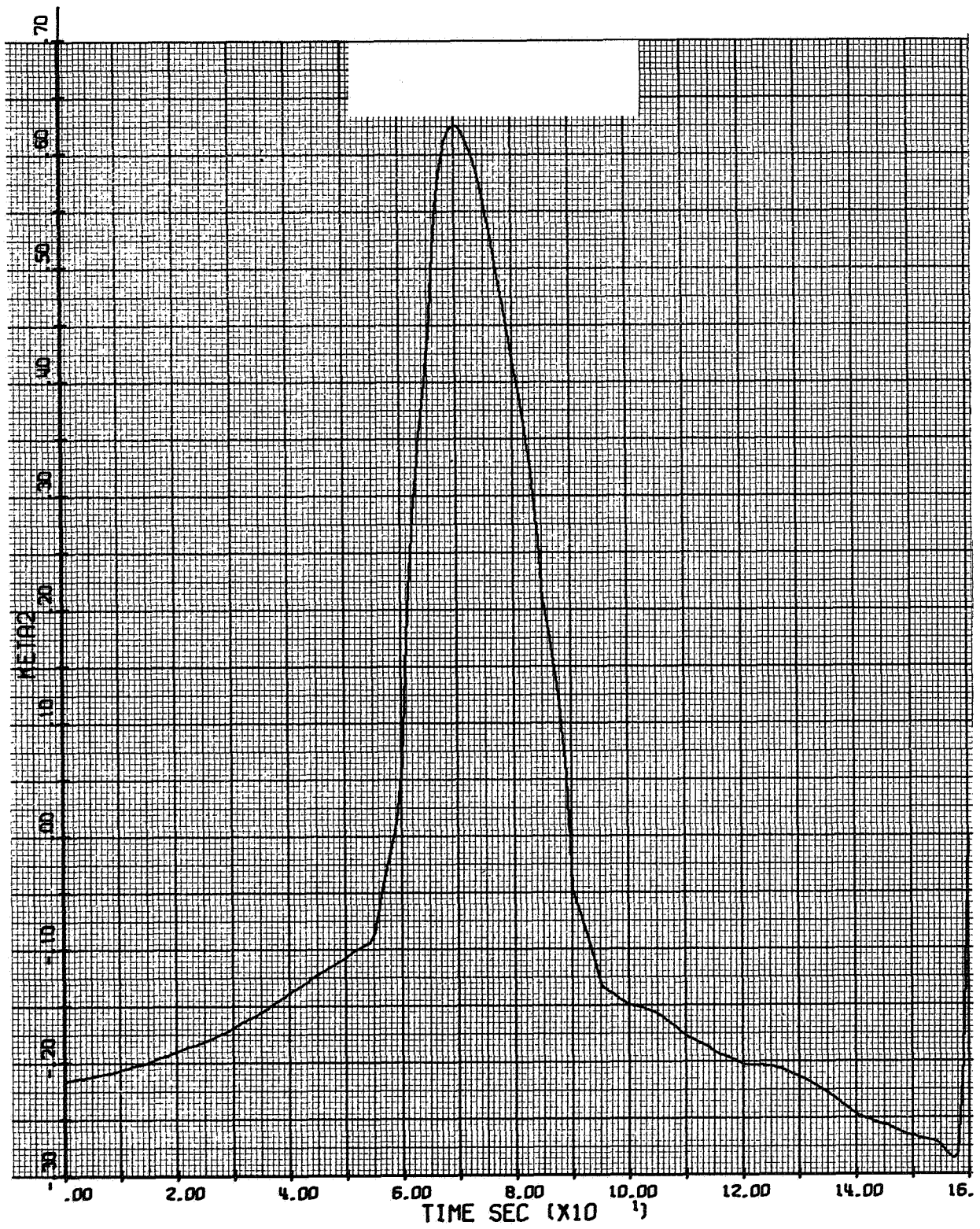
Figure D-12a. η_2 Gain for Controller A

Figure D-12b. η_2 Gain for Controller B

Figure D-13a. η_3 Gain for Controller A

Figure D-13b. η_3 Gain for Controller B

Figure D-14a. Z_{s1} Gain for Controller A
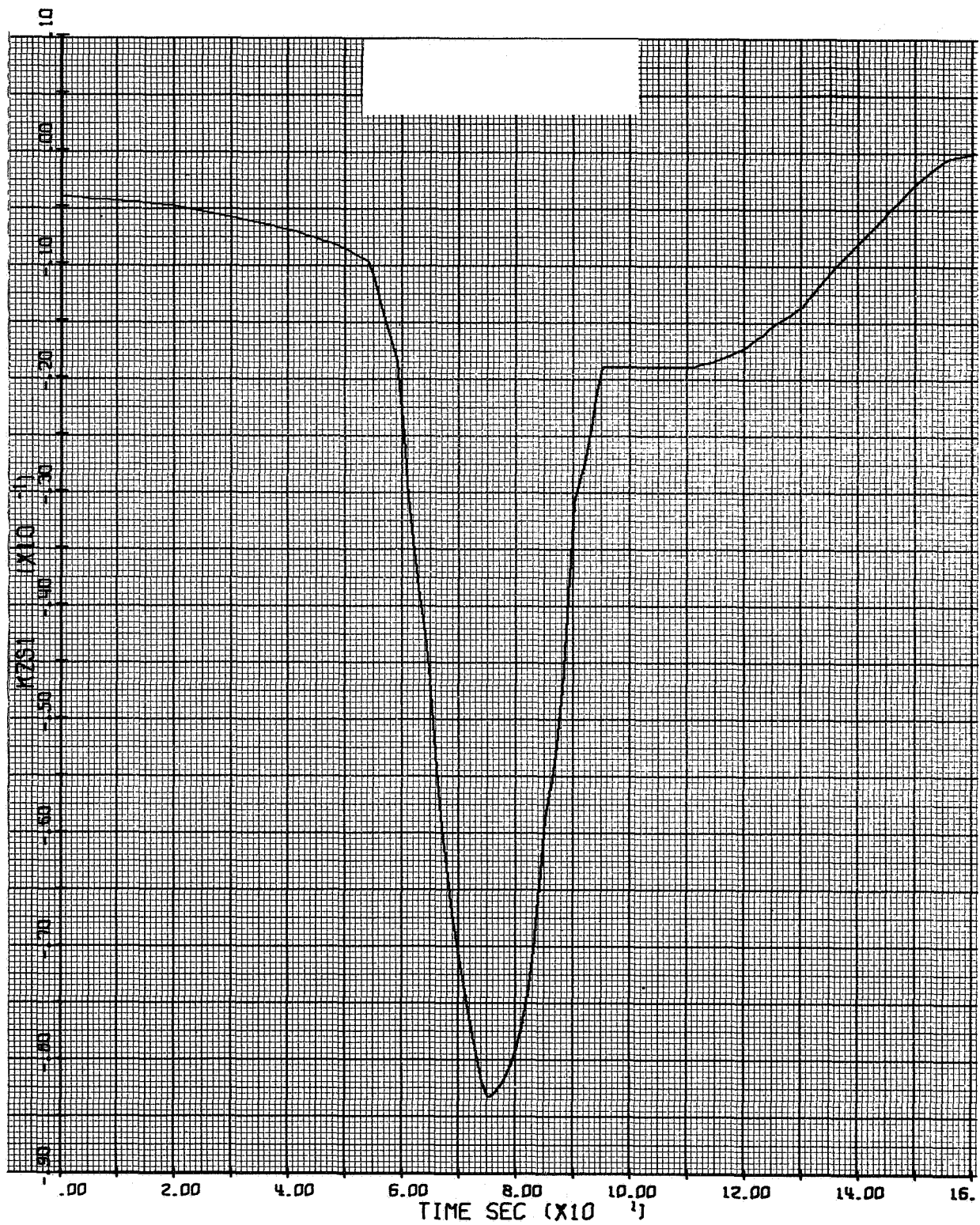
Figure D-14b. Z_{s1} Gain for Controller B
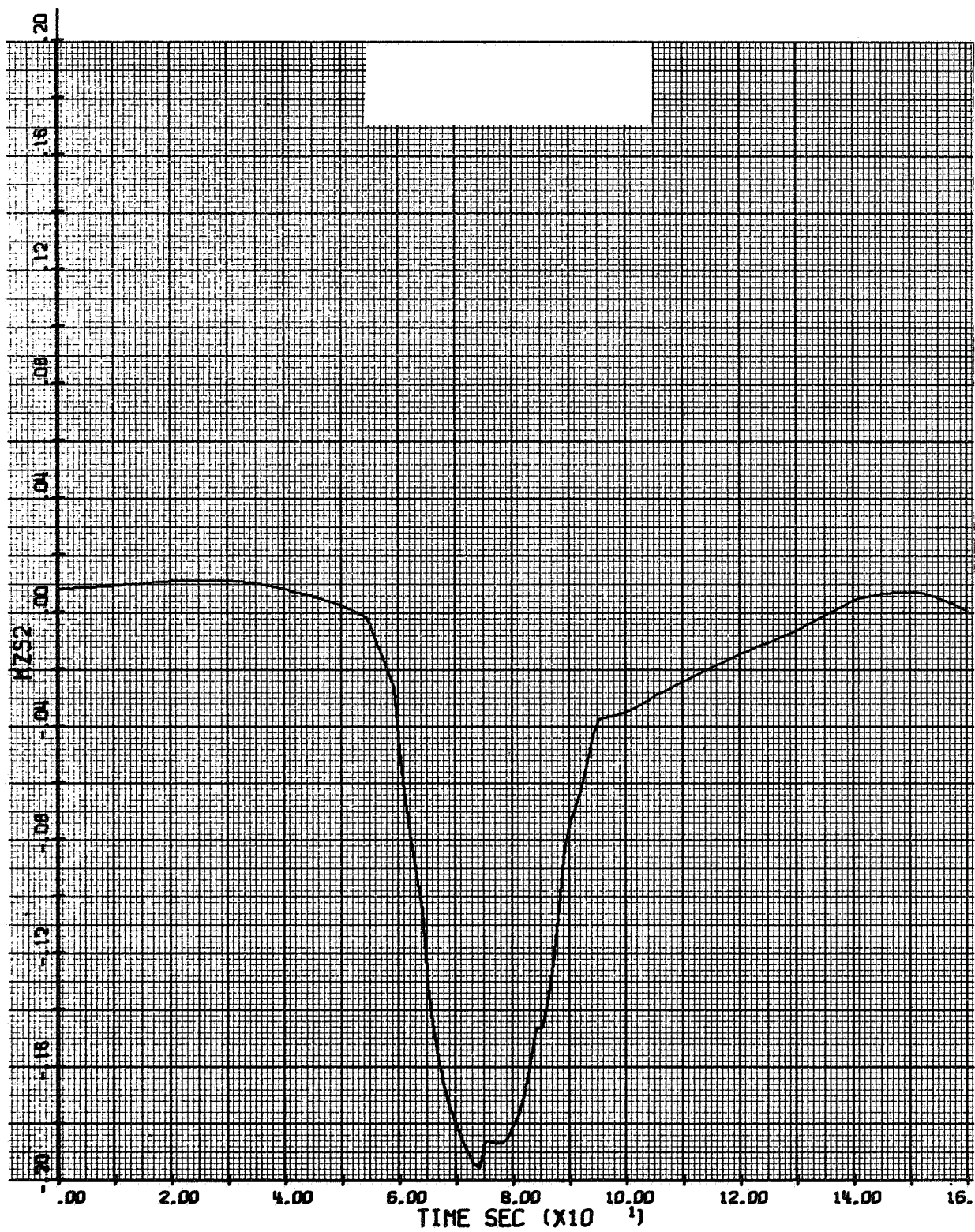
Figure D-15a. Z_{s2} Gain for Controller A

Figure D-15b. Z_{s2} Gain for Controller B
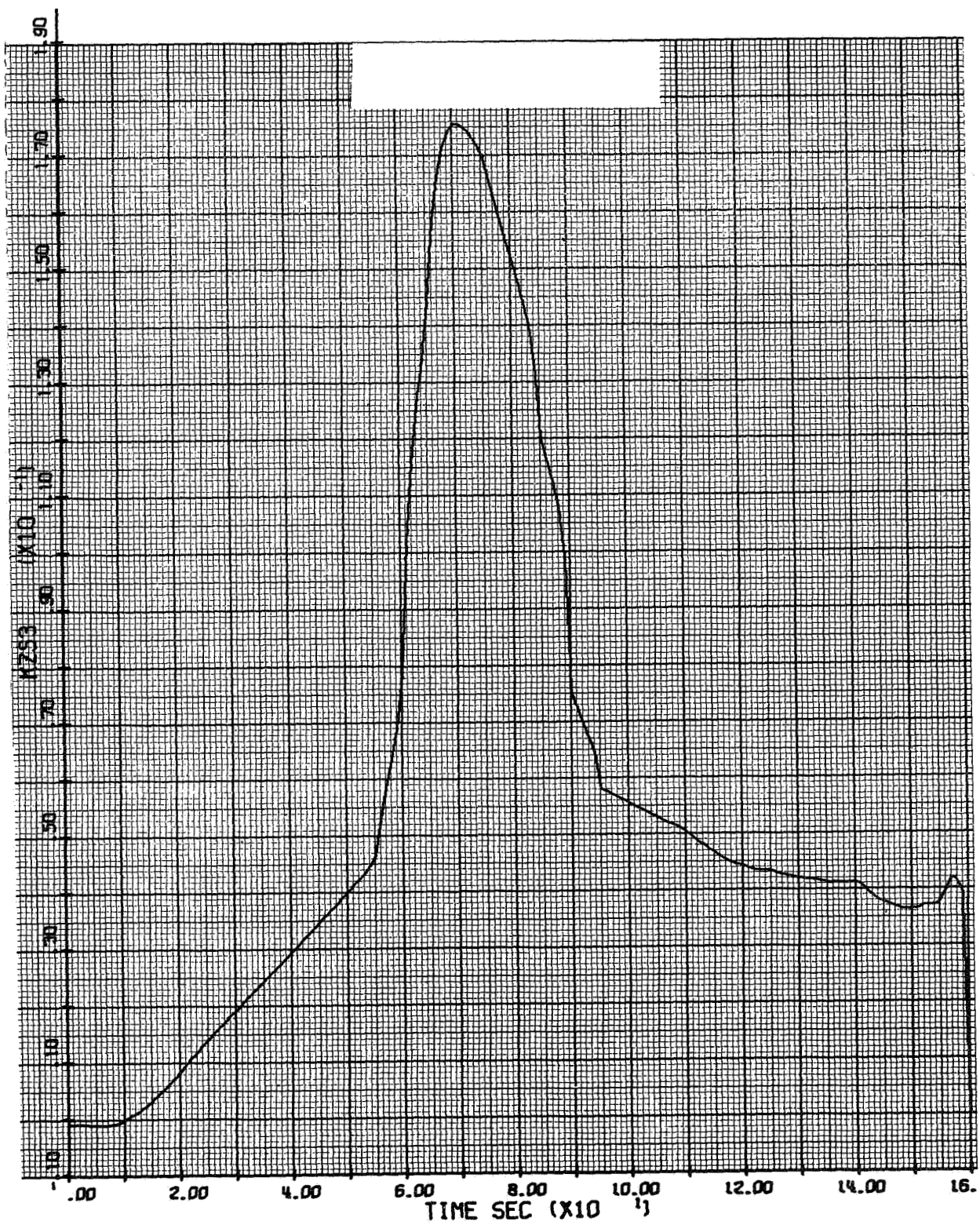
Figure D-16a. Z_{s3} Gain for Controller A

Figure D-16b. Z_{s3} Gain for Controller B

Figure D-17a. β Gain for Controller A

Figure D-17b. β Gain for Controller B
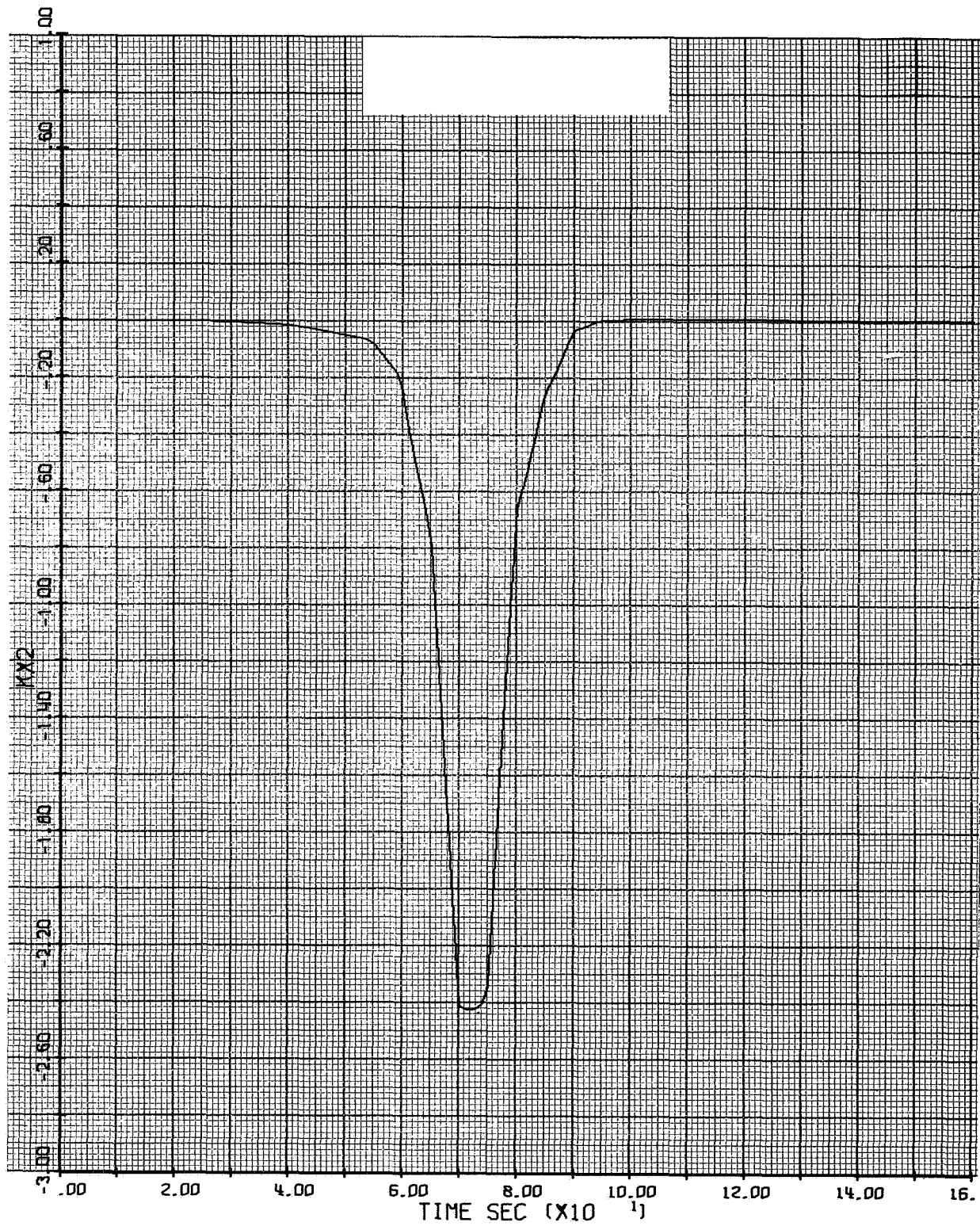
Figure D-18a. ω Gain for Controller A

Figure D-18b. ω Gain for Controller B

D36

Figure D-19a. x Gain for Controller A
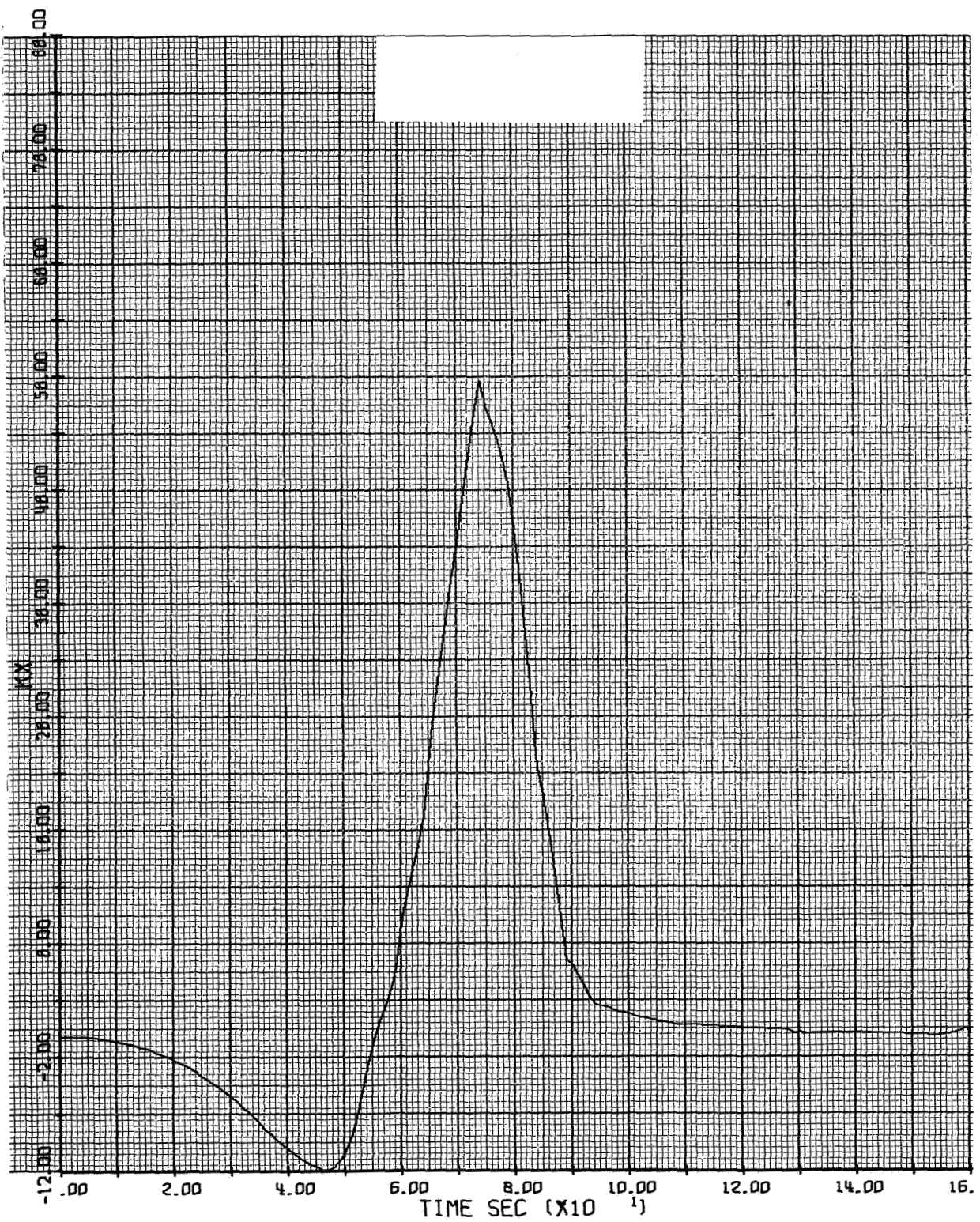
Figure D-19b. x Gain for Controller B

D38

Figure D-20a. x_1 Gain for Controller A

Figure D-20b. x_1 Gain for Controller B

D40

Figure D-21a. x_2 Gain for Controller A
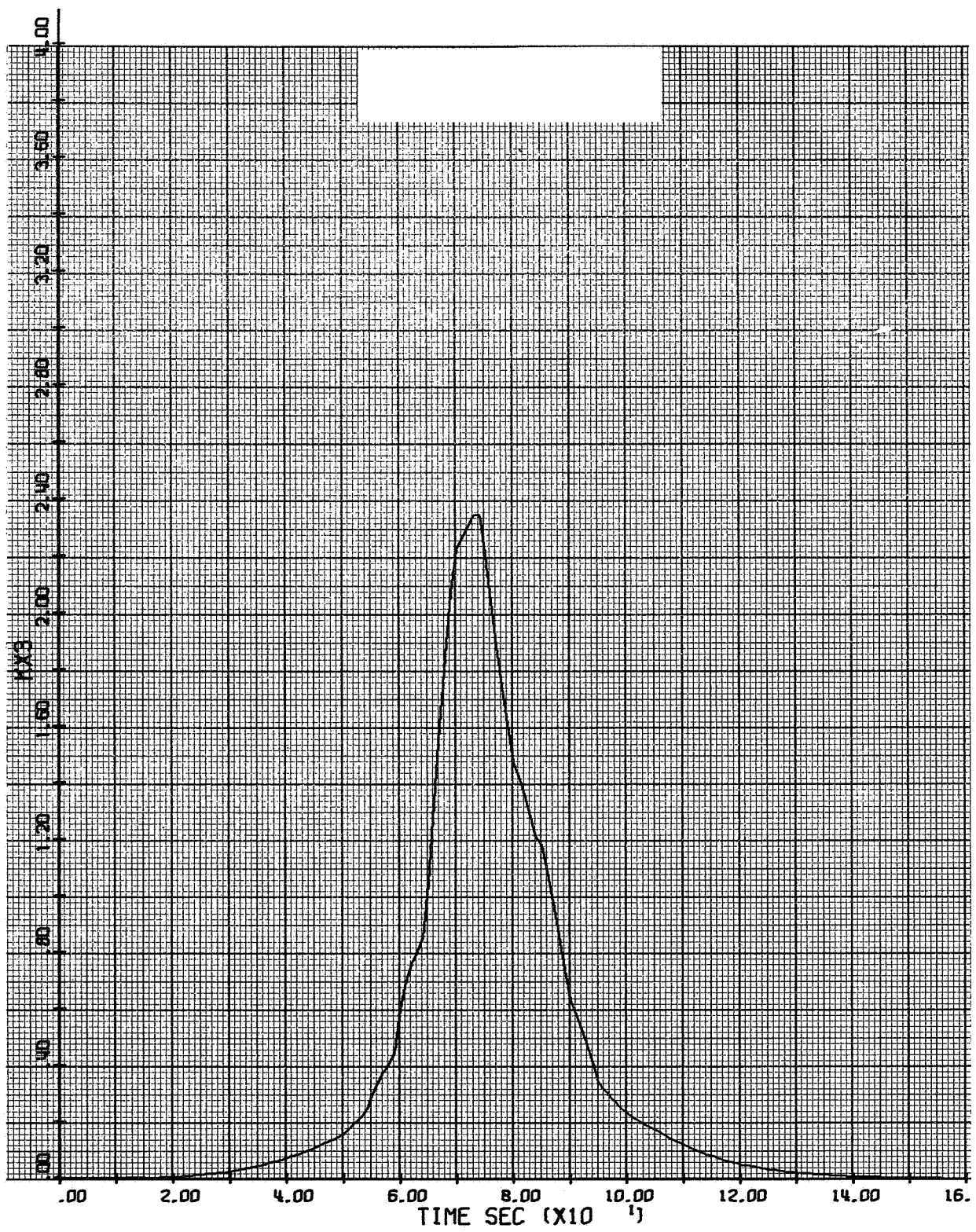
Figure D-21b. x_2 Gain for Controller B
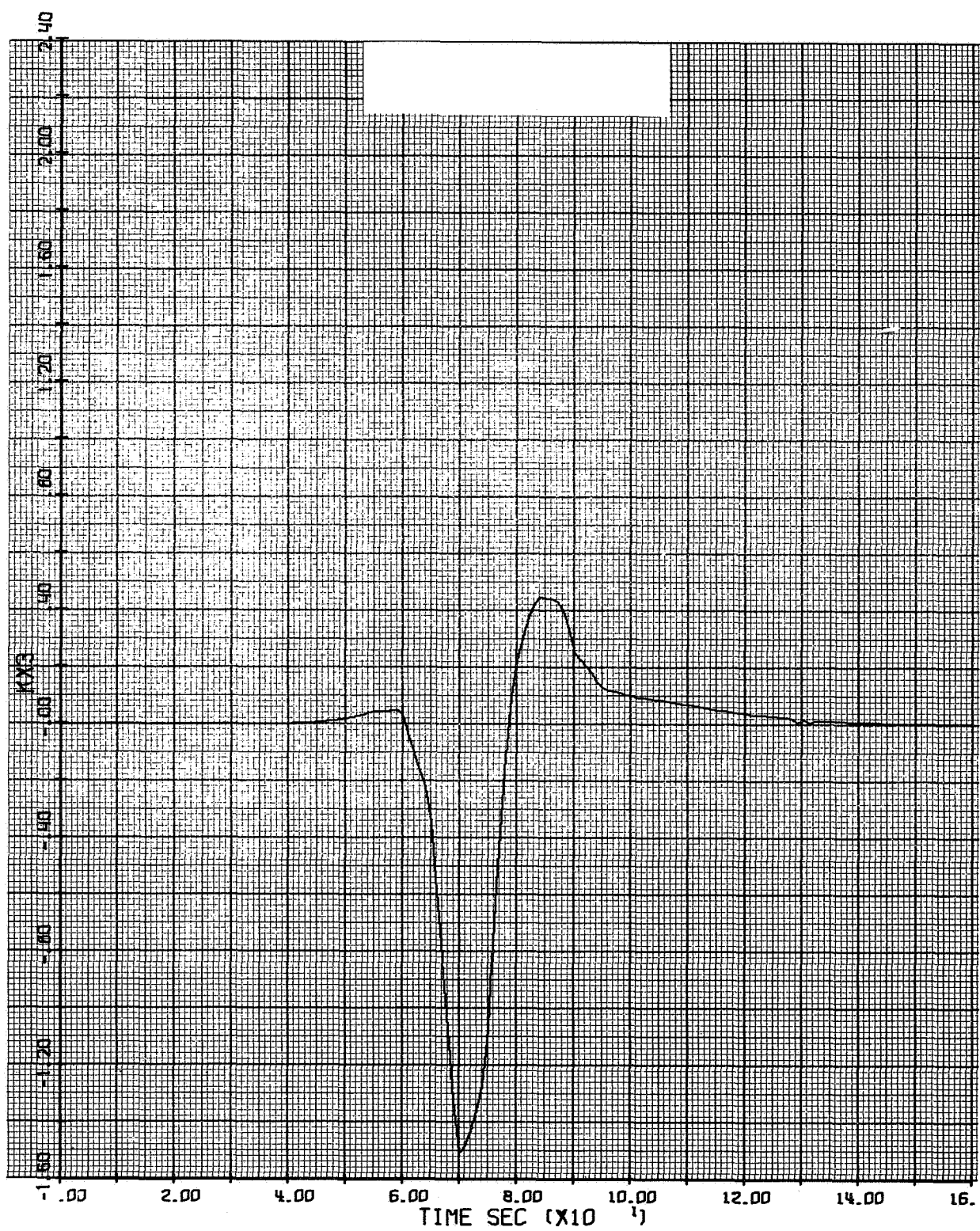
Figure D-22a. x_3 Gain for Controller A

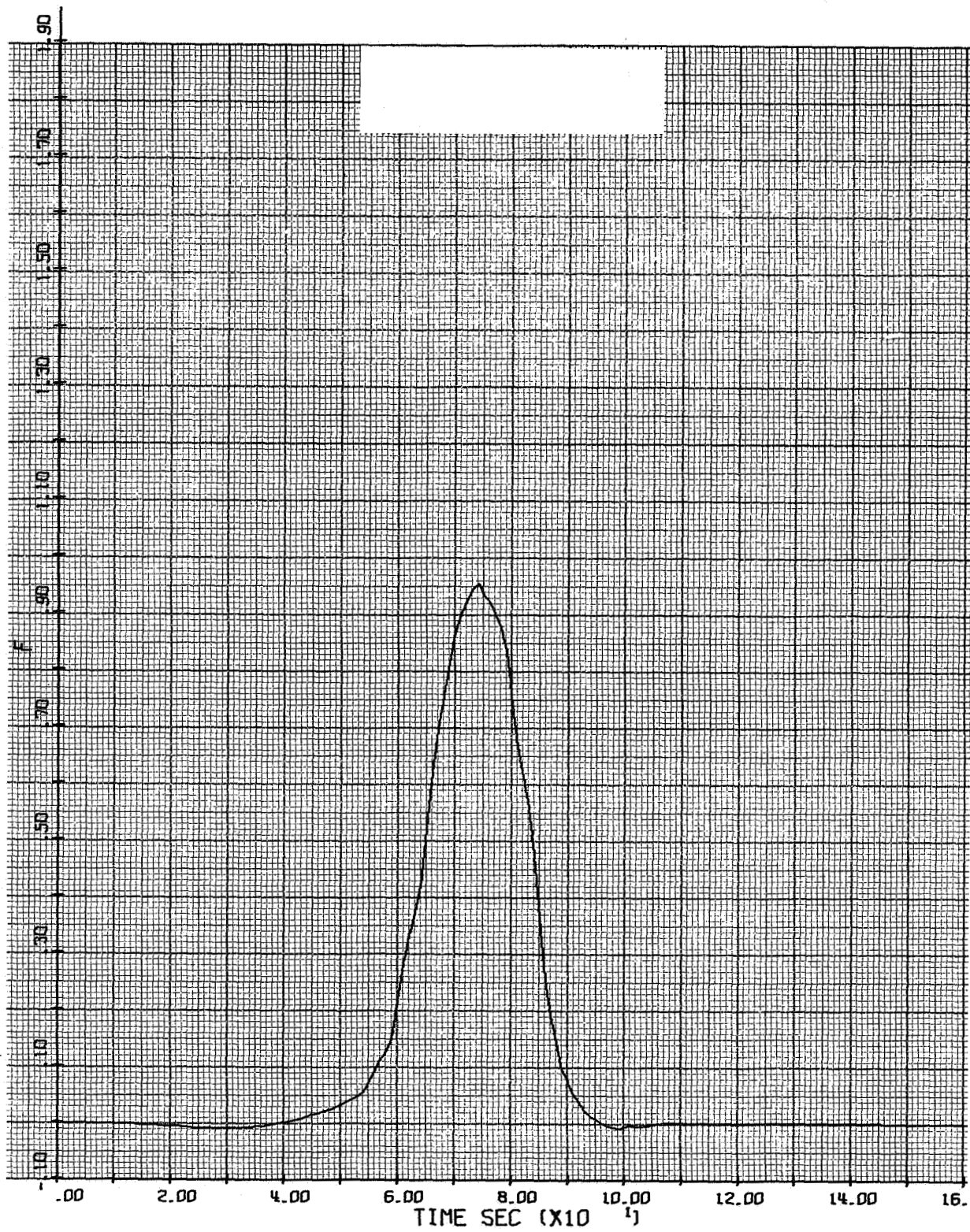Figure D-22b. x_3 Gain for Controller B

Figure D-23a. Adjusted Deterministic Input for Controller A

Figure D-23b. Deterministic Input for Controller B